

***Responses to referee comments on "Global Annual Mean Atmospheric Histories, Growth Rates and Seawater Solubility Estimations of the Halogenated Compounds HCFC-22, HCFC-141b, HCFC-142b, HFC-134a, HFC-125, HFC-23, PFC-14 and PFC-116" by Pingyang Li et al.***

We greatly thank four anonymous referees for your constructive suggestions and comments. Below, we address all the comments and describe our responses to them where we refer to the revised manuscript (Italic) by listing the page and line numbers of changes. Simple comments are sorted in "TECHNICAL CORRECTIONS" and done as it said. Similar comments are sorted together to be response, especially for the comments from Anonymous Referee #3. In the revised manuscript, all changes from the original text are marked.

Additional, we added two co-authors, Ray F. Weiss and Paul J. Fraser, as they contributed some important data and helped to revise the paper very carefully. We also changed the corresponding author to Toste Tanhua ([ttanhua@geomar.de](mailto:ttanhua@geomar.de)) as Toste is my supervisor and my email address may not be used after one or two years.

**Anonymous Referee #1**

"GENERAL COMMENTS"

Comment: The authors synthesize the atmospheric concentration history and review the solubility of HCFC-22, HCFC-141b, HCFC-142b, HFC-134a, HFC-125, HFC-23, PFC-14 and PFC-116. This study is valuable as a first step of evaluating the utility of these compounds as oceanic transient tracers. Some revisions seem to be needed. In particular, the following two revisions are needed.

Response: We thank the Reviewer for the positive comments. Following are the responding responses to the comments.

Comment: First, estimate of Ostwald solubility coefficients by LFERs (Method II) should be revised. According to Abraham et al. (2001), the solvation parameter method of Abraham relies on two linear free energy relationships, LFERs, one for processes within condensed phases, Eq. (i), and one for processes involving gas to condensed phase transfer, Eq. (ii).

$$\log SP = c + eE + sS + aA + bB + vV \text{ (i)}$$

$$\log SP = c + eE + sS + aA + bB + lL16 \text{ (ii)}$$

Here L16 is the solute gas-hexadecane partition coefficient at 298 K; l is a coefficient for L16; and other coefficients and descriptors are the same as those described in the manuscript. Therefore, Ostwald solubility coefficients in pure water (L0) can be estimated by use of Eq. (ii) (processes involving gas to condense phase transfer), while salting-out coefficients (ks) can be estimated by use of Eq. (i) (processes within condensed phases). This point should be noted clearly in the manuscript.

In this study, as seen in Eqs. 10, 12 and 13 (Sect. 2.10.2), the relationship for water to solvent (processes within condensed phases, Eq. (i)) was used to estimate Ostwald solubility coefficient in pure water (L0). It should be revised as mentioned above. Furthermore, Tables S2 and S4 should be revised. When Eq. (ii) is used to estimate L0, may the discussion in Sect. 3.3 (page 20), which includes a comparison between Method II and the Revised Method II, lead to the same result as described in the manuscript?

Response: Thank you very much for your suggestions. I understand you think that only Eq. (ii) can be used to estimate the Ostwald solubility coefficients from the expression in Abraham et al. (2001). But both Eq. (i) and Eq. (ii) can be used to do the estimations from Abraham's more studies (Abraham et al., 1994; 2012). The abstract in Abraham et al. (1994) and Table 2 in Abraham et al. (2012) both described this. Actually, Abraham et al. (2001) also described this by reporting the water-gas partition coefficients of Eq. (i) in Table 1 and the gas-water partition

coefficients of Eq. (ii) in Table 2. In Table 1, the “solvent” in “water to solvent partition coefficients” could also be a gas phase.

Here we also explain this by the definition of gas-solvent partition coefficients. Gas–water,  $K_w$ , or gas–solvent,  $K_s$ , partition coefficients can be defined in terms of equilibrium concentrations of the solute, through Eq. (1).

$$K_s = \frac{\text{Conc. of solute in solvent, in mol dm}^{-3}}{\text{Conc. of solute in the gas phase, in mol dm}^{-3}} \quad (1)$$

The Ostwald solubility coefficients usually expressed as the gas-water partition coefficients. Based on the above definition, the values calculated from Eq. (i), water-gas partition coefficients, should be the reciprocal of the real solubility coefficients. But they are not. When Abraham dealt this in studies (Abraham et al., 1994; 2001; 2012), he already treated the  $SP$  in Eq. (i) as the Ostwald solubility coefficients. So now we know that both  $SP$  estimated from Eq. (i) and Eq. (ii) could be the Ostwald solubility coefficients.

In order to explain it more clearly in the revised manuscript, we added the Eq. (ii) to estimate the Ostwald solubility coefficients ( $L_0$ ) and compared the results to the ones calculated by equations based on  $V$  (Eq. (i)) and  $V_c$  (Table 4). In order to describe Section 2.7.2 more clearly, we also adjust the text.

This addition and comparison don't influence the final results as the Ostwald solubility coefficient estimated by the equation based on the  $V_c$  (the Revised Method II) for most compounds is the best method for the pp-LFERs model method. While compared with the pp-LFERs model method, the CGW model method for estimation of water solubility is the better one to be chosen for Combined Method (Table S4).

**Comment:** Second, hydrolysis of HCFC-22 should be taken into consideration in the discussion of transient tracer potential (for example, Sect. 3.4) because rate constants for hydrolysis of HCFC-22 in alkaline aqueous solutions are much larger than those for hydrolysis of other HCFCs and HFCs [for example, le Noble, W. J. Am. Chem. Soc., 87, 2434-2438 (1965); Kutsuna, S. et al. Int. J. Chem. Kinet. 43, 639-647 (2011)].

May hydrolysis of HCFC-22 in seawater make a significant influence on transient tracer potential of HCFC-22? If hydrolysis of HCFC-22 is significant, what would be expected when HCFC-22 is used as a transient tracer?

**Response:** Thank you very much for your question. We also aware of this issue.

le Noble (1965) studied the effects of hydrostatic pressure on the rate constants of the base-catalyzed and neutral hydrolysis of HCFC-22. The rate constants of hydrolysis decrease with increasing of pressure in water at 25 °C. When HCFC-22 was in the 0.06 *N* aqueous sodium hydroxide solutions, it was deduced that substrate decomposed at least 90 % to form ion. Kutsuna et al. (2011) concluded that the removal efficiency of HCFC-22 directly through the hydrolysis in alkaline aqueous is higher than previously expected temperature, such as 353 K.

When le Noble (1965) and Kutsuna et al. (2011) discussed the rate constants for hydrolysis of HCFC-22 in alkaline aqueous, the aqueous is 0.06 *N* and 0.25-7 *mM* aqueous NaOH solutions, that is, pH is 12.78 and in the range of 10.4-11.85, respectively. However, seawater pH is typically limited to a range between 7.5 and 8.4. Moreover, ocean acidification, an emerging global problem, is getting worse. The rate constants for hydrolysis of HCFC-22 in different concentrations of alkaline aqueous would be different.

As far as we know from previous studies, HCFCs, HFCs and PFCs are relatively stable in seawater as the ocean partial lifetimes (partial atmospheric lifetimes with respect to oceanic uptake) of HCFCs and HFCs ranged from thousands to millions of years (Table 1) and PFCs have atmospheric lifetimes on the order of thousands of years and very low solubility in seawater. However, the ocean partial lifetimes were estimated without considering the biological degradation of most of these compounds in the ocean as they have not been investigated. We know from the experience with CFC-113 and CCl<sub>4</sub>, for instance, that the half time of tracers in seawater can be lower than initially predicted. This manuscript is already very long, and we focus on the source of the tracers, i.e. the atmospheric history and the solubility, in this paper. We will discuss measurements (techniques, constraints, possibilities etc.) and sinks in a follow up paper that we are preparing right now. For instance, we will discuss the stability of these compounds by comparing to measurements of SF<sub>6</sub> and CFC-12 from ocean samples collected during a few years from 3 different oceans.

Based on above discussion, “As shown in Table 1, the atmospheric lifetimes of HCFCs and HFCs with respect to hydrolysis in seawater are very long (Yvon-Lewis and Butler, 2002; Carpenter et al., 2014), ranging from thousands to millions of years, indicating that HCFCs and HFCs are relatively stable in the seawater. PFCs have atmospheric lifetimes on the order of thousands of years and very low solubilities in seawater.” have been added at page 4, line 19-22.

#### “SPECIFIC COMMENTS”

**Comment:** Page 4, lines 21-22: Combustion in thermal power station has been pointed out as a tropospheric sink of PFCs [Ravishankara, A. R. et al., Science, 259, 194-199 (1993)]. It should be cited.

**Response:** “Combustion in thermal power stations has been pointed out as a tropospheric sink of PFCs (Cicerone, 1979; Ravishankara et al., 1993; Morris et al., 1995)” has been added at page 4, line 16-17.

**Comment:** Page 4, lines 28-30, “Cutting the production and consumption of HFCs by more than 80 % over the next 30 years under the Kigali amendment of the MP”: Under the Kigali amendment, the amount of cutting the production and consumption of HFCs is based on the amount scaled by GWP of each HFC. This point had better be described.

**Response:** “Because of the high GWP of HFCs, 197 countries recently committed to cutting the production and consumption of HFCs by more than 80 % over the next 30 years under the Kigali amendment of the MP. Developed countries will reduce HFC consumption beginning in 2019.” has been changed to

“Because of the high GWP of HFCs, 197 countries recently committed to cutting the production and consumption of HFCs by more than 80% over the next 30 years under the Kigali amendment of the MP, although not all of these countries have ratified this Amendment. The reductions in HFC production and consumption are based on GWP-weighted quantities. Developed countries that have ratified the Amendment have agreed to reduce HFC consumption beginning in 2019.” at page 4, line 26-30.

**Comment:** Page 5, lines 17-18: Why were the same AGAGE calibration scales used by converting NOAA and UEA data to the AGAGE scale? Is the reason explained somewhere in the manuscript?

**Response:** NOAA and UEA data are converted to AGAGE scale as all target compounds are reported in the AGAGE network but only five and three target compounds are reported separately in the NOAA and the UEA network.

“Ambient air measurements published by the Advanced Global Atmospheric Gases Experiment (AGAGE), National Oceanic and Atmospheric Administration (NOAA) and University of East Anglia (UEA) are all considered in this study.” has been changed to

“In order to provide a comprehensive and consistent view of halogenated compounds atmospheric distribution and changes over time, ambient air measurements published by the Advanced Global Atmospheric Gases Experiment (AGAGE), the Scripps Institution of Oceanography (SIO), the Commonwealth Scientific and Industrial Research Organization (CSIRO), the National Oceanic and Atmospheric Administration (NOAA) and University of East Anglia (UEA) are considered in this study. The calibration scale differences of these networks in the form of scale conversion factors are determined. SIO and CSIRO data are reported on AGAGE scales. NOAA and UEA data are converted to AGAGE scales by these conversion factors.” at page 5, line 9-15.

**Comment:** Page 10, line 3, “The ionic strength of seawater ( $I_v$ , in  $\text{g L}^{-1}$ ): The unit of ionic strength should be checked.

**Response:** From the empirical equation (7), the ionic strength of a gas ( $I_v$ ) in seawater is  $\text{g L}^{-1}$ .

**Comment:** Page 10, Eq. (8): DS, ES and FS seems to need definition.

**Response:** Eq. (8) is the equation of state of seawater. We decide to delete it in the revised manuscript and only cite papers because the equation can be found in the oceanographic textbook. For more detail, see Millero and Poisson (1981).

$$\rho = \rho_0 + DS + ES^{3/2} + FS \quad (8)$$

Here  $\rho$  is the density of seawater in  $\text{kg m}^{-3}$ , from 0 to 40 °C and from 0.5 to 43 salinity ( $S$ ), have been used to determine a new 1-atm equation of state for seawater.

$$D = 8.24493 \times 10^{-1} - 4.0899 \times 10^{-3}t + 7.6438 \times 10^{-5}t^2 - 8.2467 \times 10^{-7}t^3 + 5.3875 \times 10^{-9}t^4 \quad (9)$$

$$E = -5.72466 \times 10^{-3} + 1.0227 \times 10^{-4}t - 1.6546 \times 10^{-6}t^2 \quad (10)$$

$$F = 4.8314 \times 10^{-4} \quad (11)$$

And  $\rho_0$  is the density of water (Bigg, 1967).

$$\rho_0 = 999.842594 + 6.793952 \times 10^{-2}t - 9.095290 \times 10^{-3}t^2 + 1.001685 \times 10^{-4}t^3 - 1.120083 \times 10^{-6}t^4 + 6.536336 \times 10^{-9}t^5 \quad (12)$$

where  $t$  is the temperature in degree Celsius (°C).

**Comment:** Page 10, line 13, unit of the McGowan's characteristic molar volume in Eq. 8: According to Abraham et al. (2001), unit of the McGowan's characteristic molar volume is not  $\text{cm}^3 \text{mol}^{-1}/100$  but  $\text{dm}^3 \text{mol}^{-1}/100$ . The unit should be checked.

**Response:** According to the original studies (Abraham and McGowan, 1987; McGowan and Mellors, 1986) and other newer studies (Abraham et al., 2012; Abraham et al., 2004), units of the McGowan's characteristic molar volumes are  $\text{cm}^3 \text{mol}^{-1}/100$ . It seems that the unit in Abraham et al. (2001) was wrongly written.

**Comment:** Page 12, line 34, Figures 2-9: The method to calculate IHG and its error (gray parts in Figures 2-9) seem to need explanation.

**Response:** "Inter-hemispheric gradients (IHG) are estimated from the annual mean atmospheric mole fractions of a gas in the NH minus the annual mean in the SH in the same year (Fig. 2a-h). Errors of the IHG were estimated based on error propagation of the annual means in the NH and the SH in the same year (Fig. 2a-h)." has been added at page 14, line 30-32.

In order to describe it more detailed, we also added the estimated method of uncertainties of hemispheric annual means in Sect. 2.6.

**Comment:** Page 14, line 11: What does it mean by "30% (median) larger"? It seems to need more explanation.

**Response:** The atmospheric mole fractions for HCFC-142b in the NH divided into the ones in the SH for each year. A series of multiples are obtained. The median of the series of multiples minus one would be the percentage. It is 30 % for HCFC-142b based on the old method, but it is 6 % based on the new method. Following are discussed based on the old results. The whole sentence means that the annual mean atmospheric mole fractions for HCFC-142b in the NH are 30 % larger than those in the SH in the same year, and the 30 % is calculated based on the median value. The median may be thought of as the "middle" value for a data set. It can be used to express the distribution based on the positions of values rather than values themselves. For average, it is easy to be influenced by an extraordinarily high or low value.

For example, the annual mean atmospheric mole fractions for HCFC-142b in the NH are 30 % larger than those in the SH in the same year based on the median. When it is the average, the percentage goes up to 75 %. That is, the annual mean atmospheric mole fractions for HCFC-142b in the NH are 75 % larger than those in the SH in the same year. This result seems to be unreasonable.

In order not to be misunderstood, similar sentences were deleted in the revised manuscript.

**Comment:** Page 16, lines 27-29: Atmospheric lifetime of HFC-23 is much longer than that of HFC-134a. Hence, time-profiles are expected to be different between HFC-134a and HFC-23 after the consumption restrictions imposed by the 2016 Kigali Amendment to the Montreal Protocol. This point should be discussed.

**Response:** “*Since the atmospheric lifetime of HFC-23 is much longer than that of HFC-134a, time-profiles and IHG change are expected to be a little different between HFC-134a and HFC-23.*” has been added at page 17, line 26-27.

**Comment:** Page 16, lines 34-35, “the growth rates in both hemispheres are really similar”: Do the growth rates mean those of HFC-125 or some target compounds? What does it mean by “really similar”?

**Response:** The growth rates mean those of all target compounds. This sentence was deleted. Following sentences has been added at page 17, line 8-13.

*“From Fig. 2a-h, it is clear that the mole fractions for target compounds in the NH are always larger than those in the SH but follow similar trends; the growth rates in both hemispheres are also similar, lagged in the SH, and the trends in IHG and in emissions/growth rates are very similar. This behavior is because the majority of the emissions (typically > 95%) occur in the NH extra-tropics (O’Doherty et al., 2009; Saikawa et al., 2012; Carpenter et al., 2014; UNEP, 2018) and the interhemispheric mixing time is around one or two years. Thus the larger (the increase) in emissions in the NH, the higher the resultant IHG.”*

**Comment:** Page 17, lines 28-29, “For compounds with shorter lifetimes. . .”: This sentence is difficult to understand. It should be revised.

**Response:** In order not to be misunderstood, the sentence was deleted in the revised manuscript.

**Comment:** Page 18, lines 7-9: The experimental data for HFC-125 are scattered as seen in Fig. S5. This point had better be described more clearly.

**Response:** “*For HFC-125, three fitted curves are shown in Fig. S2e, reflecting that data obtained by different methods do not agree with each other. Curve 1 includes data from Miguel et al. (2000), where the  $\phi$ - $\phi$  approach (the fugacity coefficient - fugacity coefficient method) has been used to predict the experimental results and the fugacity coefficients were calculated using a modified version of the Peng-Robinson equation of state, and Battino et al. (2011) where the data were collected from the International Union of Pure and Applied Chemistry (IUPAC) Solubility Data Series and, in some cases, as averages or estimates. Curve 2 includes data from Mclinden (1990) obtained from the vapour pressure of the pure substance divided by aqueous solubility (sometimes called VP/AS), and HSDB (2015) where the data were calculated with the quantitative structure–property relationship (QSPR) or a similar theoretical method. Curve 3 includes data from Reichl (1995) and Abraham et al. (2001)-observed, which are both measured values from original publications. Considering that the data which were based on measurements match with our results (Fig. S2e) calculated by Method II (only based on the physical properties of compounds), Curve 3 (the curve in the bottom) is chosen as the water solubility fit.*” has been added at page 18, line 24-34.

**Comment:** Page 18, lines 37-38: The dipolarity/polarizability (S) for C2F6 was estimated to be equal to the average of the S of CF4 and C3F8. This estimate might have substantial errors. Influence of errors of S on the salting-out coefficients of C2F6 should be evaluated.

**Response:** The general errors of S, A, B are thought to be 0.03 (Abraham et al., 1998; 2001). We assume that the error for each is 0.01 when S, A and B are all not zero and we assume that the error is 0.03 for S and 0 for A and B

when  $S$  is not zero but  $A$  and  $B$  are both zero. So the error of  $S$  would be both 0.03 for  $CF_4$  and  $C_3F_8$ . The error of  $S$  for  $C_2F_6$  is calculated to be 0.02 by the following equation:

$$\sigma_{C_2F_6} = \frac{1}{2} \cdot \sqrt{\sigma_{CF_4}^2 + \sigma_{C_3F_8}^2}$$

“and the error for the estimate of  $S$  is estimated to be 0.02 based on the error propagation” has been added at page 19, line 23-24.

**Comment:** Page 19, line 32: How is uncertainty from salting-out coefficients estimated? It seems to need more explanation.

**Response:** In the original manuscript, the descriptors  $E$ ,  $S$ ,  $A$ ,  $B$  and  $V$  are thought to be constants shown in Table 4 without errors because they are always the same values in different temperatures. The uncertainties of salting-out coefficients were estimated based on the errors of coefficients  $c$ ,  $e$ ,  $s$ ,  $a$ ,  $b$  and  $v$  (Table 3 in the revised manuscript) when the temperature pluses or minus 2 K. It was calculated by

$$\sigma_{K_s} = \sigma_c + E\sigma_e + S\sigma_s + A\sigma_a + B\sigma_b + V\sigma_v$$

Based on the propagation of uncertainty, the method above was wrong. The uncertainties of salting-out coefficients should be calculated by

$$\sigma_{K_s} = \sqrt{\sigma_c^2 + E^2\sigma_e^2 + S^2\sigma_s^2 + A^2\sigma_a^2 + B^2\sigma_b^2 + V^2\sigma_v^2}$$

But in the revised manuscript, we would like to change the estimation method of the uncertainties of salting-out coefficients considering the errors of descriptors. Abraham et al. (2001) though that it is not easy to calculate the error in the descriptors as all the descriptors are calculated simultaneously.  $E$  is calculated without error.  $V$  is the McGowan’s characteristic molar volume in  $cm^3 mol^{-1}/100$  without error. The general errors of  $S$ ,  $A$ ,  $B$  are thought to be 0.03 (Abraham et al., 1998; Abraham et al., 2001). We assume that the error for each is 0.01 when  $S$ ,  $A$  and  $B$  are all not zero. The uncertainty of salting-out coefficients could be calculated by

$$\sigma_{K_s} = \sqrt{\sigma_c^2 + E^2\sigma_e^2 + s^2S^2\left[\left(\frac{\sigma_s}{S}\right)^2 + \left(\frac{\sigma_S}{S}\right)^2\right] + a^2A^2\left[\left(\frac{\sigma_a}{a}\right)^2 + \left(\frac{\sigma_A}{A}\right)^2\right] + b^2B^2\left[\left(\frac{\sigma_b}{b}\right)^2 + \left(\frac{\sigma_B}{B}\right)^2\right] + V^2\sigma_v^2}$$

We assume that the error is 0.03 for  $S$  and 0 for  $A$  and  $B$  when  $S$  is not zero but  $A$  and  $B$  are both zero. The uncertainty of salting-out coefficients could be calculated by

$$\sigma_{K_s} = \sqrt{\sigma_c^2 + E^2\sigma_e^2 + s^2S^2\left[\left(\frac{\sigma_s}{S}\right)^2 + \left(\frac{\sigma_S}{S}\right)^2\right] + A^2\sigma_a^2 + B^2\sigma_b^2 + V^2\sigma_v^2}$$

“It is not easy to calculate the error in the descriptors as all the descriptors are calculated simultaneously (Abraham et al., 2001).  $E$  is calculated without error.  $V_c$  is the McGowan’s characteristic molar volume without error. The general errors of  $S$ ,  $A$ ,  $B$  are thought to be 0.03 (Abraham et al., 1998; 2001). We assume that the error for each is 0.01 when  $S$ ,  $A$  and  $B$  are all not zero and we assume that the error is 0.03 for  $S$  and 0 for  $A$  and  $B$  when  $S$  is not zero but  $A$  and  $B$  are both zero. So the uncertainties of salting-out coefficients could be calculated by error propagation based on different functions.” has been added at page 13, line 13-18.

**Comment:** Supplement, Eq. (2): What does it mean by  $i = 0$  in summation?

**Response:** No meaning. We changed it to start with  $i=1$ .

“TECHNICAL CORRECTIONS”

**Comment:**

Page 5, line 21: “can used” is “can be used”.

Page 6, line 32: “fin air” is “firm air”.

Page 12, line 11: “By combining Eq. (4), (12) and (14)” may be “By combining Eqs. (4), (14) and (16)”.

Page 12, line 39 – page 13, line 1: “hemispheric” is “hemisphere”.

Page 13, line 21; page 13, line 39: “This consistent” is “This is consistent”

Page 15, line 13: “These consistent” is “These are consistent”

Page 16, line 17: “ $0.038 \pm 0.007$ ” is “ $0.138 \pm 0.007$ ”.

Page 16, line 17: “ $0.033 \pm 0.008$ ” is “ $0.133 \pm 0.008$ ”.

Page 16, line 34: “This could attributed” is “This could be attributed”.

Page 17, line 9: “This consistent” is “This was consistent”.

Page 17, line 13: “countries, Moreover,” is “countries. Moreover,”.

Page 18, line 9: “is chose” is “is chosen”.

Page 18, line 32: “298.15-338.15 K” is “273.15-313.15 K”.

Page 19, line 31: “ $9.0695e-05$ ” is “ $9.0695 \times 10^{-5}$ ”.

Page 19, line 31: “ $9.1858e-05$ ” is “ $9.1858 \times 10^{-5}$ ”.

Page 21, line 38: “can be also be” is “can also be”.

[Response:](#) All technical notes and suggestions have been fully implemented.

## **Anonymous Referee #2**

[Comment:](#) This work the authors compile a large set of data to investigate the atmospheric history, growth rates, seawater solubility of a series of halocarbons. These are useful information to start understanding the suitability for these gases to be used as tracers. The paper is well-written, although I found that since a major motivation for the authors to investigate all these parameters was to assess the possibility to use these halocarbons as tracers, the title should be modified to reflect this. This paper presented an important initial step to assess the new generation of ocean tracers and should be published after minor revisions.

[Response:](#) We thank the Reviewer for the positive comments. The title is changed to be as “*Atmospheric Histories, Growth Rates and Solubilities in Seawater and other Natural Waters of the Potential Transient Tracers HCFC-22, HCFC-141b, HCFC-142b, HFC-134a, HFC-125, HFC-23, PFC-14 and PFC-116*”.

[Comment:](#) Page 5 lines 3 to 5: the terminology of “mid-February” and “mid-August” used to define means from January to March and July to September is focusing. I suggest the authors use a different terminology for these.

Page 12 lines 30 to 33: Similar to Page 5, why use such terminology? The “mid-year” mean definition for average of the monthly means also sound confusing.

[Response:](#) The terminology of “mid-February”, “mid-August” and “mid-year” changed to “JFM means”, “JAS means” and “annual means”.

### “TECHNICAL CORRECTIONS”

[Comment:](#)

Page 6 line 33: should read “The firm air data. . .”

Page 12 line 23: should read “Based on this, we reconstructed. . .”

Figures 2 through 9 and 12, a and b should be labeled.

Page 13 line 30: Define “S-Shape” here, as later in the paper, the authors mentioned it means Sigmoidal, and this should be defined before the “S-shape” terminology is used.

Page 21 line38: suggest revise to “because it is extremely volatile, therefore, it is difficult to trap and separate chromatographically”

Page 21 line 41: suggest revise to “. . .are only two of the many requirements. . .”

[Response:](#) All technical notes and suggestions have been fully implemented.

### **Anonymous Referee #3**

[Comment:](#) While the overall goal of this paper is very worthwhile, there are many issues listed below by page (P), line (L) and Table numbers (especially the major points indicated) that need to be addressed before this paper is acceptable for OS.

[Response:](#) We thank the Reviewer for the comments. Following are the responding responses to the comments.

[Comment:](#) P2 L20: MAJOR POINT-1. This is reasonable for all species for oceanic production, and for PFCs for oceanic destruction. But you provide no evidence that non-negligible destruction is ruled out for the HCFCs and HFCs that could be e.g. prone to hydrolysis. Provide this evidence or state up front that the use of these species as ocean tracers depends on their verification as stable in ocean water.

P5 L21-25: Again, MAJOR POINT-1, what about the potential in situ destructions of these H-containing species?

[Response:](#) Thank you very much for your question. We also aware of this issue.

As far as we know from previous studies, HCFCs, HFCs and PFCs are relatively stable in seawater as the ocean partial lifetimes (partial atmospheric lifetimes with respect to oceanic uptake) of HCFCs and HFCs ranged from thousands to millions of years (Table 1) and PFCs have atmospheric lifetimes on the order of thousands of years and very low solubility in seawater. However, the ocean partial lifetimes were estimated without considering the biological degradation of most of these compounds in the ocean as they have not been investigated. We know from the experience with CFC-113 and CCl<sub>4</sub>, for instance, that the half time of tracers in seawater can be lower than initially predicted. This manuscript is already very long, and we focus on the source of the tracers, i.e. the atmospheric history and the solubility, in this paper. We will discuss measurements (techniques, constraints, possibilities etc.) and sinks in a follow up paper that we are preparing right now. For instance, we will discuss the stability of these compounds by comparing to measurements of SF<sub>6</sub> and CFC-12 from ocean samples collected during a few years from 3 different oceans.

Based on above discussion, “*As shown in Table 1, the atmospheric lifetimes of HCFCs and HFCs with respect to hydrolysis in seawater are very long (Yvon-Lewis and Butler, 2002; Carpenter et al., 2014), ranging from thousands to millions of years, indicating that HCFCs and HFCs are relatively stable in the seawater. PFCs have atmospheric lifetimes on the order of thousands of years and very low solubilities in seawater.*” have been added at page 4, line 19-22.

[Comment:](#) P5 L3-6: MAJOR POINT-2. But you need to calculate polar air concentrations (where oceanic downwelling maximizes) and not entire extratropical averages. This would best be done by assimilation of all station data into a 2D or 3D model, or at least by using the high latitude AGAGE and NOAA station data only (see also the later P6 L38 comment).

P5 L14-20: The case for differences from the prior Meinshausen et al, 2017 study would be strengthened by addressing MAJOR POINT-2.

P6 L38 to P7 L2: MAJOR POINT-2 again. I do not understand why you are using only these AGAGE stations and NOAA sampling sites and neglecting AGAGE (e.g. Ny Alesund) and NOAA sites much closer to the polar downwelling regions?

[Response:](#) The main purpose of the paper is to reconstruct the atmospheric histories of target compounds for their potential to be transient tracers. As Walker et al. (2000) and Bullister (2015) did for CFCs and CCl<sub>4</sub>, we also used the data from MHD, THD and CGO to reconstruct the annual means atmospheric mole fractions in NH and SH for HCFCs, HFCs and PFCs.

Although it is very cold in polar areas, there is very little water formation in the polar regions; in the south there is a continent, and in the north there is strong stratification preventing deep water formation. In fact, most deep and

intermediate water formation takes place in the Labrador Sea, the Greenland Sea and in the Southern Ocean; at high latitudes, but not polar. Actually, the latitude of Mace Head is similar to the deep water formation region of the Labrador Sea.

From the selected sites for *in situ* or flask measurements, we reconstructed the atmospheric histories for the mid-latitude area. But actually the archived air and firn air measurements and model results are from extra-tropical regions (30°-90°). The compiled atmospheric mole fraction histories of compounds in this paper could represent the ones for extra-tropical regions.

But if someone thought that it can only represent the atmospheric history of compounds in the mid-latitude area and he or she wants to do more research for other areas (such as polar area), the latitude gradients could be used from Meinshausen et al. (2017). For example, if someone would like to work exactly on the Antarctic Intermediate Water (AAIW), the Antarctic Bottom Water (AABW) and the Weddell Sea Bottom Water (WSBW) at around 60-75°S in the south, or the Greenland Sea Deep Water (GSDW) and the Labrador Sea Water (LSW) at around 60-75°N in the north, he or she could plus or minus values from latitude gradients shown in the Supplement figures from Meinshausen et al. (2017).

Actually, scientists also took into account the correct input function (atmospheric history) of the source regions when they use CFC-12 and SF<sub>6</sub> as oceanic transient tracers (Stöven and Tanhua, 2014).

**Comment:** Also, MAJOR POINT-3, how are you weighting the ability of the NOAA (4 samples/month?) and AGAGE (900 samples/month?) measurements for computing monthly means? Surely the AGAGE monthly means are much more precise.

**Response:** In the original manuscript, the monthly average of an *in situ* data series with around 900 measurement points from the AGAGE got the same weight as the monthly average from a flask measurement program with few observations from NOAA.

In the revised manuscript, we combined the datasets to create monthly averages and standard deviations at the same hemisphere using the number of measurement-weighted averages when there were measurements from multiple different networks and sites.

We also updated our method as written in Sect. 2.6.

**Comment:** P8-P9 Section 2.9 & Supplement S1: This old smoothing spline method is not very powerful compared to recent machine learning methods (e.g. Bodesheim et al, <https://www.earth-syst-sci-data.net/10/1327/2018/>).

**Response:** Following your advice, we read the paper very carefully. Bodesheim et al. (2018) proposed the random forest regression model to predict the diurnal cycles in high-resolution based on large-scale regression models. The predicted output can be obtained from the function:

$$y^* = \frac{1}{T} \sum_{t=1}^T y_t$$

Inspired by this method, we found that we only have a decision tree. In order to avoid overfitting, the decision tree can be resampled (bootstrap aggregating or bagging) to obtain more trees and then we could do the regression. This method may be called Decision Tree Regression or Regression Tree Analysis. Following are the estimated results. We compared them with the results from our old method and a new method (Take atmospheric mole fractions of HCFC-22 in NH for example).

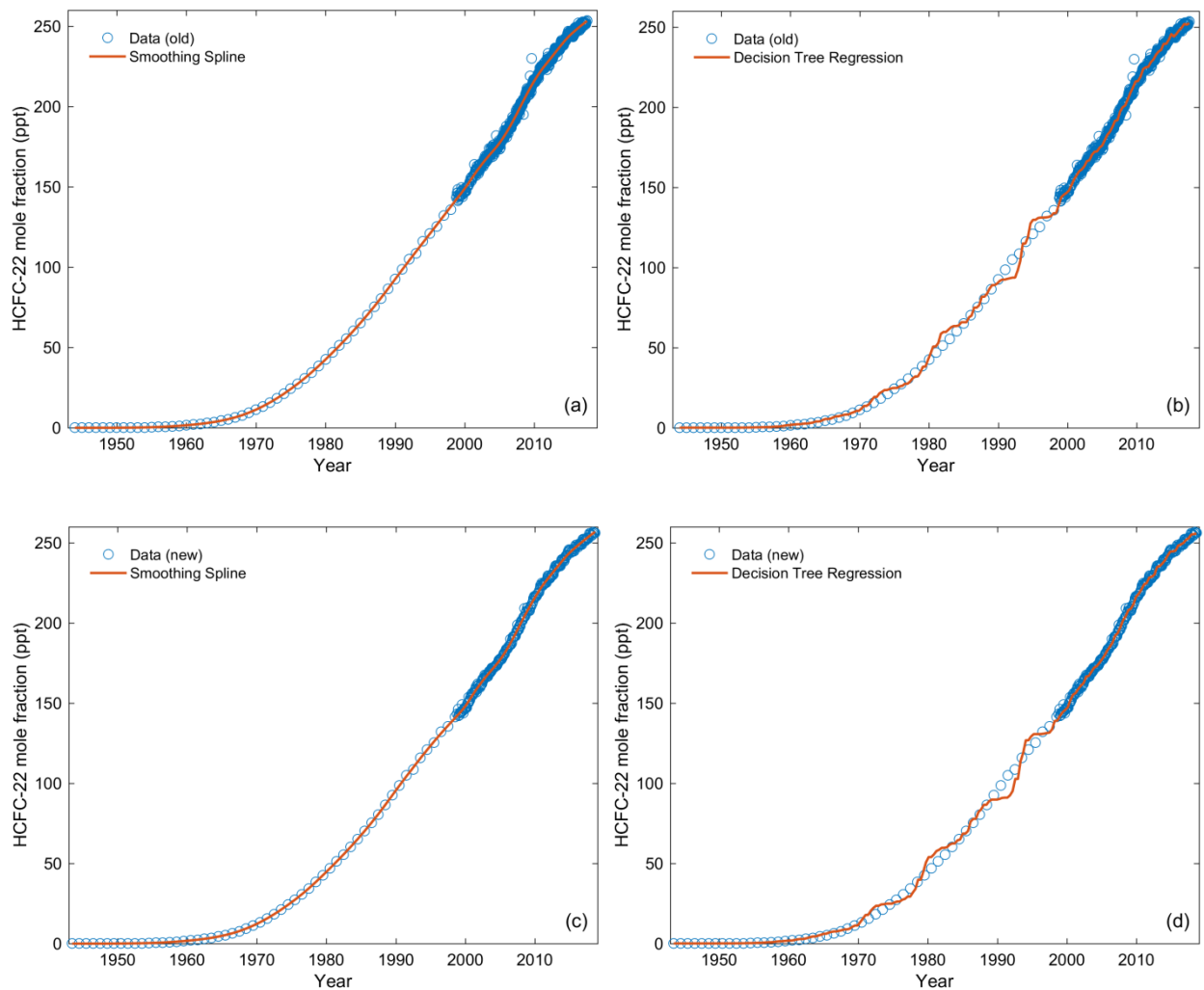


**Fig. 1** Comparison between the smoothing spline fit and the decision trees regression on the atmospheric mole fractions of HCFC-22 in NH based on the old data and new data. The difference between old data and new data is that the new data is the number of measurements-weighted monthly averages on the AGAGE *in situ* monthly means and the NOAA flask monthly mean in recent decades, and the polluted data from the NOAA flask measurements were removed in advance.

From Fig. 1, no matter for old data or new data, the total errors of estimations from decision trees regression are higher than the ones from smoothing spline fit. Based on the errors comparison, we prefer smooth spline fit.

About the method, we tried the polynomial fit, non-linear regression and smoothing spline. Following your advice, we tried decision trees regression. As our data are unevenly distributed, that is to say, we have more data with more precise in recent decades, while prior this time the data are less with less precise. For polynomial fit and non-linear regression with empirical functions, we could obtain good fit results in recent decades, while the predictions are really bad when there are fewer data. The same situation happens to decision trees regression. We thought the estimations from the three methods will be better if the original data could be more evenly distributed. Considering the purpose of the study, the smoothing spline fit works better for our estimation.

**Comment:** Also, the method appears to be using only the station/sample measurement precisions in computing the errors (see MAJOR POINT-3 about these). Also, MAJOR POINT-4, there is an additional error (“representation error”) that takes into account that these point station measurements are not measuring the large volume of the

surface atmosphere (extratropical, polar regions) that you are implicitly presuming that they do. In inverse and assimilation techniques these representation errors usually dominate the total measurement error except when mole fraction gradients are negligible (i.e. emissions are negligible). Thus, the errors you are reporting are lower limits to the real errors.

[Response:](#) The errors are re-calculated as written in Sect. 2.6.

The error for latitude gradients is not easy to estimate. If we think about the errors in latitude gradients based on the study (Meinshausen et al., 2017), the errors will be really significant.

[Comment:](#) P22 L4-7: This conclusion suggesting "in a way that is optimized" is presently debatable given MAJOR POINTS 2,3,4.

[Response:](#) It is not optimized. The hemispheric annual means were calculated to be the source functions of transient tracer studies rather than the real hemispheric means based on all the atmospheric observations themselves.

[Comment:](#) P8 L5-18: Some/many of these appear out of date. Check Prinn, Weiss et al, 2018b (their Section 2.6) for SIO-year calibrations, and their Table 5 for latest AGAGE/NOAA conversion factors.

Table 3: Some/many of these may be out of date. Check Prinn, Weiss et al, 2018b Section 2.6 for SIO (year) values and Table 5 for AGAGE/NOAA conversion factors.

[Response:](#) The AGAGE/NOAA conversion factors have been changed for Section 2.5 and Table 2.

#### “TECHNICAL CORRECTIONS”

[Comment:](#)

P3 L5: P4: Please also cite relevant ALE/GAGE/AGAGE papers.

P3 L13: Please also cite relevant ALE/GAGE/AGAGE papers.

P3 L21: “They” not “He”

P4 L14: Need references for this doubling statement.

P5 L35: Change to Prinn, Weiss et al 2018a (new CDIAC website) and add Prinn, Weiss et al 2018b (references are given at end of this review).

P5 L38-39: Much more relevant for making this point are the Prinn, Cunnold et al 1992 and Prinn, Weiss et al 2000 studies for the Samoa and Barbados sites showing the way ENSO and Atlantic Hurricanes enhance interhemispheric mixing and thus affect the measurements at these stations.

P6 L9-10: Add Prinn, Weiss et al, 2018b reference for latest instrumentation.

P6 L10-11: Add Prinn, Weiss et al, 2018b (their Table 1) reference for precisions of ALL 8 of your compounds.

P8 L5: Please reference instead of the main AGAGE website (agage.mit.edu) that connects to this daughter website only after potential users have read the substantial guidelines for ethical use of AGAGE data on the main website.

Tables 2a-2h: Change Prinn et al, 2016 to Prinn, Weiss et al 2018a (new CDIAC website) and add Prinn, Weiss et al 2018b (ESSD paper).

[Response:](#) All technical notes and suggestions have been fully implemented.

#### **Anonymous Referee #4**

[Comment:](#) The authors have provided two important components for the use of eight halogenated compounds as tracers of ocean circulation. They have reconstructed the atmospheric source functions and estimated their solubilities in water and seawater. These two items should enable reconstructions of the surface seawater concentrations of these compounds as a function of time. However the utility of these compounds as transient tracers depends more strongly on whether they are conservative in seawater, and whether they can be precisely and

accurately measured on relatively small volumes of seawater in a timely fashion. A cautionary tale can be found in the use of CFC-113 as a tracer in the ocean. A great deal of time and effort went into developing the analytical method and determining its solubility. However CFC-113 exhibits non-conservative behavior in seawater. This paper needs to be revised before publication. There are a few scientific issues to be addressed and numerous grammatical corrections.

**Response:** We thank the Reviewer for the comments. As far as we know from previous studies, HCFCs, HFCs and PFCs are relatively stable in seawater as the ocean partial lifetimes (partial atmospheric lifetimes with respect to oceanic uptake) of HCFCs and HFCs ranged from thousands to millions of years (Table 1) and PFCs have atmospheric lifetimes on the order of thousands of years and very low solubility in seawater. However, the ocean partial lifetimes were estimated without considering the biological degradation of most of these compounds in the ocean as they have not been investigated. We know from the experience with CFC-113 and CCl<sub>4</sub>, for instance, that the half time of tracers in seawater can be lower than initially predicted. This manuscript is already very long, and we focus on the source of the tracers, i.e. the atmospheric history and the solubility, in this paper. We will discuss measurements (techniques, constraints, possibilities etc.) and sinks in a follow up paper that we are preparing right now. For instance, we will discuss the stability of these compounds by comparing to measurements of SF<sub>6</sub> and CFC-12 from ocean samples collected during a few years from 3 different oceans.

Based on above discussion, “As shown in Table 1, the atmospheric lifetimes of HCFCs and HFCs with respect to hydrolysis in seawater are very long (Yvon-Lewis and Butler, 2002; Carpenter et al., 2014), ranging from thousands to millions of years, indicating that HCFCs and HFCs are relatively stable in the seawater. PFCs have atmospheric lifetimes on the order of thousands of years and very low solubilities in seawater.” have been added at page 4, line 19-22.

Scientific Issues:

**Comment:** Why not direct the reader to the AGAGE website (<https://agage.mit.edu/data/agage-data>) for the recent atmospheric measurements?

**Response:** P6, L6-7, “where historic and newest atmospheric measurements are reported” has been added behind “The data are available at the AGAGE website ([http://agage.eas.gatech.edu/data\\_archive/](http://agage.eas.gatech.edu/data_archive/))”.

**Comment:** Why were these eight compounds chosen out of the many compounds measured by AGAGE?

**Response:** The atmospheric mole fractions of CFCs, HCFCs, HFCs, PFCs, Halons, very shorted-lived compounds (-Cl, -Br, -I) are reported by the AGAGE website (<https://agage.mit.edu/data/agage-data>). CFCs have been studied for transient tracers since the 1980s. Halons are not suitable for tracer studies because their atmospheric mole fractions are decreasing obviously. The very shorted-lived compounds (-Cl, -Br, -I) are also not proper to be alternative tracers because their lifetimes are too short and they are not stable in seawater apparently. Thus HCFCs, HFCs and PFCs are chosen as the potential transient tracers. Besides, the atmospheric mole fractions of most HCFCs, HFCs and PFCs are increasing in the atmosphere.

For HCFCs, the atmospheric mole fractions of only HCFC-22, HCFC-141b and HCFC-142b are reported. For HFCs, HFC-134a is the most abundant HFC in the atmosphere. The trends of atmospheric mole fractions of HFC-125 and HFC-32 are different from other HFCs. The lifetime of HFC-125 (31 years) is longer than HFC-32 (4.9 years) in the atmosphere. HFC-23 is chosen because it has a relatively long lifetime in the atmosphere (228 years). For PFCs, they have very long lifetimes in the atmosphere and are very stable in seawater. The concentrations of PFCs are not easy to be detected considering their low solubility in seawater. Therefore, only PFC-14 and PFC-116 with relatively high atmospheric mole fractions are chosen to be studied.

**Comment:** The authors provide late winter atmospheric concentrations for these compounds. Are these values much different than a linear interpolation between the mid-year values? Is there a systematic offset that makes it important to include the NH Feb and SH Aug concentrations?

**Response:** The annual means were calculated by averaging the monthly means of the corresponding 12 months. The JFM and JAS means are obtained by averaging the monthly means of January, February and March and the monthly means of July, August and September of the same year. The median of relative standard deviation (RSD) for JFM between calculated means and linear interpolated ones are 0.15%, 0.59%, 0.20%, 0.47%, 1.96 %, 0.20%, 0.006% and 0.06% for HCFC-22, HCFC-141b, HCFC-142b, HFC-134a, HFC-125, HFC-23, PFC-14 and PFC-116. The median of RSD for JAS between calculated means and linear interpolated ones are 0.22%, 0.44%, 0.05%, 0.40%, 1.03%, 0.05%, 0.002% and 0.03% for HCFC-22, HCFC-141b, HCFC-142b, HFC-134a, HFC-125, HFC-23, PFC-14 and PFC-116. These values are not much different from a linear interpolation between the annual means, but these calculated values are more precise than the interpolated ones.

**Comment:** Most of the use of transient tracers is to study the ventilation of waters colder than 10 °C. However the measured freshwater solubility presented in this manuscript do not constrain the solubility curves at temperatures colder than 298 K where the temperature dependence of the solubility becomes significant.

**Response:** As shown in Table 5, the measured freshwater solubility presented in this manuscript constrain the solubility curves at temperatures 5-80 °C for HCFC-22, HCFC-141b, HCFC-142b, HFC-134a; 10-70 °C for HFC-125; 5-75 °C for HFC-23; 0-55 °C for PFC-14; 5-55 °C for PFC-116 and 0-75 °C for CFC-12. Therefore, except HFC-125 and PFC-116, the measured freshwater solubility of other compounds constrains the solubility curves at temperatures colder than 10 °C. Moreover, the measured freshwater solubility of HFC-125 and PFC-116 also constrain the solubility curves at temperatures between 10 °C and 25 °C.

Editorial Comments:

**Comment:** P2,L10 – CFC concentrations are not “variables”

**Response:** It has been changed to “indices”.

**Comment:** P2, L41 – Define MOZART

**Response:** “MOZART model” has changed to “*the Model for OZone And Related chemical Tracers (MOZART)*”.

**Comment:** P3, L29 – Is it important that HFC-125 is the 5th most abundant HFC? It makes me wonder why the 2nd through 4th most abundant HFCs are not considered by the authors.

**Response:** It is not important that HFC-125 is the 5<sup>th</sup> (changed to third after re-check) most abundant HFC. The reason why HFC-125 is chosen is that the trends of atmospheric mole fractions of HFC-125 and HFC-32 are different from other HFCs and the lifetime of HFC-125 (31 years) is longer than HFC-32 (4.9 years) in the atmosphere.

**Comment:** P4, L31 – The atmospheric growth rate can be reversed – not the concentrations

**Response:** “reverse” has changed to “decline”.

**Comment:** P4, L40 – intercalibrated rather than consistent?

**Response:** It is “consistent”.

**Comment:** P6, L10 – “see studies”?

**Response:** It has been changed to “see Prinn et al. (2018a)”.

Comment: P6, L18 – be more specific than America

Response: “Northern Hemisphere (NH) samples used for this paper were filled during background conditions mostly at Trinidad Head, but also at La Jolla, California, Cape Meares, Oregon (courtesy of the Oregon Graduate Centre via CSIRO, Aspendale, and the Norwegian Institute for Air Research, Oslo, Norway), and Point Barrow, Alaska (courtesy of Robert Rhew, University of California, Berkeley)” has been added to replace “America” in P6, L31-34.

Comment: P6, L21 – all data for HFC134a are first reported for HFC134a?

Response: AGAGE HFC-134a air archive data are reported here for the first time.

Comment: P7, L34 – “by in”

Response: “in” has been deleted.

Comment: P9, EQN1 – csapsGCV not defined

Response: “csapsGCV” has been deleted.

Comment: P10, EQN8 – D,E,F not defined

Response: Eq. (8) is the equation of state of seawater. We decide to delete it in the revised manuscript and only cite papers because the equation can be found in the oceanographic textbook. For more detail, see Millero and Poisson (1981).

$$\rho = \rho_0 + DS + ES^{3/2} + FS \quad (8)$$

Here  $\rho$  is the density of seawater in  $\text{kg m}^{-3}$ , from 0 to 40 °C and from 0.5 to 43 salinity ( $S$ ), have been used to determine a new 1-atm equation of state for seawater.

$$D = 8.24493 \times 10^{-1} - 4.0899 \times 10^{-3}t + 7.6438 \times 10^{-5}t^2 - 8.2467 \times 10^{-7}t^3 + 5.3875 \times 10^{-9}t^4 \quad (9)$$

$$E = -5.72466 \times 10^{-3} + 1.0227 \times 10^{-4}t - 1.6546 \times 10^{-6}t^2 \quad (10)$$

$$F = 4.8314 \times 10^{-4} \quad (11)$$

And  $\rho_0$  is the density of water (Bigg, 1967).

$$\rho_0 = 999.842594 + 6.793952 \times 10^{-2}t - 9.095290 \times 10^{-3}t^2 + 1.001685 \times 10^{-4}t^3 - 1.120083 \times 10^{-6}t^4 + 6.536336 \times 10^{-9}t^5 \quad (12)$$

where  $t$  is the temperature in degree Celsius (°C).

Comment: P10, L14 – “some properties”?

Response: Abraham (1993) presented a paragraph as “The dependent variable  $\log SP$  refers to some property of a series of solutes in a fixed phase (or phases) Thus  $SP$  could be  $L$ , the gas-liquid partition coefficient for a series of solutes in a given liquid or it could be  $P$ , the partition coefficient for a series of solutes between water and, say, octanol. In the case of biological properties, where  $SP$  can be some biological response as an  $LC_{50}$ , equations 13 and 14 then represent two new families of quantitative structure-activity relationships (QSARs).”

It should be “some property”. The “some property” could be the gas-liquid partition coefficient, the liquid-liquid partition coefficient and  $LC_{50}$  etc. Considering the comments from Reviewer #1, we revised the text to be “In these equations, the dependent variable  $\log SP$  is some property of a series of solutes in a given system. Therefore,  $SP$  could be partition coefficient,  $P$ , for a series of solutes in a given water-solvent system in Eq. (9), or  $L$ , for a series of solutes in a given gas-solvent system in Eq. (10).” at P12, L1-3.

Comment: P10, L25 – There is no  $V_c$  in the equations

Response: Considering the comments from Reviewer #1, we revised the text. Please see Sect. 2.7.2 in the revised manuscript.

Comment: P11, L13 – Use approximately when dropping significant figures

**Response:** *“The salt concentration in seawater is equivalent to 0.6 M NaCl”* has been changed to *“The salt concentration in seawater is approximately equivalent to 0.6 M NaCl”*.

**Comment:** P11, L16 – “so as to”?

**Response:** “so as to” has been changed to “to”.

**Comment:** P11, L30 – Note that CGW model method does not provide a method for estimating  $L_0$

**Response:** When the salinity ( $S$ ) is zero, the CGW model provides a method for estimating freshwater solubility ( $L_0$ ).

**Comment:** P12, L2 – Methods do not think

**Response:** *“Method II thinks more about the physical properties of compounds.”* has been changed to *“Consideration of the physical properties of compounds is more important in Method II”* at P13, L34-35.

**Comment:** P12, L18 – A better description of the ventilation process is needed (e.g. the mixed layer deepens...)

**Response:** *“During this process, the mixed layer deepens and older water (usually with lower transient tracer mole fractions) is brought in contact with the atmosphere. The mixed layer is gaining density and tends to be transported towards the ocean interior through diffusive, advective and/or convective processes. This water then carries with it a signature of the atmospheric mole fraction, pending the saturation state of the water as it leaves the surface layer. For tracers with rapidly increasing atmospheric mole fractions and for deep mixed layers under saturation of the tracers has frequently been reported (e.g. Tanhua et al. (2008b))”* is added at P14, L10-14 in Sect. 3.1.

**Comment:** P13, L4 – Curves and symbols in the upper panels of many figures are difficult to distinguish.

**Response:** Fig. 2a-9a were moved to the Supplement and renamed as Fig. S1 (a-h). Fig. S1 (ai-hi) show the original data and estimated annual means. Fig. S1 (aii-hii) shows the enlarged views of Fig. S1 (ai-hi) for the recent 5-6 years.

**Comment:** P13, L14 – “stable” is not the correct word

**Response:** *“This initial increase and then stable in the growth rate of HCFC-22 coincide with the large production and consumption reported for between the 1950s and 1990s (Fig. 1) and a freeze of production magnitudes in the developed countries in 1996.”* has been changed to

*“Growth rates for HCFC-22 rose steadily until 1990, followed by a slight decrease, which coincides with the large production and consumption reported between the 1950s and 1990s (Fig. 1) and a freeze of production magnitudes in the developed countries in 1996.”* at P14, L36-38.

**Comment:** P13, L36 – As written “they” refers to the interhemispheric gradients

**Response:** No. “They” is “The annual growth rates”. This sentence has been deleted.

**Comment:** P14, L13 – Bimodal has a specific meaning, choose a more appropriate word for describing this curve.

**Response:** This sentence has been deleted.

**Comment:** P14, L15 – “other one” implies a second plateau.

**Response:** Yes. The growth rates show a double-peak distribution pattern. The first plateau ..., the growth rates of the other one ....

In order not to misunderstand, this sentence has been deleted.

**Comment:** P14, L17 – verb missing

**Response:** “are” has been added.

**Comment:** P15, L8 – How do the authors distinguish “exponential” from “quadratic” from “linear”?

Response: The three ones are distinguished by curve fit. P values were compared. The higher P value, the better fit.

Comment: P15, L13 – missing verb

Response: “are” has been added.

Comment: P16, L12-13 – sentence needs rewritten

Response: This sentence has been deleted.

Comment: P16, L22 – What does “annual growth rates exhibit a normal distribution” mean?

Response: “*annual growth rates exhibit a normal distribution*” has been changed to “*annual growth rates exhibit the shape of Gaussian distribution*” at P17, L19.

Comment: P17, L10 – “accelerated phase out” not correct

Response: “*accelerated phase out*” has been changed to “*phased-out sooner than originally mandated*” at P18, L5.

Comment: P17, L11 – “bank of HCFC-22 exists” ?

Response: “*bank*” has been changed to “*emission source*” at P18, L9-10.

Comment: P17, L29 – “even out” is not a noun

Response: In order not to misunderstand, this sentence has been deleted.

Comment: P18, L18 – Warner and Weiss did use a salting out coefficient as defined in Eqn 6

Response: No, they didn’t. Eq. (6) is from the method of Deeds et al. (2008), not from the method of Warner and Weiss (1985). Only Eq. (3) is from the method of Warner and Weiss (1985).

Comment: P18, L24 – Fitting the solubility at temperatures between 25-65 C is not an important finding

Response: Sorry to wrote it wrong. It has been changed to 0-40 °C.

Comment: P18, L29 and L31 – What happened to the factor of  $10^{15}$ ?

Response: In the study of Warner and Weiss (1985), the average of  $K_S$  is  $0.229 \pm (1.41 \cdot 10^{-15}) \text{ L g}^{-1}$  at 298.15 K when the salinity is in the range of 0-40. It means that  $K_S$  is independent of salinity.

Comment: P21, L2 – the Cl radical is the culprit, not the prime suspect

Response: “prime suspect” has been changed to “culprit”. In order to shorten the paper, we delete most of sentences in this paragraph.

“TECHNICAL CORRECTIONS”

Comment:

P14, L21 – “rapid” instead of “raid”

P14, L31 – “are” not “were”

P15, L10 – larger instead of “large”

P15, L35 – “reduced”

P21, L10 – Use e.g. before presenting a subset of the manuscripts that use the CFCs as ocean tracers

Response: All technical notes and suggestions have been fully implemented.

## **Additional Corrections**

### For tables:

Original Table 2 (collected data) was moved to the Supplement (Table S1) to shorten the manuscript.

Original Table 3 (primary scales) was renamed to be the new Table 2.

New Table 3 was added to sort the coefficients and descriptors of partition coefficients for Sect. 2.7.2.

Position of Table 4 and Table 5 was exchanged.

Original Table S1 (atmospheric mole fractions) in the Supplement was renamed as Table S2.

Original Table S2 was renamed to be Table S4 (comparison of solubility calculated by  $V$ ,  $V_c$  and  $\log L^{16}$ ).

Original Table S4 was renamed to be Table S5 (Ostwald solubility functions estimated by Method II).

### For figures:

To response one comment from Anonymous Referee #4, Fig. 2a-9a were moved to the Supplement and renamed as Fig. S1 (a-h). Fig. S1 (ai-hi) show the original data and estimated annual means. Fig. S1 (aii-hii) shows the enlarged views of Fig. S1 (ai-hi) for the recent 5-6 years.

Original Figure 2b-9b was renamed as Fig. 2 (a-h).

Original Figure 10-12 was renamed as Fig. 3-5.

Original Figure S1-S9 was renamed as Fig. S2 (a-i).

Original Figure S10 was renamed as Fig. S3.

Content of Tables and Figures for the Supplement was added.

### For manuscript:

The titles of sections have been changed as follows:

1 Introduction
2 Data and Methods
2.1 AGAGE in situ Measurements and Instrumentation
2.2 AGAGE archived air
2.3 AGAGE firm air
2.4 NOAA flask measurements
2.5 NOAA archived air
2.6 UEA archived air
2.7 Models
2.8 Calibration scale
2.9 Smoothing spline fit and uncertainty
2.10 Seawater solubility estimation method
2.10.1 Method I: the CGW model
2.10.2 Method II: the pp-LFER model
2.10.3 Combined Method: combined the CGW model and the pp-LFER model
3 Results and Discussion
3.1 Atmospheric histories and growth rates
3.1.1 HCFC-22
3.1.2 HCFC-141b
3.1.3 HCFC-142b
3.1.4 HFC-134a
3.1.5 HFC-125
3.1.6 HFC-23
3.1.7 PFC-14
3.1.8 PFC-116
3.2 Growth Patterns
3.3 Solubility in seawater
3.4 Transient Tracer potential and comparison with CFC-12
4 Conclusions
Acknowledgments
References

Original sections titles

1 Introduction
1.1 Potential transient tracers
1.2 Production and ban histories
2 Data and Methods
2.1 Data from the AGAGE network
2.1.1 AGAGE in situ measurements and instrumentation
2.1.2 AGAGE measurements of CSIRO and SIO archived air
2.1.3 AGAGE measurements of CSIRO firm air
2.2 Data from the NOAA network
2.2.1 NOAA flask measurements
2.2.2 NOAA measurements of archived and shipborne air samples
2.2.3 NOAA measurements of firm air
2.3 Data from the UEA network
2.3.1 UEA archived air
2.4 Data from models
2.5 AGAGE, NOAA and UEA calibration scales
2.6 Hemispheric annual means and uncertainties estimation
2.7 Seawater solubility estimation method
2.7.1 Method I: the CGW model
2.7.2 Method II: the pp-LFER model
2.7.3 Combined Method: combined CGW model and pp-LFER model
3 Results and Discussion
3.1 Atmospheric histories and growth rates
3.1.1 HCFC-22
3.1.2 HCFC-141b
3.1.3 HCFC-142b
3.1.4 HFC-134a
3.1.5 HFC-125
3.1.6 HFC-23
3.1.7 PFC-14 (CF4)
3.1.8 PFC-116
3.2 Growth Patterns
3.3 Solubility in seawater
3.3.1 Solubility in freshwater
3.3.2 Salting-out coefficient
3.3.3 Solubility in seawater based on Combined Method
3.3.4 Comparison of solubility in seawater based on three methods
3.4 Transient Tracer potential and comparison with CFC-12
4 Conclusions
Acknowledgments

Revised sections titles

This work can be applied for more waters. *“Even though our intention is for application in oceanic research, the work described in this paper is potentially useful for tracer studies in a wide range of natural waters, including freshwater and saline lakes, and, for the more stable compounds, groundwaters.”* has been added at page 1, line 40-42.

The manuscript was shortened by deleted some background information in Introduction (Sect. 1), some very detailed description of atmospheric histories and growth rates of target compounds (Sect. 3.1), the last two paragraphs in Sect. 3.2, and most sentences in the first paragraph in Sect. 3.4 (background information of production and use history of CFC-12). The manuscript was checked and revised very carefully again. For detail, see following revised paper.

# Atmospheric Histories, Growth Rates and Solubilities in Seawater and other Natural Waters of the Potential Transient Tracers HCFC-22, HCFC-141b, HCFC-142b, HFC-134a, HFC-125, HFC-23, PFC-14 and PFC-116

Pingyang Li <sup>1</sup>, Jens Mühle <sup>2</sup>, Stephen A. Montzka <sup>3</sup>, David E. Oram <sup>4</sup>, Benjamin R. Miller <sup>3</sup>, Ray F. Weiss <sup>2</sup>, Paul J. Fraser <sup>5</sup> and Toste Tanhua <sup>1</sup>

<sup>1</sup>GEOMAR Helmholtz Centre for Ocean Research Kiel, Kiel, 24105, Germany

<sup>2</sup>Scripps Institution of Oceanography, University of California, San Diego, La Jolla, California, 92093, USA

<sup>3</sup>Earth System Research Laboratory, National Oceanic and Atmospheric Administration, Boulder, Colorado, 80305, USA

<sup>4</sup>National Centre for Atmospheric Science, Centre for Ocean and Atmospheric Sciences, School of Environmental Sciences, University of East Anglia, Norwich, NR4 7TJ, UK

<sup>5</sup>Climate Science Centre, Commonwealth Scientific and Industrial Research Organization Oceans and Atmosphere, Aspendale, Victoria, 3195, Australia

Correspondence to: Toste Tanhua, (ttanhua@geomar.de)

**Abstract.** We present consistent annual mean atmospheric histories and growth rates for the mainly anthropogenic halogenated compounds HCFC-22, HCFC-141b, HCFC-142b, HFC-134a, HFC-125, HFC-23, PFC-14 and PFC-116, all potentially useful oceanic transient tracers (tracers of water transport within the ocean), for the Northern and Southern Hemisphere with the aim of providing input histories of these compounds for the equilibrium between the atmosphere and surface ocean. We use observations of these halogenated compounds made by the Advanced Global Atmospheric Gases Experiment (AGAGE), the Scripps Institution of Oceanography (SIO), the Commonwealth Scientific and Industrial Research Organization (CSIRO), the National Oceanic and Atmospheric Administration (NOAA), and the University of East Anglia (UEA). Prior to the direct observational record, we use archived air measurements, firn air measurements and published model calculations to estimate the atmospheric mole fraction histories. The results show that the atmospheric mole fractions for each species, except HCFC-141b and HCFC-142b, have been increasing since they were initially produced. Recently, the atmospheric growth rates are decreasing for the HCFCs (HCFC-22, HCFC-141b and HCFC-142b), are increasing for the HFCs (HFC-134a, HFC-125, HFC-23), and are stable with small fluctuation for the PFCs (PFC-14 and PFC-116) investigated here. The atmospheric histories (source functions) and natural background mole fractions show that HCFC-22, -141b and -142b and HFC-134a, -125 and -23 have the potential to be oceanic transient tracers for the next few decades only because of the recently imposed bans on production and consumption. When the atmospheric histories of the compounds are not monotonically changing, the equilibrium atmospheric mole fraction (and ultimately the age associated with that mole fraction) calculated from their concentration in the ocean are not unique, reducing their potential as transient tracer. Moreover, HFCs have potential to be oceanic transient tracers for a longer period in the future than HCFCs as the growth rates of HFCs are increasing and those of HCFCs are decreasing in the background atmosphere. PFC-14 and PFC-116, however, have the potential to be the tracers for longer periods into the future due to their extremely long lifetimes, steady atmospheric growth rates and no explicit ban on their emissions. In this work, we also derive solubility functions for HCFC-22, HCFC-141b, HCFC-142b, HFC-134a, HFC-125, HFC-23, PFC-14 and PFC-116 in water and seawater to facilitate their use as oceanic transient tracers. These functions are based on the Clark-Glew-Weiss (CGW) water solubility functions fit and salting-out coefficients estimated by the poly-parameter linear free energy relationships (pp-LFERs). Here we also provide three methods of seawater solubility estimation for more compounds. Even though our intention is for application in oceanic research, the work described in this paper is potentially useful for tracer studies in a wide range of natural waters, including freshwater and saline lakes, and, for the more stable compounds, groundwaters.

Deleted: Global Annual Mean

Deleted: Solubility Estimations

Deleted: Halogenated Compounds

Deleted: <sup>5</sup>

Deleted: , San Diego

Deleted: nited States

Deleted: <sup>5</sup>Centre for Ocean and Atmospheric Sciences, School of Environmental Sciences, University of East Anglia, Norwich, NR4 7TJ, UK

Deleted: Pingyang Li

Deleted: pli

Deleted: for

Deleted: here available w

Deleted: utilise

Deleted: and

Deleted: estimated the atmospheric history concentrations from other sources such as

Deleted: ir

Deleted: values

Deleted: HCFCs (

Deleted: HCFC

Deleted: HCFC

Deleted: )

Deleted: HFCs (

Deleted: HFC

Deleted: HFC

Deleted: )

Deleted: concentration

Deleted: s

Deleted: concentration

Deleted: thanks

## 1 Introduction

Oceanic and natural waters transient tracers have time-varying sources and/or sinks. Chlorofluorocarbons (CFCs) have been used traditionally as oceanographic transient tracers because of their continuously increasing atmospheric mole fractions until some years ago. They are powerful tools in oceanography where they are used to, for instance, deduce transport times, estimate mixing rates between water masses, study formation rates of new water masses, and determine the anthropogenic carbon ( $C_{\text{ant}}$ ) content of seawater (Weiss et al., 1985; Waugh et al., 2006; Fine, 2011; Schneider et al., 2012; Stöven et al., 2016). The production and consumption of CFCs have been phased-out as a consequence of the implementation of the Montreal Protocol (MP) on Substances that Deplete the Ozone Layer (first in developed nations by 1996, followed by developing nations by 2010) designed to halt the degradation of the Earth's protective ozone layer (Fig. 1). The atmospheric mole fractions of the major CFCs have been decreasing since the mid-1990s/mid-2000s (Carpenter et al., 2014; Bullister, 2015), and although CFCs are valuable indices to quantify deep water transport, the use of CFCs as oceanographic transient tracers has become more difficult for recently ventilated water masses. During recent decades sulfur hexafluoride ( $\text{SF}_6$ ) has been added to the suite of transient tracers measured in the ocean (Tanhua et al., 2004; Bullister et al., 2006). Its atmospheric mole fractions are still increasing and its atmospheric distribution is measured widely. However,  $\text{SF}_6$  is also facing restrictions; for example, in Europe it has been banned for release as a tracer gas and in all applications except high-voltage switchgear since 1 January 2006 (Fig. 1). Since a combination of transient tracers is needed to constrain ventilation (Waugh et al., 2002; Stöven et al., 2015), it is necessary to explore other transient tracers with positive growth rates for the study of mixing and transport processes in the oceans and in other natural waters.

### 1.1 Potential transient tracers

Generally, several requirements for a useful oceanic transient tracer can be defined: the tracer should have a well-established, transient, source function (or well-defined decay function); have a low or well-known natural background; be conservative (not produced or destroyed) in the marine environment and be measured relatively inexpensively, accurately, and rapidly. Potential candidates as transient tracers that fulfill at least some of the requirements listed above include hydrochlorofluorocarbons (HCFCs) such as HCFC-22, HCFC-141b and HCFC-142b, hydrofluorocarbons (HFCs) such as HFC-134a, HFC-125 and HFC-23 and perfluorocarbons (PFCs) such as PFC-14 and PFC-116. As a first step in evaluating the usefulness of these compounds as oceanic transient tracers, we synthesize their atmospheric mole fraction histories, and review their solubilities. An upcoming work will evaluate the in-field data of these compounds.

**HCFC-22:** Chlorodifluoromethane ( $\text{CHClF}_2$ ) is the most abundant HCFC in the global atmosphere. It was first synthesized in 1928 and commercial use started in 1936 (Calm and Domanski, 2004). It has been used dispersedly in domestic and commercial refrigeration, as a spray-can propellant, and in extruded polystyrene foam industries (McCulloch et al., 2003; Jacobson, 2012), and non-dispersedly as the feedstock in fluoropolymer production (Miller et al., 2010). HCFC-22 was first measured in the atmosphere in 1979 (Rasmussen et al., 1980), a pronounced increase of its abundance in the 1990s was found in both hemispheres as HCFC-22 became an interim replacement for CFC-12 since the late 1980s (Xiang et al., 2014). There are no known natural emission sources for HCFC-22 (Saikawa et al., 2012). A considerable amount of literature has been published on the atmospheric histories of HCFC-22. Montzka et al. (1993) presented the NOAA network measurements and historic mole fractions from a 2-box model for HCFC-22 from 1980 to 1993, and these have since been updated and augmented with measurements from Antarctic firm air and box models to construct an atmospheric history and emissions for HCFC-22 from 1944 to 2014 (Montzka et al., 2010a; 2015). Sturrock et al. (2002) presented CSIRO HCFC-22 data from 1940 to 2000 based on analysis of Antarctic firm air samples using the AGAGE instrumentation. In 2012, Saikawa et al. (2012) reported observations and archived air measurements from multiple networks, combined with the Model for Ozone And Related chemical Tracers (MOZART), to present the atmospheric mole fractions for HCFC-22 from 1995 to 2009.

- Deleted: The o
- Deleted: are chemical tracers with
- Deleted: a
- Deleted:
- Deleted: as
- Deleted: concentration
- Deleted: has
- Deleted: phased
- Deleted: from
- Deleted: stop
- Deleted: the
- Deleted: earth's
- Deleted: ir
- Deleted: variables
- Deleted: is
- Deleted: levels
- Deleted: '
- Deleted: the most
- Deleted: of all the potential tracers in (...)
- Deleted: But
- Deleted: in Europe
- Deleted: understanding
- Deleted: ¶
- Formatted: English (U.K.)
- Deleted: concentration
- Deleted: in seawater
- Deleted: of
- Deleted: utility
- Deleted: concentration
- Deleted: y
- Deleted: y in this study
- Deleted: discovered
- Deleted: but
- Deleted: little used until after the Wor (...)
- Deleted: ization
- Deleted: as
- Deleted: ,
- Deleted: because
- Deleted: In 1993,
- Deleted: scattered
- Deleted: model results of
- Deleted: an
- Deleted: air archive
- Deleted: build
- Deleted: 55
- Deleted: In 1998, Miller et al. (1998) (...)
- Deleted: have
- Deleted: on updated AGAGE and NOAA
- Deleted: model

**HCFC-141b:** 1,1-dichloro-1-fluoroethane ( $\text{CH}_2\text{CCl}_2\text{F}$ ) has been widely used as a foam-blowing agent in rigid polyurethane foams for insulation purposes and in integral skin foams as a replacement for CFC-11. It was also employed as a solvent for lubricants, coatings and cleaning fluids for aircraft maintenance and electrical equipment as a replacement for CFC-113 (Derwent et al., 2007). The industrial production and use of HCFC-141b have greatly increased since the early 1990s, as did its global mole fractions and emissions (Oram et al., 1995; Sturrock et al., 2002; Montzka et al., 2015; Prinn et al., 2018a).

**HCFC-142b:** 1-chloro-1,1-difluoroethane ( $\text{CH}_3\text{CClF}_2$ ) has largely been emitted from extruded polystyrene board stock as a foam-blowing agent combined with small emissions from refrigeration applications as a replacement for CFC-12 (TEAP, 2003). Previous studies described measurements of HCFC-141b and HCFC-142b from the AGAGE network, UEA and CSIRO including measurements of the Cape Grim Air Archive (CGAA) and Antarctic firm air (Oram et al., 1995; Sturrock et al., 2002; Simmonds et al., 2017; Prinn et al., 2018a), NOAA flask and firm air measurements for both compounds have also been reported (Montzka et al., 1994; 2009; 2015).

**HFC-134a:** 1,1,1,2-tetrafluoroethane ( $\text{CH}_2\text{FCF}_3$ ) is the most abundant HFC in the Earth's atmosphere. It was first synthesized by Albert Henne in 1936 (Matsunaga, 2002). Extensive production and emission of HFC-134a began in the early 1990s. It was used as a preferred refrigerant in domestic, commercial and automotive air conditioning and refrigeration to replace CFC-12. It is also used to a lesser extent as foam blowing agent, cleaning solvent, fire suppressant, and propellant in metered-dose inhalers and aerosols (Simmonds et al., 2015; 2017). Continuous and substantially increasing atmospheric levels of HFC-134a were found over the past two decades (Xiang et al., 2014). A number of researchers have reported the atmospheric history of HFC-134a. The observational record of HFC-134a started from near-zero levels in the background atmosphere (Oram et al., 1996). In the same year, Montzka et al. (1996) reported initial measurements from the NOAA network for HFC-134a from the late 1980s to mid-1995, which have since been updated (Montzka et al., 2015). Simmonds et al. (1998) presented AGAGE observations for HFC-134a from 1994 to 1997, updated by O'Doherty et al. (2004) from 1998 to 2002, by Rigby et al. (2014) and by Prinn et al. (2018a) to recent times.

**HFC-125:** Pentafluoroethane ( $\text{CHF}_2\text{CF}_3$ ) is currently the third most abundant HFC. It is used primarily in refrigerant blends for commercial refrigeration applications, has a minor use in fire-fighting equipment as a replacement for halons. Atmospheric mole fractions of HFC-125 are also rising consistently as one of the substitutes of CFCs (O'Doherty et al., 2009; Rigby et al., 2014; Prinn et al., 2018a). In 2009, O'Doherty et al. (2009) reported *in situ* and archived air measurements from Mace Head and Cape Grim, combined with the AGAGE 2-D 12-box model results for HFC-125 from 1977 to 2009. In 2015, Montzka et al. (2015) reported results of flask measurements of HFC-125 spanning from 2007 to 2013.

**HFC-23:** Fluoroform or trifluoromethane ( $\text{CHF}_3$ ) is a by-product from the industrial production of HCFC-22. Historically it has been considered as waste and simply vented to the atmosphere, although process optimization and abatement can eliminate most or all emissions. HFC-23 was also used as a feedstock for Halon-1301 ( $\text{CBrF}_3$ ) production. Small amounts are reportedly used in semiconductor (plasma etching) fabrication, in very low-temperature refrigeration (dispersive), and in specialty fire suppressant systems (dispersive) (McCulloch and Lindley, 2007). HFC-23 was first reported in the background atmosphere by Oram et al. (1998) in samples dating back to 1978. It continued to increase in the atmosphere (Miller et al., 2010; Rigby et al., 2014; Simmonds et al., 2018) despite the voluntary and regulatory efforts in developed nations and abatement measures in developing nations financially-supported by the United Nations Framework Convention on Climate Change (UNFCC) Clean Development Mechanism (CDM) project. In the past three decades, a number of researchers have reported the atmospheric mole fractions of HFC-23. In 1998, Oram et al. (1998) reported measured and model-generated mole fractions of HFC-23 at Cape Grim from 1978 to 2005. Updated in situ AGAGE measurements and results from the AGAGE 2-D atmospheric 12-box chemical transport model for HFC-23 from 1978 to 2010 and from 1950 to 2016 have been presented by Miller et al. (2010) and Simmonds et al. (2018), respectively. A history derived from multiple firm air sample collections was also published in 2010 (Montzka et al., 2010a).

- Deleted:** of
- Deleted:** for motor vehicle dashboards, steering wheels and soles of shoes
- Deleted:** y
- Deleted:** has
- Deleted:** concentration
- Deleted:** have reported the atmospheric mole fractions of both HCFC-141b and HCFC-142b. In 2002, Sturrock et al. (2002) reported the observations and reconstructed records for HCFC-141b and HCFC-142b based on firm air samples collected in 1993 and in 1997-98 in the Antarctic. In 1995, Oram et al. (1995) published a paper in which they
- Deleted:** the concentrations
- Deleted:** in the Cape Grim a
- Deleted:** archive
- Deleted:** between 1978 and 1994
- Deleted:** The
- Deleted:** archived
- Deleted:** from NOAA were
- Deleted:** by
- Deleted:** He presented the measurements for HFC-134a at Cape Grim, Tasmania over the period of 1978-1995 and at Mace Head, Ireland between July 1994 and May 1995.
- Deleted:** In 1998,
- Deleted:** measurements
- Deleted:** recorded at Mace Head, Ireland
- Deleted:** October
- Deleted:** March
- Deleted:** . In 2004,
- Deleted:** showed the *in situ* AGAGE measurements made at Mace Head, Ireland and Cape Grim, Tasmania for HFC-134a
- Deleted:** In the same year, Culbertson et al. (2004) published a paper in which they described measurements of HFC-134a air archived at Cape Meares, Oregon, from 1978 to 1997, at Point Barrow, Alaska, from 1995 to 1998, and at Palmer Station, Antarctica, from 1991 to 1997.
- Deleted:** fifth
- Deleted:** (O'Doherty et al., 2009)
- Deleted:** measurements
- Deleted:** ,
- Deleted:**
- Deleted:** detect
- Deleted:** in 1978
- Deleted:** mandatory
- Deleted:** concentration
- Deleted:** over the period
- Deleted:** -
- Deleted:** In 2004, Culbertson et al. (2004) published a paper in which they described measurements of HFC-23 air archived at (...)
- Deleted:** -

**PFC-14:** Tetrafluoromethane or carbon tetrafluoride (CF<sub>4</sub>) is the most abundant perfluorocarbon (PFC) in the Earth's atmosphere and is one of the most long-lived tracer gases with an atmospheric lifetime of more than 50,000 years. The presence of carbon tetrafluoride in the atmosphere was first deduced by Gassmann (1974) from analysis of contaminant levels of PFC-14 in high-purity krypton samples. The first atmospheric measurements of PFC-14 were made by Rasmussen et al. (1979). It has a background atmospheric mole fraction due to its natural source from the rocks and soils, especially tectonic activity (Deeds et al., 2015). The pre-industrial level was 34.05 ± 0.33 ppt for PFC-14 (Trudinger et al., 2016). The primary anthropogenic sources of PFC-14 are aluminum production and the semiconductor industry (Khalil et al., 2003; Mühle et al., 2010; Fraser et al., 2013) and perhaps the production of rare Earth elements. Consequently, atmospheric mole fractions have approximately doubled since the early 20<sup>th</sup> century (Mühle et al., 2010; Trudinger et al., 2016; Prinn et al., 2018a).

**PFC-116:** Hexafluoroethane (C<sub>2</sub>F<sub>6</sub>) is another long-lived tracer gas with an atmospheric lifetime of at least 10,000 yr. The tropospheric abundance of PFC-116 was first determined by Penkett et al. (1981). It has a small natural abundance (Mühle et al., 2010; Trudinger et al., 2016); the pre-industrial level having been estimated to be 0.002 ppt (Trudinger et al., 2016). Like CF<sub>4</sub> it is also emitted as a by-product of aluminum production (Fraser et al., 2013) and during semiconductor manufacturing.

## 1.2 Production and ban histories

The major atmospheric degradation pathway of HCFCs and HFCs is through reaction with hydroxyl radicals (OH) in the troposphere (Montzka et al., 2010b). Combustion in thermal power stations has been pointed out as a tropospheric sink of PFCs (Cicerone, 1979; Ravishankara et al., 1993; Morris et al., 1995). The atmospheric lifetimes, ocean partial lifetimes, the Ozone Depleting Potentials (ODP), and the Global Warming Potentials (GWP) for HCFC-22, HCFC-141b, HCFC-142b, HFC-23, HFC-134a, HFC-125, PFC-14 and PFC-116 are listed in the Table 1. As shown in Table 1, the atmospheric lifetimes of HCFCs and HFCs with respect to hydrolysis in seawater are very long (Yvon-Lewis and Butler, 2002; Carpenter et al., 2014), ranging from thousands to millions of years, indicating that HCFCs and HFCs are relatively stable in the seawater. PFCs have atmospheric lifetimes on the order of thousands of years and very low solubilities in seawater. The production and use histories of CFC-12, SF<sub>6</sub>, HCFCs, HFCs, and PFCs are plotted in Fig. 1. HCFCs have been regulated with the aim to cease production and consumption by 2020 for non-Article 5 (developed) countries and 2030 for Article 5 (developing) countries (although this only covers dispersive applications) and phase-out beginning with a freeze in 1996 for developed nations and in 2013 for developing nations under the MP and its more recent amendments. Because of the high GWP of HFCs, 197 countries recently committed to cutting the production and consumption of HFCs by more than 80% over the next 30 years under the Kigali amendment of the MP, although not all of these countries have ratified this Amendment. The reductions in HFC production and consumption are based on GWP-weighted quantities. Developed countries that have ratified the Amendment have agreed to reduce HFC consumption beginning in 2019. Most developing countries will freeze consumption in 2024, some in 2028. This measure most likely will slow down HFC growth rates, leading eventually to a decline in their atmospheric mole fraction, similar to what is observed for the CFCs.

In order to explore if these halogenated compounds can be used as transient ocean tracers, their atmospheric history (source functions) and natural background should be established. Previous work has reconstructed annually-averaged atmospheric mole fraction histories for some trace gases for use in tracer oceanographic applications. For example, Walker et al. (2000) reported annual mean atmospheric mole fractions for CFC-11, CFC-12, CFC-113, and CCl<sub>4</sub> for the period 1910-1998 and updated the data to 2008 at the website (<http://bluemoon.ucsd.edu/pub/cfchist/>). On the basis of Walker's work, Bullister (2015) reported atmospheric histories for CFC-11, CFC-12, CFC-113, CCl<sub>4</sub>, SF<sub>6</sub>, and N<sub>2</sub>O for the period 1765-2015. Previous work related to our target compounds, have mainly focussed on the atmospheric history over specific periods, often at a high temporal resolution. We have listed these works above. For our purposes, we are interested in a consistent record of the full atmospheric history at annual temporal resolution. As Trudinger et al. (2016) presented the consistent atmospheric histo-

Deleted: earth's

Deleted: concentration

Deleted: concentration

Deleted: has

Deleted: A more gradual increase in emission for PFC-116 was found in 1900.

Deleted: ¶

Deleted: The only identified atmospheric loss pathway of PFCs is through reaction with atmospheric ions

Deleted: ,

Deleted: and atmospheric lifetimes

Deleted: and

Deleted:

Deleted:

Deleted: will

Deleted: and

Deleted: reverse

Deleted: concentration

Deleted: of HFCs

Deleted: now

Deleted: values

Deleted: concentration

Deleted: r

Deleted: concentrated

Deleted: for a

ries of PFC-14 and PFC-116 from 1900 to 2014, we only study the growth rates for these two compounds and evaluate their utility as oceanic transient tracers.

In this study, drawing on previous literature and published data, we present atmospheric mole fractions (JFM means, annual means and JAS means) and growth rates for HCFC-22, HCFC-141b, HCFC-142b, HFC-134a, HFC-125, HFC-23, PFC-14 and PFC-116 for both the Northern (NH) and Southern Hemisphere (SH). The JFM means (the average of monthly means in January, February and March) and JAS means (the average of monthly means in July, August and September) are chosen to coincide with the coldest part of the year in the NH and SH, respectively, i.e. the time of (deep) water mass formation when ambient trace gases are carried from the surface to the interior ocean. The reconstructed atmospheric histories have been compiled from a combination of air measurements and model calculations. In order to provide a comprehensive and consistent view of halogenated compounds atmospheric distribution and changes over time, ambient air measurements published

by the Advanced Global Atmospheric Gases Experiment (AGAGE), the Scripps Institution of Oceanography (SIO), the Commonwealth Scientific and Industrial Research Organization (CSIRO), the National Oceanic and Atmospheric Administration (NOAA) and University of East Anglia (UEA) are considered in this study. The calibration scale differences of these networks in the form of scale conversion factors are determined. SIO and CSIRO data are reported on AGAGE scales. NOAA and UEA data are converted to AGAGE scales by these conversion factors. For years prior to atmospheric observations, the reconstructed dry mole fractions for each species were provided by a combination of atmospheric models, firm air measurements and the analysis of archived air samples. The aim of this work is to synthesize existing data and model results into one consistent data product of atmospheric history with annual values useful for ocean tracer applications; it is not intended to replace more detailed atmospheric studies. All reported values in this study are dry air mole fractions. In a similar work, Meinshausen et al. (2017) provided consolidated datasets of historical atmospheric mole fractions of 43 Greenhouse Gases (GHGs). Compared with this earlier study, the differences and added value of this study is that we: 1) incorporated UEA data not included in the Meinshausen et al. (2017) study, 2) report data on a common calibration scale, (AGAGE) by converting NOAA and UEA data to AGAGE scales, 3) estimated annual means based on baseline data with local pollution events removed, 4) estimated the propagated uncertainties based on the original standard deviations of monthly means or data points, 5) used a different method for data fitting, and 6) presented the atmospheric histories for winter (JFM means in the NH and JAS means in the SH) which is especially useful for oceanic transient tracers studies.

In addition, we explore whether these compounds can be used as oceanic transient tracers, by reporting on the solubility characteristics of each of the gases. There are no literature estimates that directly provide solubility functions of all target compounds in seawater, only very limited studies (with several data points) on the solubility of these compounds in seawater have been reported. Scharlin and Battino (1995) published four solubility data points in the temperature range 15-30 °C and a salinity of 35.086 of PFC-14 in seawater. In the present analysis, the water and seawater solubility functions of HCFC-22, HCFC-141b, HCFC-142b, HFC-134a, HFC-125, HFC-23, PFC-14 and PFC-116 are derived by the Combined Method based on the combination of the Clark-Glew-Weiss (CGW) fit to estimate their water solubility function and the poly-parameter linear free energy relationships (pp-LFERs) to estimate their salting-out coefficients. Three concluded methods (the Revised Method II only based on the pp-LFERs, the Combined Method and the Experimental Method) on seawater solubility estimation are also provided for more compounds. Although the atmospheric histories and solubility functions in water and seawater of target compounds are intended for oceanic research, the work described in this paper is potentially useful for studying a range of natural waters, including freshwater, saline lakes and groundwaters.

ries of PFC-14 and PFC-116 from 1900 to 2014, we only study the growth rates for these two compounds and evaluate their utility as oceanic transient tracers.

Deleted: 2015

Deleted: to be

Deleted: annual mean

Deleted: mid-February, mid-year and mid-August

Deleted:

Deleted: (SH)

Deleted: mid-February

Deleted: mid-August

Deleted: is

Deleted: concentration

Deleted: A

Deleted: all

Deleted: reported through March or July 2017

Deleted: concentrations (

Deleted: )

Deleted: add

Deleted: the data from the

Deleted: used the same

Deleted: calibration scales

Deleted: the

Deleted: 3

Deleted: 4

Deleted: 5

Deleted: mid-February

Deleted: mid-August

Deleted: that

Deleted: if

Deleted: for

Deleted: were

Deleted: g kg<sup>-1</sup>

## 2 Data and Methods

### 2.1 Data from the AGAGE network

#### 2.1.1 AGAGE *in situ* measurements and instrumentation

*In situ* atmospheric measurements have been made by the Advanced Global Atmospheric Gases Experiment (AGAGE) (Prinn et al., 2000; O'Doherty et al., 2004; 2009; Miller et al., 2010; Mühle et al., 2010; Prinn et al., 2018a; 2018b). The data are available at the AGAGE website ([http://agage.eas.gatech.edu/data\\_archive/](http://agage.eas.gatech.edu/data_archive/)) where historic and newest atmospheric measurements are reported. AGAGE provides measurements of more than 40 compounds, whereas we focus only on HCFC-22, HCFC-141b, HCFC-142b, HFC-134a, HFC-125, HFC-23, PFC-14 and PFC-116 (Table S1). There are more than 10 AGAGE and affiliated stations globally, mostly located at coastal or mountain sites. Here we exclude all AGAGE stations at tropical latitudes which are periodically subjected to air masses originating in the other hemisphere (Prinn et al., 1992; 2000; Walker et al., 2000). Observations at the AGAGE remote stations Mace Head, Ireland (MHD, 53°N, 10°W) and Trinidad Head, California (THD, 41°N, 124°W) were assumed to represent 30-90°N atmospheric mole fractions, whereas observations at Cape Grim, Tasmania (CGO, 41°S, 145°E) represent 30-90°S mole fractions. Small latitudinal gradients in the AGAGE Mace Head and Trinidad Head observations of different compounds are present but assumed to be of minor importance to this work. These stations, their locations and the date ranges of the samples used in this study are listed in Table S1. The “pollution-free” monthly mean atmospheric mole fractions and standard deviations for all target compounds are used in this study.

All ambient air measurements were carried out using two similar measurement technologies over time, based on the cryogenic pre-mole fraction with gas chromatography separation and mass spectrometry detection (GC-MS) system. The initial used instrument was the ADS (adsorption-desorption system)-GC-MS, but in the early/mid-2000 this was replaced by the Medusa-GC-MS with a doubled sampling frequency, upgraded sample pre-mole fraction methodologies, extended compound selection, and improved measurement precisions. For more information on the instrumentation and the working standards, see studies (Simmonds et al., 1995; Miller et al., 2008; Arnold et al., 2012; Prinn et al., 2018a). For the measurement precision, see Prinn et al. (2018a).

#### 2.1.2 AGAGE measurements of CSIRO and SIO archived air

To extend the available mole fraction records back in time, NH and SH air archive samples collected by CSIRO and SIO were measured using AGAGE instrumentation for target compounds. Southern Hemisphere Cape Grim Air Archive (CGAA) samples, which are background or “baseline” air, were collected at the Baseline Air Pollution Station, Cape Grim, Tasmania by CSIRO and the Bureau of Meteorology. The samples were cryogenically collected into 34 L electro-polished stainless steel canisters (Langenfelds et al., 1996; Fraser et al., 2017) since 1978. The CGAA samples were analyzed on Medusa-9 in the CSIRO laboratory at Aspendale (Miller et al., 2010). Northern Hemisphere (NH) samples used for this paper were filled during background conditions mostly at Trinidad Head, but also at La Jolla, California, Cape Meares, Oregon (courtesy of the Oregon Graduate Centre via CSIRO, Aspendale, and the Norwegian Institute for Air Research, Oslo, Norway), and Point Barrow, Alaska (courtesy of Robert Rhew, University of California, Berkeley) and analyzed at SIO, La Jolla, on laboratory-based Medusa-GC-MS instruments (Medusa-1, Medusa-7) (O'Doherty et al., 2009). A stepwise tightening filtering algorithm was applied based on their deviations from a fit through all data from each semi-hemisphere (including pollution-free monthly mean *in situ* data) to remove outliers (Mühle et al., 2010; Vollmer et al., 2016). HFC-134a air archive data obtained using AGAGE instrumentation at CSIRO and SIO are reported here for the first time (Table S1d). The archived air measurements for HFC-125 reported by O'Doherty et al. (2009) are used in this study (Table S1e) and have been updated to include more present data. The CGAA archived air measurements for HCFC-22 reported by Miller et al. (1998) are used here. CGAA Medusa-3/Medusa-9 measurements for HFC-23 from AGAGE reported by Miller

Deleted: Measurements ...easureme ...

Formatted: Heading 3

Deleted: 2

Deleted: .33... .., 9.9...0° ... and ...

Deleted: both on the basis of...ased on ...

Deleted: studies

Formatted: Heading 3

Deleted: concentration...ole fraction ...

Deleted: based ...n Medusa-9 at ...

Deleted: All NH archived air samples were collected in America...and analyze ...

Deleted: These samples were mostly collected during clean air conditions. The data have been filtered followed by statistical outlier exclusion (Cunnold, 2002)

Deleted: All ...FC-134a air archive da ...

Deleted: 2...1e) and have been update ...

Deleted: The Southern Hemisphere ...

et al. (2010) are also reported here (Table S1f). CSIRO SH and SIO NH archived air samples have been analysed on AGAGE GC-MS instrumentation at CSIRO, Aspendale and at SIO, La Jolla, for PFC-14 and PFC-116 (Mühle et al., 2010).

Deleted: 2

### 2.1.3 AGAGE measurements of CSIRO firn air

The firn layer is unconsolidated snow overlaying an ice sheet. Large volumes (hundreds of liters) of air trapped in firn can be extracted for subsequent analysis. From the measured firn depth profiles, atmospheric histories can be derived using firn diffusion models. Firn air histories typically cover the period from the present day (or drilling date) to up to 100 years ago.

Deleted: enable analysis of trace gases requiring larger volumes of air than is available from ice cores (Sturrock et al., 2002). The air

The firn air samples for HCFC-141b and HCFC-142b were collected from six depths at Law Dome, Antarctic in 1997-98 at the DSSW20K site (Table S1b and Table S1c) (Sturrock et al., 2002). The firn air samples were measured on the AGAGE ADS-GC-MS instrument at Cape Grim. Antarctic firn air samples have also been used for the reconstruction of the atmospheric histories of PFC-14 and PFC-116 (Trudinger et al., 2016).

Formatted: Do not check spelling or grammar

Deleted: around ...p to 100 years ago (...)

Moved down [8]: The first measurements of HCFC-141b and HFC-134a in firn were made by Butler et al. (1999) and showed that there are no natural sources for these compounds.

## 2.2 Data from the NOAA network

### 2.2.1 NOAA flask measurements

Flask air measurements of the compounds considered in this study have been made by the National Oceanic and Atmospheric Administration (NOAA) as early as 1992 (Montzka et al., 1994; 1996; 2009; 2015). The data are available at the NOAA website (ftp://ftp.cmdl.noaa.gov/hats/) where the latest atmospheric measurements are reported. There are many NOAA and affiliated stations globally. In order to be consistent with the chosen AGAGE stations, NOAA observations at only Mace Head, Ireland (MHD, 42 meters above sea level (masl)) for HCFC-22, HCFC-141b, HCFC-142b and HFC-134a, and Trinidad Head, USA (THD, 120 masl) for HCFC-22, HCFC-141b, HCFC-142b HFC-134a and HFC-125 are used for representing atmospheric mole fractions from 30-90°N. The observations at Cape Grim, Australia (CGO, 164 masl) represent the 30-90°S mole fractions. These stations, their locations and the sampling dates of the samples used in this study are listed in Table S1 and are essentially identical to the corresponding the AGAGE stations.

Deleted: The firn air data is estimated from the published figures (Table 2)... (...)

Deleted: 4

Deleted: is ...re available at the NOAA (...)

Air samples are analyzed in the NOAA/ESRL/GMD Boulder laboratory by GC-MS techniques for HCFC-22, HCFC-141b, HCFC-142b, HFC-134a and HFC-125. More details are given (Montzka et al., 1993; 1994; 1996; 2015). The working standards and measurement precision are also reported in the studies.

Deleted: ies...by gas chromatography (...)

Deleted: , (Montzka et al., 1994), (Montzka et al., 1996) and (Montzka et al., 2015)

Deleted: above

Formatted: Heading 3

Deleted: 5

Deleted: cruise

Deleted: fill...btained at the Niwot Ridge (...)

### 2.2.2 NOAA measurements of archived and shipborne air samples

Archived air and shipborne air measurements from both hemispheres for HCFC-141b and HCFC-142b are given in Thompson et al. (2004). The archived air samples for HCFC-141b and HCFC-142b were obtained at the Niwot Ridge (NWR, 40°N, 106°W) since 1986. The cruise air samples were collected during the Soviet-American Gas and Aerosol Experiment (SAGA) II cruise in the Pacific Ocean in 1987 (37°N-30°S, 160°W-170°W).

Deleted: cruise...air measurements for (...)

Deleted: The archived air s...amples (...)

Archived air and shipborne air measurements for HFC-134a were presented by Montzka et al. (1996). Samples were collected at Niwot Ridge (NWR). Samples were obtained shipboard during two cruises, one in the Pacific Ocean in 1987 (SAGA II above) and in 1994 (41°N-47°S, 127°W-76°W) and another in the Atlantic Ocean in 1994 (46°N-48°S, 14°W-60°W).

### 2.2.3 NOAA measurements of firn air

The first measurements of HCFC-141b and HFC-134a in firn air were made by Butler et al. (1999) and showed that there are no natural sources for these compounds.

Moved (insertion) [8]

## 2.3 Data from the UEA network

### 2.3.1 UEA archived air

University of East Anglia (UEA) measurements on Cape Grim Air Archive sub-samples (since 1978) and flask samples collected at Cape Grim are updated following the original publications for HCFC-141b, HCFC-142b (Oram et al., 1995) and HFC-134a (Oram et al., 1996). The Cape Grim archived air contains trace gas records known to be representative of background air in the Southern Hemisphere. UEA has analysed sub-samples of the Cape Grim Air Archive, whereas the CGAA has been analysed directly on AGAGE instrumentation at Cape Grim, CSIRO, Aspendale and at the SIO, La Jolla (Sect. 2.1.2).

The Cape Grim Archived Air, which is located at CSIRO, Aspendale, was sub-sampled for the UEA at Aspendale and the UEA flask air samples were collected directly at Cape Grim; both were analyzed by GC-MS at the UEA for HCFC-141b, HCFC-142b and HFC-134a (Oram et al., 1995; 1996) (Table S1b and Table S1c). The working standards and measurement uncertainties were also shown in the above mentioned studies.

### 2.4 Data from models

In order to estimate atmospheric mole fractions before direct atmospheric measurements commenced, the results from published models, a 2-box model for HCFC-22 (Montzka et al., 2010a) and the AGAGE 2-D atmospheric 12-box chemical transport model for HFC-23 (Cunnold et al., 1983; 1994; Miller et al., 2010; Rigby et al., 2011) and for PFC-14 and PFC-116 (Trudinger et al., 2016), are also included in this study (Table S1g and Table S1h).

The 2-box model for HCFC-22 from Montzka et al. (2010a) considers the atmosphere as two boxes, one box representing each hemisphere. Each hemisphere is assumed to be well mixed and a standing vertical gradient is assumed. Using the 2-box model, Montzka et al. (2010a) derived the atmospheric mole fractions from 1944 to 2009 for HCFC-22 by assuming a constant 0.95 scaling of global emissions estimated by the Alternative Fluorocarbons Environmental Acceptability Study (AFEAS).

The AGAGE two-dimensional atmospheric 12-box chemical transport model used here for HFC-23, PFC-14 and PFC-116 mole fractions and emissions, contains four lower tropospheric boxes, four upper tropospheric boxes and four stratospheric boxes, with boundaries at 30°N, 0° and 30°S in the horizontal, and 500 and 200 hPa in the vertical (Cunnold et al., 1983; 1994; Rigby et al., 2011). It has previously used to estimate mole fractions and emissions of CFC-11 and CFC-12 and various other trace gases, Miller et al. (2010) derived mole fractions for HFC-23 for the period 1978-2009, prior to the AGAGE in situ measurements, by an inversion technique using this 2-D 12-box model, but not back to zero atmospheric mole fraction. Trudinger et al. (2016) calculated the atmospheric mole fractions of PFC-14 and PFC-116 in each semi-hemisphere since 1900 by combining the data from ice core, firn, air archive and *in situ* measurements, extending the work of Mühle et al. (2010).

### 2.5 AGAGE, NOAA and UEA calibration scales

The latest AGAGE absolute calibration scales for various trace gases are displayed on the AGAGE website (agage.mit.edu and http://agage.eas.gatech.edu/data\_archive/agage/AGAGE\_scale\_2018\_v1.pdf). AGAGE *in situ* measurements have been reported on the latest SIO absolute calibration scales for HCFC-22 (SIO-05), HCFC-141b (SIO-05), HCFC-142b (SIO-05), HFC-134a (SIO-05), HFC-125 (SIO-14), HFC-23 (SIO-07), PFC-14 (SIO-05) and PFC-116 (SIO-07), as have archived air measurements for HFC-134a and HFC-23. The archived air measurements for HFC-125 reported by O'Doherty et al. (2009) on the calibration scale UB-98 (UB: University of Bristol) were converted to the latest scale SIO-14 by the conversion factor (SIO-14/UB-98 = 1.0826) (See Table 2). The archived air measurements for HCFC-22 reported by Miller et al. (1998) on the calibration scale SIO-93 were converted to the latest scale SIO-05 by the combined conversion factors (NOAA-1992/SIO-93

Deleted: 6

Formatted: Heading 3

Deleted: The Cape Grim air archive measurements from

Deleted: The UEA has analyzed whole air samples from the Cape Grim Baseline Air Pollution Station in Tasmania, Australia since 1978. ...he Cape Grim archived air (...)

Deleted: archived ...rched air ...ir, (...)

Deleted: 2...1b and Table S1c). The (...)

Deleted: 7 ... Data from M (...)

Deleted: fill the gap ...efore direct (...)

Deleted: 2

Deleted: ; ...- one box representing ea (...)

Deleted: calculated ...erived the (...)

Deleted: s...four lower tropospheric (...)

Deleted: and Rigby et al. (2011)

Deleted: was...used to estimate the (...)

Deleted: inferred the model...erived m (...)

Deleted: 8 ... AGAGE, NOAA and (...)

Deleted: The ...GAGE *in situ* (...)

Formatted: Font: 10 pt

Deleted: 3

= 0.997 ± 0.004, NOAA-2006/NOAA-1992 = 1.005, NOAA-2006/SIO-05 = 0.9971 ± 0.0027 (See Table 2). The firm air measurements for HCFC-141b and HCFC-142b were reported in the calibration scale UB-98. Conversion factors (NOAA-1994/UB-98 = 1.006 ± 0.003, NOAA-1994/SIO-05 = 0.9941 ± 0.0049) are used to transfer data to the latest calibration scale SIO-05 for HCFC-141b (Prinn et al., 2000; Simmonds et al., 2017). For HCFC-142b, the data can be converted from scale UB-98 to be the latest calibration scale SIO-05 by conversion factors (NOAA-1994/UB-98 = 0.937 ± 0.003, NOAA-1994/SIO-05 = 0.9743 ± 0.0052) (Prinn et al., 2000; Simmonds et al., 2017).

All NOAA absolute calibration scales for various trace gases are shown on <https://www.esrl.noaa.gov/gmd/ccl/scales.html>, NOAA flask measurements were reported on the latest NOAA calibration scale for HCFC-22 (NOAA-2006), HCFC-141b (NOAA-1994), HCFC-142b (NOAA-1994), HFC-134a (NOAA-1995) and HFC-125 (NOAA-2008). NOAA archived air measurements for HCFC-141b and HCFC-142b were also reported in the latest scale. All data reported on NOAA scales are converted here to AGAGE calibration scale for both compounds. The conversion factors between AGAGE and NOAA are shown in Table 2 and were derived on the basis of Table 12 from Prinn et al. (2000), Table S4 from Simmonds et al. (2017) and Table 5 from Prinn et al. (2018a). The scale conversions between NOAA-1994 and SIO-98 for HCFC-22 in former study were based on the comparison of gas mole fractions in air samples in 1994-1995 and the scale conversions between NOAA-1994 and UB-98 for HCFC-141b and HCFC-142b were based on the measurements against NOAA standard and UB standard in 1997-1998. In the latter study, the scale conversions between NOAA and AGAGE were based on the comparison of gas mole fractions in air samples in 1998-2017 for HCFC-22, HCFC-141b, HCFC-142b, and HFC-134 at CGO, SMO, THD and MSD (Prinn et al., 2018a). For HFC-125, the NOAA/AGAGE ratio was based on the comparison in 2007-2015 at CGO, SMO and THD (Simmonds et al., 2017).

Archived air measurements from UEA are obtained on the NOAA-1994 scale for HCFC-141b and HCFC-142b, and on the NOAA-1995 scale for HFC-134a. It is important to note that the original UEA calibration scale for HCFC-141b, HCFC-142b, and HFC-134a (Oram et al., 1995; 1996) has been superseded by NOAA scale. All UEA measurements obtained on the NOAA scale are converted to the AGAGE calibration scale by the conversion factors shown in Table 2.

## 2.6 Hemispheric annual means and uncertainties estimation

We assembled data from *in situ*, flask, archived air and firm air measurements from the AGAGE, SIO, CSIRO, NOAA and UEA networks/laboratories and from AGAGE and NOAA model calculations (Table S1a-h). As the AGAGE baseline monthly means are nominally pollution-free data, the flask measurements from the NOAA network were processed by a statistical procedure to identify measurements which may have been influenced by regional pollution. Briefly, monthly means were calculated by averaging around 4 values for each month. Then the resultant standard deviations for each month were estimated by error propagation. For each month, values exceeding three standard deviations above the monthly mean were rejected as polluted. Afterwards, the monthly means for flask measurements were re-calculated without pollution events, combined with UEA data, and converted to AGAGE scales. The combined data from all networks/laboratories then formed the database used here.

The initial database containing replicate times have been converted into a value without such replicates by using the number of measurement-weighted averages at each replicate time. That is to say, when measurements from different networks and sites are combined, hemispheric monthly averages were first calculated by weighted averages to give monthly means more weight as they are based on many individual measurements.

Hemispheric monthly means for each compound were estimated by a smoothing spline fit to the combined and sorted data. The inverses of the square of the standard deviations ( $(\delta y_i)^{-2}$ ) of each monthly mean or data points are used as the weights for the spline fit. Although there are no significant differences between the AGAGE and the NOAA monthly means in the same hemisphere, the hemispheric monthly means are closer to the AGAGE monthly means due to the much higher number

- Deleted: 003
- Deleted: 3
- Deleted: on
- Deleted:
- Deleted:
- Deleted: 005
- Deleted: displayed
- Deleted: their website (
- Deleted: )
- Deleted: A
- Deleted: on
- Deleted: the
- Deleted: the
- Deleted: 3
- Deleted: study
- Deleted: and
- Deleted: study
- Deleted: concentration
- Deleted: concentration
- Deleted: 06
- Deleted: wa
- Deleted: The a
- Deleted: ,
- Deleted: the
- Deleted: (
- Deleted: 3
- Deleted: )
- Deleted: 9
- Deleted: Smoothing spline fit
- Deleted: y

of measurements in a given month from the AGAGE network (every 2 h, around 100-300 pollution-free samples/month for each site) compared to the NOAA network (weekly flask, around 4 samples/month for each site).

Hemispheric annual means were calculated by averaging the monthly means of the corresponding 12 months. The JFM means and JAS means are estimated by averaging monthly means of January, February, and March and monthly means of July, August and September of the same year.

The smoothing spline fit method discussed above was based on previous studies (Reinsch, 1967; Craven and Wahba, 1978; Wahba, 1983; Hutchinson and De Hoog, 1985; Wahba, 1990). The method is briefly described below. For more details, see Sect. S1 in the Supplement.

For a set of  $n$  data points taking values  $y_i$  at times  $t_i$ , the smoothing spline fit  $g(t)$  of the function  $g(t_i)$  is defined to be the minimizer of

$$p \sum_{i=1}^n \left[ \frac{g(t_i) - y_i}{\delta y_i} \right]^2 + \int g''(t)^2 dt \quad (1)$$

Generally, the function is given an initial guess by sampling various values of the smoothing parameter  $p$ , from  $10^{-4}$ ,  $10^{-3}$ , ...,  $10^{10}$ . The initial guess is the first local maximum. If it does not exist, the minimum location is used instead. The generalized cross-validation is used to estimate the smoothing parameter  $p$ . After estimating the optimal smoothing parameter, the estimated variance (VAR) and 95% Bayesian confidence intervals (CI) are calculated. The weights ( $W$ ) are assumed to be the inverse of the square of standard deviations ( $(\delta y_i)^{-2}$ ) associated with the observed variables. It calculates the spline the way Reinsch (1967) specified.

The uncertainties of the final annual means are calculated based on the original uncertainties of the monthly means (e.g. for AGAGE in situ data, a standard deviation from 100-300 pollution-free measurements/month for each site) or the measurement precisions for individual data points. The uncertainties in the original pollution-free AGAGE monthly means and the calculated NOAA monthly means include uncertainties in the measurements themselves (precision), scale propagation errors and sampling frequency errors. When the monthly means of the NOAA and UEA measurements were converted to AGAGE scales, scale conversion errors were also propagated. Following error propagation, the errors of the hemispheric monthly means were first calculated by the number of measurement-weighted root-mean-square (RMS) of the standard deviation of replicate values. The final uncertainties of hemispheric monthly means are calculated based on the misfit between the smoothing spline fit and the observed values. The uncertainties of hemispheric annual means were calculated as the square root of the squared errors from each of the 12 months.

## 2.7 Seawater solubility estimation method

Solubility has been reported in terms of the Henry's Law solubility coefficient  $H$  ( $\text{mol L}^{-1} \text{atm}^{-1}$ ), the mole fraction solubility  $x$  ( $\text{mol mol}^{-1}$ ), the Bunsen solubility coefficient  $\beta$  ( $\text{L L}^{-1}$ , in STP condition), the Ostwald solubility coefficient  $L$  ( $\text{L L}^{-1}$ ), the weight solubility coefficient  $c_w$  ( $\text{mol kg}^{-1} \text{atm}^{-1}$ ) or the K unen solubility coefficient  $S$  ( $\text{L g}^{-1}$ ). The definitions of solubility are shown in studies (Young et al., 1987; Gamsj ager et al., 2008; 2010). The relationship between different solubility terms are:

$$H = \frac{x}{(1-x) \cdot p^\ominus \cdot V_m} = \frac{\beta}{R \cdot T^\ominus} = \frac{L}{R \cdot T} = \frac{c_w \cdot M_i}{V_m} = \frac{S \cdot M_g}{R \cdot T^\ominus \cdot V_m} \quad (2)$$

where  $T^\ominus = 273.15 \text{ K}$  and  $p^\ominus = 101.325 \text{ kPa} = 1 \text{ atm}$  are the standard temperature and pressure (STP);  $V_m$  is molar volume of the solvent,  $V_m = 18.01528 \cdot 10^{-3} \text{ L mol}^{-1}$  is the molar volume of water;  $R$  is the ideal gas constant,  $8.314459848 \text{ L kPa K}^{-1} \text{ mol}^{-1}$  (or  $0.08205733847 \text{ L atm K}^{-1} \text{ mol}^{-1}$ );  $T$  is the temperature in Kelvin and  $M_i$  is the molar mass of the solvent, which is  $18.01528 \text{ g mol}^{-1}$  for water. Next, we present three methods to estimate the solubility of compounds in freshwater and seawater.

Deleted: The monthly means for target compounds were obtained by fitting all data from different institutes with the smoothing spline.

Deleted: ere

Deleted: the

Deleted: csapsGCV =

Deleted: gets

Deleted:

Deleted:  $\delta y_i$

Deleted: 10

Deleted: the

Deleted: for

Deleted: Molar

Deleted: Here are

Deleted: two complete

### 2.7.1 Method I: the CGW model

The following method to estimate the solubility of gases in seawater was reported in Deeds (2008), and briefly described here. The Clark-Glew-Weiss (CGW) solubility equation can be used to calculate the solubility of gases in freshwater and seawater. It is derived from the integrated van 't Hoff equation and the Setchenow salinity dependence (Weiss, 1970, 1974) and expressed as a function of temperature and salinity.

$$\ln L = a_1 + a_2 \cdot \left(\frac{100}{T}\right) + a_3 \cdot \ln\left(\frac{T}{100}\right) + S[b_1 + b_2 \cdot \left(\frac{T}{100}\right) + b_3 \cdot \left(\frac{T}{100}\right)^2] \quad (3)$$

where  $L$  is the Ostwald solubility coefficient in  $L L^{-1}$  of a gas in seawater,  $T$  is the absolute temperature in Kelvin,  $S$  is the salinity in ‰ (or  $g kg^{-1}$ ) and  $a_i$  and  $b_i$  are constants.

When  $S = 0$ , this equation becomes the freshwater solubility equation for a gas:

$$\ln L_0 = a_1 + a_2 \cdot \left(\frac{100}{T}\right) + a_3 \cdot \ln\left(\frac{T}{100}\right) \quad (4)$$

where  $L_0$  is the Ostwald solubility in  $L L^{-1}$  of a gas in freshwater.

We did not find complete studies on the solubility of our target gases in seawater based on experiments. Fortunately, the solubility of a gas in seawater can be determined from their freshwater solubility, which can be represented by a modified Setschenow equation (Masterton, 1975):

$$\ln(L_0/L) = k_s \cdot I_V \quad (5)$$

Here  $L_0$  is the freshwater solubility,  $L$  is the solubility in a mix-electrolyte solution, such as seawater,  $k_s$  is the salting-out coefficient and  $I_V$  is the ionic strength of the solution.  $k_s$  is an empirically-derived, temperature-dependent constant. It can be estimated as a function of temperature using the freshwater and seawater solubility data by a least-square fit with a second-order polynomial (Masterton, 1975).

$$k_s = c_1 t^2 + c_2 t + c_3 = c_1(T - 273.15)^2 + c_2(T - 273.15) + c_3 \quad (6)$$

where  $t$  is the temperature in Celsius,  $T$  is the temperature in Kelvin and  $c_i$  are the constants.

The ionic strength of seawater  $I_V$  ( $g L^{-1}$ ) can be calculated from its salinity ( $S$ ) (Deeds, 2008):

$$I_V = \frac{0.03600}{1.80655} \times S \times \rho(T, S) \quad (7)$$

where  $\rho(T, S)$  is the density of seawater in  $kg L^{-1}$ , estimated using the equation of state of seawater (Millero and Poisson, 1981). This equation is suitable for temperature ( $T$ ) from 273.15 K (0 °C) to 313.15 K (40 °C) and salinities ( $S$ ) from 0.5 to 43.

The seawater solubility of the target compounds based on Method I can therefore be estimated by combining Eq. (4), (5), (6), and (7):

$$\ln L = \left[ a_1 + a_2 \cdot \left(\frac{100}{T}\right) + a_3 \cdot \ln\left(\frac{T}{100}\right) \right] \cdot \exp[-(c_1(T - 273.15)^2 + c_2(T - 273.15) + c_3)] \times \frac{0.03600}{1.80655} \times S \times \rho(T, S) \quad (8)$$

### 2.7.2 Method II: the pp-LFER model

The solubility estimation of compounds is based on a cavity model, the poly-parameter linear free energy relationships (pp-LFERs) of Abraham (1993). The pp-LFER model has been applied and validated for many types of partition coefficients (Abraham et al., 2004; 2012). In this model, the process of dissolution of a gaseous or liquid solute in a solvent involves setting up various exoergic solute-solvent interactions. Each of these interactions is presented in relevant solute parameters or descriptors. The selected Abraham model solute descriptors are the excess molar refraction ( $E$ ) in  $cm^3 mol^{-1}/10$ , the solute dipolarity/polarizability ( $S$ ), the overall solute hydrogen-bond acidity ( $A$ ) and basicity ( $B$ ), the McGowan's characteristic molar volume ( $V$ ) in  $cm^3 mol^{-1}/100$  and the gas to hexadecane partition coefficient ( $\log L^{16}$ ) at 298.15 K.

Deleted: 10

Deleted: build

Deleted: . It is

Deleted: it

Deleted: There are not

Deleted: the

Deleted: and/or the CGW model

Deleted: the following form using

Deleted: the

Deleted: is

Deleted: (

Deleted: , in

Deleted: can be calculated by

Deleted: an

Deleted: for

Deleted: ¶  
 $\rho = \rho_0 + DS + ES^{3/2} + FS$

Deleted: then

Deleted: the freshwater solubility

Deleted: and Eq.

Deleted: (7)

Deleted: 8

Deleted: 9

Deleted: 10

Moved (insertion) [2]

Deleted: s

Deleted: ve

Deleted: in

Field Code Changed

Deleted: of

Deleted: are

Deleted:

Deleted: and

$$\log SP = c + eE + sS + aA + bB + vV \quad (9)$$

$$\log SP = c + eE + sS + aA + bB + l \log L^{16} \quad (10)$$

In these equations, the dependent variable  $\log SP$  is some property of a series of solutes in a given system. Therefore,  $SP$  could be partition coefficient,  $P$ , for a series of solutes in a given water-solvent system in Eq. (9), or  $L$ , for a series of solutes in a given gas-solvent system in Eq. (10).

In this work,  $\log SP$  refers to some solubility-related property of a series of gaseous solutes in water.  $SP$  is the gas-water partition coefficient  $K_w$ , which can be defined in terms of equilibrium mole fractions of the solute, through Eq. (11).

$$K_w = \frac{\text{Conc. of solute in water, in mol dm}^{-3}}{\text{Conc. of solute in the gas phase, in mol dm}^{-3}} \quad (11)$$

The Ostwald solubility coefficient  $L_0$  (in  $L L^{-1}$ ) usually expressed as the gas-water partition coefficients  $K_w$ , which can be estimated by Eq. (10). But  $L_0$  can be determined by both Eq. (9) and Eq. (10) because the "solvent" in "water-solvent partition coefficient" could also be gas phase (Abraham et al., 1994; 2001; 2012). Based on the definition of gas-water partition coefficients in Eq. (11), the values calculated from Eq. (9), water-gas partition coefficients, should be the reciprocal of the real solubility coefficients. But they are not. When Abraham dealt this in his work (Abraham et al., 1994; 2001; 2012), he already treated the  $SP$  in Eq. (9) as the Ostwald solubility coefficients  $L_0$ . So  $L_0$  can be determined by both Eq. (12) and Eq. (13) by rewriting Eq. (9) and Eq. (10):

$$\log L_0 = c + eE + sS + aA + bB + vV \quad (12)$$

$$\log L_0 = c + eE + sS + aA + bB + l \log L^{16} \quad (13)$$

Inspired by Endo et al. (2012) and Goss et al. (2006) using the pp-LFER model to estimate the salting-out coefficients based on corrected  $V$  ( $V_c$ ) (described afterwards),  $V_c$  replaced  $V$  in Eq. (12) with the same coefficients and other descriptors, was also used to calculate the Ostwald solubility coefficient in water, expressed as Eq. (14), for comparison.

$$\log L_0 = c + eE + sS + aA + bB + vV_c \quad (14)$$

$L_0$  estimated by Eqs. (12), (13) and (14) based on  $V$ ,  $\log L^{16}$  and  $V_c$  were compared with the observed values. The estimated  $L_0$  which is closest to the observed values will be chosen as the one to estimate the Ostwald solubility coefficients in water for the pp-LFER model method.

The set of coefficients,  $c$ ,  $e$ ,  $s$ ,  $a$ ,  $b$ ,  $v$ , and  $l$  characterize a solvent phase in terms of specific solute/solvent interactions. They are determined by multiple linear regression (MLR) analysis. The coefficients  $c$ ,  $e$ ,  $s$ ,  $a$ ,  $b$  and  $v$  for Eqs. (12), (13) and (14) at 298.15 K and 310.15 K are shown in Table 3 (Abraham et al., 1994; 2001; 2012). The Abraham model solute descriptors  $E$ ,  $S$ ,  $A$ ,  $B$ ,  $V$ ,  $V_c$  and  $\log L^{16}$  are calculated based on different methods and shown in Table 4. The  $E$  descriptor describes the polarizability of a solute.  $E$  for target compounds except HCFC-22 and PFC-116 can be obtained from Abraham et al. (2001).

For HCFC-22, the value of the  $E$  descriptor was calculated by Eq. (15) on the basis of the number of iodine, bromine, chlorine and fluorine atoms ( $nI$ ,  $nBr$ ,  $nCl$  and  $nF$ ) in a halocarbon (Abraham et al., 2012), obtained from a regression analysis of 221 compounds. The methods of determining  $S$ ,  $A$ ,  $B$  descriptors are reported in previous studies (Abraham et al., 1989; 1991; 1993). The  $V$  descriptor, which is the measure of the size of a solute, is the molar volume of a solute calculated from McGowan's approach (McGowan and Mellors, 1986; Abraham and McGowan, 1987). The  $V_c$  descriptor is the corrected McGowan's characteristic molar volume with the characteristic atomic volume for a fluorine atom (Goss et al., 2006).  $L^{16}$  is the solute gas/hexadecane partition coefficient or the Ostwald solubility coefficient in hexadecane at 298.15 K, which can be obtained from previous studies (Abraham et al., 1987; 2001; 2012).

$$E = 0.641nI + 0.328nBr + 0.140nCl - 0.0984nF \quad (15)$$

$$n = 221, \text{SD} = 0.083$$

The solubility of a compound in salt solution can be determined from its solubility in water by Eq. (16). This equation is also the method for the quantitative description of the salting-out effect in neutral organic solutes, expressed in the following form using a modified Setschenow relationship (Sander, 1999; Schwarzenbach et al., 2003; Endo et al., 2012):

Deleted: 10

Deleted: i

Deleted: ies

Deleted: phase (or phases)

Deleted:  $L$ , the partition coefficient for a series of solutes in a given gas-solvent system or it could be  $P$ , the water-solvent partition coefficient for a series of solutes.

Moved up [2]: The pp-LFERs have been applied and validated in many types of partition coefficients (Abraham et al., 2004; Abraham et al., 2012).

Moved (insertion) [3]

Deleted: ies

Deleted: W

Deleted: expressed as t

Deleted: For HCFC-141b, HCFC-142b, HFC-134a, HFC-125, HFC-23 and PFC-14, the values of

Deleted: descriptor

Deleted: were given by

Deleted: 11

Deleted: . It is

Deleted: based on the

Deleted: n

Deleted: . Note that

Deleted: needs correction from  $10.48 \text{ cm}^3 \text{ mol}^{-1}$  to be  $12.48 \text{ cm}^3 \text{ mol}^{-1}$

Deleted: 11

Moved up [3]: In this work,  $\log SP$  refers to some solubility-related properties of a series of gaseous solutes in water.  $SP$  is the gas-water partition coefficient  $K_w$ , expressed as the Ostwald solubility coefficient  $L_0$  (in  $L L^{-1}$ ).

Deleted: In this work,  $\log SP$  refers to some solubility-related properties of a series of gaseous solutes in water.  $SP$  is the gas-water partition coefficient  $K_w$ , expressed as the Ostwald solubility coefficient  $L_0$  (in  $L L^{-1}$ ). The solubility of 408 gaseous...

Deleted: the

Deleted: on

Deleted: . Both can be represented

Deleted: by

$$\log(L_0/L) = K_S \cdot [\text{salt}] \quad (16)$$

where  $L_0$  is the Ostwald solubility coefficient in pure water (in  $\text{L L}^{-1}$ ),  $L$  is the Ostwald solubility coefficient in the salt solution (in  $\text{L L}^{-1}$ ),  $K_S$  is the molality-based Setschenow (or salting-out) coefficient ( $\text{M}^{-1}$ ) for the salinity- and common logarithm-based Setschenow equation and is independent of [salt], and [salt] is the molality of the salt in  $\text{mol L}^{-1}$ . The relationship between [salt] and salinity ( $S$ ,  $\text{g L}^{-1}$ ) in seawater is  $[\text{salt}] = S/M_{\text{NaCl}}$ .  $M_{\text{NaCl}}$  is the molar mass of sodium chloride ( $\text{NaCl}$ ,  $58.44 \text{ g mol}^{-1}$ ). So the salt mole fraction in seawater is approximately equivalent to 0.6 M NaCl (i.e.,  $[\text{NaCl}] = \text{ca. } 0.6 \text{ M}$ ). It is best to define the salt solution based on molality. Adding dry salt to a solution does not change the molality of other solutes as the molality is the mass of the solvent rather than the solution (Sander, 1999).

The salting-out coefficient  $K_S$  should be estimated to calculate the solubility of a compound in a salt solution.  $K_S$  can be estimated by the poly-parameter linear free energy relationships (pp-LFERs) since  $K_S$  is formally comparable with the Common Logarithm of the partition coefficient between the 1 M NaCl solution and freshwater (Abraham et al., 2012; Endo et al., 2012).

$$K_S = c + eE + sS + aA + bB + vV_c \quad (17)$$

The coefficients  $c$ ,  $e$ ,  $s$ ,  $a$ ,  $b$  and  $v$  for Eq. (17) at  $298.15 \pm 2 \text{ K}$  are shown in Table 3 (Endo et al., 2012).  $E$ ,  $S$ ,  $A$ ,  $B$ , and  $V_c$  are same as the ones described above. It is not easy to calculate the error in the descriptors as all the descriptors are calculated simultaneously (Abraham et al., 2001).  $E$  is calculated without error.  $V_c$  is the McGowan's characteristic molar volume without error. The general errors of  $S$ ,  $A$ ,  $B$  are thought to be 0.03 (Abraham et al., 1998; 2001). We assume that the error for each is 0.01 when  $S$ ,  $A$  and  $B$  are all not zero and we assume that the error is 0.03 for  $S$  and 0 for  $A$  and  $B$  when  $S$  is not zero but  $A$  and  $B$  are both zero. So the uncertainties of salting-out coefficients could be calculated by error propagation based on different functions. Using the above pp-LFER model, the Setschenow coefficient  $K_S$  can be estimated for numerous compounds with various functional groups (Endo et al., 2012).

The solubility of compounds in seawater based on the pp-LFER model can be estimated by combining one of the Eq. (12), (13), (14) with Eqs. (16) and (17):

$$L = L_0 \cdot 10^{-K_S \frac{S}{M_{\text{NaCl}}}} \quad (18)$$

In order to distinguish between Abraham's original method and the revised method based on his method in estimating Ostwald solubility coefficients in water, which we define as Method II when  $L_0$  is calculated by Eq. (12) or Eq. (13) and Revised Method II when  $L_0$  is calculated by Eq. (14).

### 2.7.3 Combined Method: combined CGW model and pp-LFER model

The main difference between the two methods described above to estimate the solubility of compounds in seawater is the different methods to estimate the water solubility and salting-out coefficients. Method I, reported in Deeds (2008), is mainly based on the Clark-Glew-Weiss (CGW) solubility model. The water solubility functions of compounds are constructed based on the CGW model and the salting-out coefficients are estimated as a function of temperature using the freshwater and seawater solubility data by the least-square fit with a second-order polynomial. In Method I, more solubility measurements in water and seawater are needed and chemical properties of compounds are considered. Method II is based on the poly-parameter linear free energy relationships (pp-LFERs). The water solubility of compounds and salting-out coefficients are both estimated based on the pp-LFERs. Consideration of the physical properties of compounds is more important in Method II. Both Methods have shortages and advantages. For Method I, there are frequently too few seawater solubility measurements for target compounds in order to construct the second-order polynomial between the salting-out coefficient and temperature. For Method II, the water solubility functions for target compounds are only constructed at 298.15 K and 310.15 K (Abraham et al., 2001; 2012).

The best approach is a combination of Method I and II to construct the solubility of compounds in water and seawater. The freshwater solubility functions of compounds can be constructed based on the Clark-Glew-Weiss (CGW) solubility model

Deleted: 4

Deleted: Sodium ...odium chloride (N...

Deleted: so as ...o calculating...the ...

Deleted: 15

Deleted: and ...B, and  $V_c$  are same as (...)

Moved (insertion) [4]

Moved up [4]: Using the above pp-LFER model, the Setschenow coefficient  $K_S$  can be estimated for numerous compounds with various functional groups.

Deleted: The Setschenow coefficient  $K_S$  of 43 diverse neutral compounds in NaCl solutions at  $298.15 \pm 2 \text{ K}$  have been correlated through Eq. (16) (Endo et al., 2012)

Deleted: 10...2), (12...3), (14) with E...

Formatted

Deleted:  $10^{[-K_S \cdot S/M_{\text{NaCl}} + c + eE + sS + aA + bB + vV]}$

Formatted

Deleted: 17

Deleted: 10...3 Combined Method: ...

Deleted: re are ...main difference betw...

Deleted: M...ore solubility measurem...

Deleted: way ...pproach is the ...

(Method I) with the advantage of validity over a larger temperature range. The seawater solubility functions of compounds can be constructed on the basis of the pp-LFERs in estimating the salting-out coefficients (Method II) with the advantage of working for more compounds. By combining Eq. (4), (16) and (17), the solubility of compounds in seawater ( $L$ , Ostwald solubility coefficient in  $L L^{-1}$ ) based on the Combined Method can be estimated by the following equation. This equation is used to estimate the seawater solubility of the target compounds in this paper.

$$L = 10^{-K_S \cdot S / M_{NaCl}} \cdot \exp \left[ a_1 + a_2 \cdot \left( \frac{100}{T} \right) + a_3 \cdot \ln \left( \frac{T}{100} \right) \right] \quad (19)$$

### 3 Results and Discussion

#### 3.1 Atmospheric histories and growth rates

During late winter, typically January, February and March in the Northern Hemisphere and July, August and September in the Southern Hemisphere, heat is lost from the surface seawater which results in an increased density of the surface seawater.

During this process, the mixed layer deepens and older water (usually with lower transient tracer mole fractions) is brought in contact with the atmosphere. The mixed layer is gaining density and tends to be transported towards the ocean interior through diffusive, advective and/or convective processes. This water then carries with it a signature of the atmospheric mole fraction, pending the saturation state of the water as it leaves the surface layer. For tracers with rapidly increasing atmospheric mole fractions and for deep mixed layers under saturation of the tracers has frequently been reported (e.g. Tanhua et al. (2008b)). Since we are interested in reporting the annual means for the compounds for their use as oceanic tracers of water masses, it is useful to know the atmospheric mole fractions of these compounds in late winter compared to annual means. JFM and JAS are nominally the coldest times in the Northern and Southern Hemispheres, respectively, and normally the main periods when water masses are formed. Therefore, we reconstructed JFM means and JAS means atmospheric mole fractions for all species in the Northern and the Southern Hemispheres. The annual mean atmospheric mole fractions of these compounds are mainly given to allow comparison to the annual mean atmospheric mole fractions for CFC-11, CFC-12, CFC-113, and  $CCl_4$  given in previous studies (Walker et al., 2000; Bullister, 2015).

As described in Sect. 2, there are a number of data sets available for HCFC-22, HCFC-141b, HCFC-142b, HFC-134a, HFC-125, HFC-23, PFC-14 and PFC-116 (Table S1, Fig. S1a-h). Once consolidated onto a single data set via a common calibration scale, all data were fitted by a smoothing spline to determine the monthly means for each compound. The hemispheric annual means, JFM means (NH) and JAS means (SH) atmospheric dry air mole fractions in parts per trillion (ppt) are then estimated and shown in Fig. S1a-h and the top panels of Fig. 2a-h. The associated uncertainties were estimated by error propagation and shown in the top panels of Fig. 2a-h. The mole fractions and associated uncertainties are also given with JFM means (e.g. 2000.125), annual means (e.g. 2000.500) and JAS means (e.g. 2000.625) and shown in Table S2. Annual growth rates were calculated based on the annual means, combined with their associated errors, and shown in the lower panels of Fig. 2a-h. Inter-hemispheric gradients (IHG) are estimated from the annual mean atmospheric mole fractions of a gas in the NH minus the annual mean in the SH in the same year (Fig. 2a-h). Errors of the IHG were estimated based on error propagation of the annual means in the NH and the SH in the same year (Fig. 2a-h).

##### 3.1.1 HCFC-22

HCFC-22 (Fig. 2a, Table S2 and Fig. S1a); Annual mole fractions of HCFC-22 are  $253.2 \pm 0.4$  ppt (NH) and  $231.2 \pm 0.3$  ppt (SH) in 2017, 23% increase from 2009 (Montzka et al., 2010a). The inter-hemispheric gradient (IHG) initially increased but has been diminishing since 2010 because of a decline in emission (growth rates). Growth rates for HCFC-22 rose steadily until 1990, followed by a slight decrease, which coincides with the large production and consumption reported between the 1950s and 1990s (Fig. 1) and a freeze of production magnitudes in the developed countries in 1996. A rapid increase oc-

Deleted: in...larger temperature range

Deleted: 18

Deleted: The surface water tends to sink toward the ocean interior, and in the process carries concentration signals of atmospheric gases that have been equilibrated with the surface water in preceding months. ...ur

Deleted: different ...ata sets available

Deleted: Figures 2-9 show annual means and growth rates in the northern (NH) and southern (SH) hemisphere lower tropospheric HCFC-22, HCFC-141b, HCFC-142b, HFC-134a, HFC-125, HFC-23, PFC-14 and PFC-16 concentrations in parts-per-trillion (ppt) and the associated uncertainty. The concentrations are given with mid-February (e.g. 2000.125), mid-year (e.g. 2000.500) and mid-August (e.g. 2000.625) and expressed as the mole fraction of the trace gas in dry air (Table S1). ¶ Global annual mean mole fractions of HCFCs, HFCs and PFCs have increased continuously in the background atmosphere throughout the whole atmosphere history record (Fig. 2-9). The mole fractions for all target compounds in the northern hemisphere are larger than those in the southern hemisphere. In general, recent growth rates are decreasing for HCFCs, increasing for HFCs and are stable for PFCs. ¶

Deleted: The monthly means atmospheric history of ...CFC-22 (Fig. 2a, Table S2

Deleted: The atmospheric mole fractions for HCFC-22 in the NH are 14% (median) larger than those in the SH over the entire record. The i...ter-hemispheric

Deleted: ¶ The g...rowth rates for HCFC-22 rose

5 ~~curred~~ between 2005 and 2008. Corresponding step changes were also ~~seen~~ in 2005 in both observations (upper panel in Fig. 2a) and emissions (Xiang et al., 2014), in response to the United Nations Environment Programme (UNEP) production changes (UNEP, 2018). The growth rate peaked in ~~2007 (NH) at 8.4 ppt yr<sup>-1</sup> and in 2008 (SH) at 7.6 ppt yr<sup>-1</sup>~~ before sharp 91% decline ~~to 2016~~ at an annual average rate of ~~0.8 ppt yr<sup>-2</sup> (NH) and 0.7 ppt yr<sup>-2</sup> (SH)~~. This suggests that global emissions are not growing as rapidly as before 2008, as reported by Montzka et al. (2015) and Grazioli et al. (2015), consistent with the accelerated phase-out ~~in the dispersive application~~ of HCFCs ~~since 2007~~ (Grazioli et al., 2015).

### 3.1.2 HCFC-141b

10 ~~HCFC-141b (Fig. 2b, Table S2, and Fig. S1b):~~ HCFC-141b ~~annual mole fractions~~ increased ~~from 1990~~, a slowdown ~~occurred~~ in the second-half of the 2000s, ~~corresponding to a sharp drop in production and consumption in 2005~~ (Montzka et al., 2015). HCFC-141b annual ~~mole fractions~~ ~~have~~ increased to a maximum of ~~26.0 ± 0.1 ppt (NH) in 2016 and 23.6 ± 0.1 ppt (SH) in 2017, representing 36% (NH) and 41% (SH) increases from 2005 and 7% (NH) and 12% (SH) increases from 2012.~~ This also suggests that the annual mole fractions in the NH began to decrease, ~~Rapid growth rates was seen before 1993 (NH) and 1995 (SH), coinciding with intensified industrial production and consumption of HCFCs in the 1990s. This is followed by a comparatively stable plateau period, 1994-1999 (NH) and 1995-1999 (SH), consistent with UNEP production~~ (Montzka et al., 2015) and consumption changes (UNEP, 2018). Subsequently, the growth rate declined until ~~around 2005~~. Since 2005, ~~production has increased substantially in developing countries, so growth rates recovered to higher values in 2006-2007.~~ Growth rates ~~in 2012~~ appear to be ~~109% (NH) and 59% (SH) decline to 2016 of -0.07 ppt yr<sup>-1</sup> (NH) and 0.36 ppt yr<sup>-1</sup> (SH).~~ The growth rates in 2016 are very close to the growth rates ~~seen in the 1980s~~. This decline coincides with the global production and consumption of HCFCs being capped in 2013 ~~in developing countries~~ (Montzka et al., 2015).

### 3.1.3 HCFC-142b

25 ~~HCFC-142b (Fig. 2c, Table S2, and Fig. S1c):~~ Annual mean mole fractions show a slow initial increase until 1989 followed by a sharp increase in the 1990s, the same slowdown in the mid-2000s as ~~seen with HCFC-141b~~, and finally a plateau in recent years. Annual mole fractions reached a maximum of ~~23.4 ± 0.1 ppt (NH) and 21.9 ± 0.1 ppt (SH) in 2017 at the end of the time series, representing a 39% (NH) and 48% (SH) increase since 2005.~~ Annual mole fractions in the NH show a ~~declining trend. The JHG and growth rates~~ exhibit two peaks, one in the 1990s, and another in 2007/2008 followed by a substantial drop. There are ~~minima~~ in growth rates around 2005 for all three HCFCs. The peak-valley-peak distribution patterns of HCFCs are consistent with the UNEP consumption changes (UNEP, 2018). This is followed by a dramatic 99% (NH) and 94% (SH) decline to 2015 ~~from 2007/2008~~ at an annual average rate of ~~0.14 ppt yr<sup>-2</sup>~~ for both hemispheres. This decline in both atmospheric mole fractions and emissions follows reduced production and consumption in developed countries and a levelling off of production and consumption in developing countries (Carpenter et al., 2014). The current growth rates are similar to those ~~seen~~ in the 1980s before the rapid increase in emissions.

### 3.1.4 HFC-134a

35 ~~HFC-134a (Fig. 2d, Table S2, and Fig. S1d):~~ Annual mean mole fractions have increased continuously since the 1990s. The monotonical increase is reflected in emissions (Xiang et al., 2014; Montzka et al., 2015; Simmonds et al., 2017). HFC-134a annual mole fractions reached a maximum of ~~102.7 ± 0.2 ppt (NH) and 89.4 ± 0.2 ppt (SH), by the end of the current time-series, representing 163% (NH) and 191% (SH) increases since 2005 and 40% (NH) and 42% (SH) increases since 2012.~~ JHG and growth rates started to increase around 1992, then rapidly increased in 1995-2004, followed by a ~~stabilization of growth rate in 2009-2012 and then an increase since 2012.~~ The maximum growth rates are shown at the end of the time-series of ~~6.5 ppt yr<sup>-1</sup> (NH) and 6.0 ppt yr<sup>-1</sup> (SH), representing 41% (NH) and 42% (SH) increases from 2005 and 26% (NH) and 25% (SH) increases from 2012.~~

Deleted: was found in Fig. 2b...

Deleted: 2008 ...007 (NH) at 8.45 ...

Deleted: . This...consistent with the

Deleted: For HCFC-22, the dispersive application was phased out. This suggests that the 2007 Adjustments played a role. The annual growth rates of HCFC-22 are 3.73 ± 0.30 ppt yr<sup>-1</sup> for NH and 4.03 ± 0.32 ppt yr<sup>-1</sup> for SH in 2016.

Deleted: The monthly means atmospheric history of HCFC-141b (Fig. 3a) is obtained by using the smoothing spline to fit the combined data shown in Table 2b. The mid-February, mid-year and mid-August annual mean atmospheric history and annual growth rates of HCFC-141b are shown in Fig. 3b.

Deleted: The annual mean mole fractions of ...CFC-141b annual mole fractions

Deleted: The ...CFC-141b annual

Deleted: with the reason mentioned above... But s...since 2005, the ...product

Deleted: The monthly means atmospheric history of HCFC-142b (Fig. 4a) used the data sources from Table 2c. The mid-February, mid-year and mid-August annual means atmospheric history and annual growth rates of HCFC-142b are shown in Fig. 4b. The a...annual mean mole fractio

Deleted: 19 ...4 ppt yr<sup>-1</sup>

Deleted: seen

Deleted: The monthly means atmospheric history of HFC-134a (Fig. 5a) is obtained by using the smoothing spline to fit the combined data in Table 2d. The mid-February, mid-year and mid-August annual means atmospheric history and annual growth rates of HFC-134a are shown in Fig. 5b. The a...annual mean mole fractions of

Deleted: The ...FC-134a annual mole

### 3.1.5 HFC-125

HFC-125 (Fig. 2e, Table S2, and Fig. S1e): Annual mean mole fractions, JHG and growth rates increased throughout the atmospheric history record, which reflects a continuing increase in emissions (O'Doherty et al., 2009; Montzka et al., 2015; Simmonds et al., 2017). Annual mole fractions reached a maximum of  $25.7 \pm 0.1$  ppt (NH) and  $21.7 \pm 0.05$  ppt (SH) at the end of the time-series, representing 199% (NH) and 216% (SH) increases since 2009 (O'Doherty et al., 2009). The growth rate reached a peak of  $3.1$  ppt yr<sup>-1</sup> (NH) and  $2.6$  ppt yr<sup>-1</sup> (SH) by the end of the time-series, representing 117% (NH) and 138% (SH) increases from 2009. The increase in growth rate of HFC-125 is more than three times the growth rate increase for HFC-134a.

### 3.1.6 HFC-23

HFC-23 (Fig. 2f, Table S2 and Fig. S1f): Annual mean mole fractions have increased since 1978. HFC-23 atmospheric mole fractions peaked at  $30.7 \pm 0.05$  ppt (NH) and  $29.2 \pm 0.06$  ppt (SH) by the end of the time-series (in 2017), representing 33% (NH) and 32% (SH) increases since 2009 (Miller et al., 2010). JHG and growth rates exhibit an increasing trend with large fluctuations over the time-series, with local maxima in the growth rate in 2006 and 2013, and a minimum in 2009, which reflect changes in emissions (Carpenter et al., 2014; Simmonds et al., 2018). The slowing in growth rate was in response to emission reductions in developed countries that began in the late 1990s, combined with the UNFCCC CDM destruction program for the developing countries that started around 2007 (Miller and Kuijpers, 2011; Carpenter et al., 2014). The higher values in growth rates could be attributed to the increase in production of HCFC-22 with no subsequent incineration of HFC-23 (Miller and Kuijpers, 2011; Carpenter et al., 2014). The current annual growth rates are  $1.1$  ppt yr<sup>-1</sup> (NH) and  $0.86$  ppt yr<sup>-1</sup> (SH), representing 100% (NH) and 68% (SH) increases since 2009.

### 3.1.7 PFC-14 (CF<sub>4</sub>)

PFC-14 (Fig. 2g, Table S2, and Fig. S1g): Trudinger et al. (2016) used a firm diffusion model to determine the atmospheric abundance of PFC-14 since 1900 from ice core, firm air, archived air and in situ measurements. Here we updated and extended the time series assembled by Trudinger et al. (2016). PFC-14 has a natural background of  $34.05 \pm 0.33$  ppt (Trudinger et al., 2016). Annual mean mole fractions and growth rates began to increase around 1900, with a local maximum in growth rate around 1943. The maximum reflects changing emissions from increasing aluminium production during World War II (Barber and Tabereaux, 2014; Trudinger et al., 2016), for example for the construction of aircraft. Mole fractions of PFC-14 began to increase rapidly in the 1970s. Since then it has continued to grow, reaching a maximum of  $84.30 \pm 0.04$  ppt (NH) and  $83.05 \pm 0.03$  ppt (SH) at the end of the time-series (in 2017), representing 8% (NH) and 7% (SH) increases from 2009. The growth rates began to increase from the 1950s and peaked in 1980 before declining. The decline is attributed to a concerted effort by the aluminium and semiconductor industries to reduce their emissions (Trudinger et al., 2016). The growth rate minimum in 2009 could be related to the Global Financial Crisis (Trudinger et al., 2016). PFC-14 growth rates have increased again during the last five years probably due to increased aluminium production, and perhaps rare Earth element production in developing countries (Vogel and Friedrich, 2018). The current growth rates are  $0.91$  ppt yr<sup>-1</sup> (NH) and  $0.85$  ppt yr<sup>-1</sup> (SH), representing 48% (NH) and 49% (SH) increases from 2009.

### 3.1.8 PFC-116

PFC-116 (Fig. 2h, Table S2, and Fig. S1h): We updated and extended the time series previously shown in Trudinger et al. (2016). PFC-116 has a pre-industrial background of  $0.002$  ppt (Trudinger et al., 2016). PFC-116 shows a similar atmospheric trend to PFC-14. Annual mean mole fractions have increased since 1900, with a step up around 1943 (discussed above, PFC-116 is co-produced with PFC-14 during aluminium production), then increased significantly in the 1970s, reaching  $4.73 \pm 0.007$  ppt (NH) and  $4.06 \pm 0.007$  ppt (SH) by the end of the record, representing 16% increases from 2009. PFC-116

**Deleted:** The monthly means atmospheric history of HFC-125 (Fig. 6a) is obtained by using the smoothing spline to fit the combined data in Table 2e. The mid-February, mid-year and mid-August annual means atmospheric mole fractions and annual growth rates of HFC-125 are shown in Fig. 6b. The annual mean mole fractions, I...

**Deleted:** The HFC-125 annual mole ...

**Deleted:** for HFC-125 also ... each a ...

**Deleted:** ¶

**Deleted:** The monthly means atmospheric history of HFC-23 (Fig. 7a) is determined by combining the data in Table 2f. The mid-February, mid-year and mid-August annual means atmospheric history and annual growth rates of HFC-23 are shown in Fig. 7b. The annual mean mole ...

**Deleted:** The ...HG and growth ...

**Deleted:** HFC-23 ...rowth rate was in ...

**Deleted:** at the end of the time-series for HFC-23 ...re  $1.1078 \pm 0.02$  ...ppt yr<sup>-1</sup> ...

**Deleted:** The monthly means atmospheric history of PFC-14 (Fig. 8a) is estimated using the smoothing spline to fit the data in Table 2g.

**Deleted:** inferred ...rom ice core, ...

**Deleted:** The mid-February, mid-year and mid-August annual means atmospheric history and annual growth rates of PFC-14 are shown in Fig. 8b. ...FC-14 has a nat...

**Deleted:** The annual mean mole ...

**Deleted:** Afterwards, the m...ole ...

**Deleted:** dip ...rowth rate minimum in ...

**Deleted:** The ...rowth rates of PFC- ...

**Formatted** ...

**Deleted:** maybe because of the increased primary aluminium production year after year (Trudinger et al., 2016) and the global economic recovery. The growth rates for PFC-14 have initial increased slowly, experienced a small peak in 1943/1944, stayed a relatively stable period, followed by a big peak in 1980/1981 and subsequently decreased to a stable value with small fluctuations. The small peak values are  $0.41 \pm 0.05$  ppt yr<sup>-1</sup> and  $0.34 \pm 0.04$  ppt yr<sup>-1</sup> for each hemisphere whereas the large peak values are  $1.22 \pm 0.05$  ppt yr<sup>-1</sup> for NH and  $1.18 \pm 0.04$  ppt yr<sup>-1</sup> for SH

**Deleted:** stable average...urrent growth ...

**Deleted:** The monthly means atmospheric history of PFC-116 (Fig. 9a) used the data source in Table 2h. ...Here w... updated ...

**Deleted:** The mid-February, mid-year and mid-August annual means atmospheric history and annual growth rates of PFC-116 are shown in Fig. 9b. ...FC-116 has a pr...

**Deleted:** The annual mean mole ...

growth rates began to increase slowly, followed by maxima around 1943 (discussed above for PFC-14). Then they have declined and stayed relatively stable until 1965, when they started to climb to a maximum at the end of the 1990s. Subsequently, they declined and stayed relatively stable at 0.104 ppt yr<sup>-1</sup> (NH) and 0.09 (SH) ppt yr<sup>-1</sup>, representing increases of 31% (NH) and 38% (SH) from 2009.

Global annual mean mole fractions of HCFCs, HFCs and PFCs, except HCFC-141b and HCFC-142b, have increased continuously in the background atmosphere throughout the whole atmosphere history record (Fig. 2a-h). Recent growth rates are decreasing for HCFCs, are increasing for HFCs and are stable for PFCs. From Fig. 2a-h, it is clear that the mole fractions for target compounds in the NH are always larger than those in the SH but follow similar trends; the growth rates in both hemispheres are also similar, lagged in the SH, and the trends in IHG and in emissions/growth rates are very similar. This behavior is because the majority of the emissions (typically > 95%) occur in the NH extra-tropics (O'Doherty et al., 2009; Saikawa et al., 2012; Carpenter et al., 2014; UNEP, 2018) and the interhemispheric mixing time is around one or two years. Thus the larger (the increase) in emissions in the NH, the higher the resultant IHG. If all emissions stop, long-lived compounds would expect to reach near-identical mole fractions in both hemispheres.

### 3.2 Growth Patterns

The atmospheric history trends of target compounds generally follow expected patterns based on the history of their known industrial applications and production bans. We can make out three distinct behavioural patterns where we could predict the trend of annual mean mole fractions of these compounds. Pattern I: the annual mean mole fractions show sigmoidal (S-shaped) growth and the annual growth rates exhibit the shape of Gaussian distribution over the whole time period, such as HCFC-141b and HCFC-142b. This means that annual mole fractions of these compounds are going to decrease or are decreasing. Pattern II: the annual mean mole fractions show initial exponential growth followed by a period of linear increase, whilst the growth rates show a sigmoidal pattern but slightly increase recently, such as HFC-134a and HFC-23 (combined the modelled mole fractions output of HFC-23 from 1950 to 2016 in Fig. 1, Simmonds et al. (2018)). This means that mole fractions of these compounds are going to continuously increase with relatively slower growth rates in the near future. Afterward, they will likely experience a plateau phase, followed by a decline following the restrictions imposed by the 2016 Kigali Amendment to the Montreal Protocol. Since the atmospheric lifetime of HFC-23 is much longer than that of HFC-134a, time-profiles and IHG change are expected to be a little different between HFC-134a and HFC-23. Pattern III: The annual mean mole fractions and growth rates both show exponential (J-shaped) growth, such as HFC-125. So the atmospheric history and growth rates of HFC-125 are going to increase for a longer period of time than HFC-134a and HFC-23, and then will likely follow a similar path to the compounds in Pattern II as they are subjected to the same regulations.

The annual mean mole fractions of the remaining halogenated compounds, HCFC-22, PFC-14 and PFC-116, have also increased throughout the time-series and continue to increase today. The growth rates of these compounds initially increased and experienced a peak before declining. The growth trend for HCFC-22 is more likely to experience a plateau and then decrease and follow the trends of HCFC-141b and HCFC-142b as they are subjected to the same regulations. Different from all other target compounds, the annual mean growth rates of PFC-14 and PFC-116 have stabilized after a short decline without specific restrictions on emissions. This could be attributed to the changing sources of both PFC-14 and PFC-116. PFC emissions from the aluminium industry dominated for a long time but have likely been declining for the past decade or so, while emissions by the electronics industry (Kim et al., 2014) and probably the rare earth elements industry became more important. The very long lifetimes of PFCs in the atmosphere makes a decrease in the atmospheric mole fraction unlikely in the foreseeable future.

Considering the combined growth patterns and the production and consumption histories for these gases (Fig. 1), the sequence of atmospheric change of HCFCs and HFCs coincide with the replacement sequence of CFCs. In 1980s, CFCs were

Deleted: for PFC-116

Deleted: u

Deleted: experience a higher value in

Deleted: /1944,

Deleted: comparatively

Deleted: for a period of time,

Deleted: ed gradually

Deleted: large peak in

Deleted: and s

Deleted: to a

Deleted: value with small fluctuations. The higher value of PFC-116 in 1940s has the same reasons as PFC-14. The large peak values of PFC-116 are  $0.038 \pm 0.007$  ppt yr<sup>-1</sup> for NH and  $0.033 \pm 0.008$  ppt yr<sup>-1</sup> for SH. The growth rates by the end of the time-series are

Deleted:  $078 \pm 0.003$

Deleted: for both hemispheres

Moved (insertion) [7]

Deleted: As for HCFCs, global and regional studies (Montzka et al., 2009; Saikawa et al., 2012; Carpenter et al., 2014) suggest a shift of HCFC emissions from mid-latitudes to lower latitudes, corresponding to recent shifts of production and consumption from developed countries to developing countries (mostly distributed at lower latitudes).

Deleted: Sigmoidal

Deleted: a

Deleted: normal

Deleted: for example

Deleted: The largest inter-hemispheric gradients approximately coincide with the maximum annual growth rates. In recent times the inter-hemispheric gradients of (...)

Deleted: Sigmoidal

Deleted: for example

Deleted: l

Deleted: from

Deleted: T

Deleted: atmospheric concentration hi (...)

Deleted: consumption

Deleted: )

Deleted: for example

Deleted: T

Deleted: Common for both Pattern II a (...)

Deleted: carbons

Deleted: The annual mean mole fractio (...)

Deleted: stayed stable

Deleted: a ban

Deleted: E

Deleted: . These are offset by increasing

Deleted: from

Deleted: concentration

found to be a threat to the ozone layer (Molina and Rowland, 1974; Rowland and Molina, 1975). To facilitate the **phase-out** of the more potent **ozone depleting CFCs**, HCFC production and consumption increased rapidly in developed countries in the 1990s and in developing countries in the mid-2000s as industrial/**domestic** usage as CFCs was curtailed. Thus, atmospheric growth rates of HCFCs reached a peak in the 1990s and/or 2000s. Following the 2007 amendment to the Montreal Protocol, the production and consumption of HCFCs was **phased-out sooner than originally mandated**. With a large **emission source** of HCFC-22 existing in refrigeration systems **and stockpiling**, emissions are expected to continue (Carpenter et al., 2014). The atmospheric mole fractions of HCFCs tend toward stable values or decline as a consequence of the freeze of HCFC production and consumption for dispersive uses in 2013 in Article 5 countries. Moreover, the growth rates of HCFCs are decreasing. HFCs have been developed as potential substitutes for both CFCs and HCFCs because they pose no harm to the ozone layer. Their production and consumption has increased rapidly over the past decade or so. This accounts for the **rapid** growth of the atmospheric mole fractions of many HFCs and the J-shaped or S-shaped patterns of their growth rates.

### 3.3 Solubility in seawater

The seawater solubility functions for HCFC-22, HCFC-141b, HCFC-142b, HFC-134a, HFC-125, HFC-23, PFC-14 and PFC-116 are estimated, based on their freshwater **solubilities** as no direct studies of the solubility functions of the target compounds in seawater have been published.

#### 3.3.1 Solubility in freshwater

Available freshwater solubility data **for HCFC-22, HCFC-141b, HCFC-142b, HFC-134a, HFC-125, HFC-23, PFC-14 and PFC-116** from previous studies were compiled. These data were converted to a common solubility unit (Ostwald solubility,  $L_0$ , in  $L L^{-1}$ ) and fitted with the Clark-Glew-Weiss (CGW) function of temperature to **construct** the freshwater solubility equations **shown in** Fig. S2a-h. Only the observed **values of** water solubility from Abraham et al. (2001) are involved in the fits. Those calculated **values** using the (Revised) Method II (described below) are **shown** only for comparison. The water solubility functions in Ostwald solubility units for HCFC-22, HFC-134a, HFC-125, HFC-23 and PFC-116 (Fig. S2a, d, e, f, h) **are** compared with the results from Deeds (2008) **and agree well, except for HFC-125**.

For HFC-125, **three fitted curves are** shown in Fig. S2e, **reflecting that data obtained by different methods do not agree with each other**. **Curve 1 includes data from** Miguel et al. (2000), **where the  $\phi$ - $\phi$  approach (the fugacity coefficient - fugacity coefficient method) has been used to predict the experimental results and the fugacity coefficients were calculated using a modified version of the Peng-Robinson equation of state, and Battino et al. (2011) where the data were collected from the International Union of Pure and Applied Chemistry (IUPAC) Solubility Data Series and, in some cases, as averages or estimates. Curve 2 includes data from Mclinden (1990) obtained from the vapour pressure of the pure substance divided by aqueous solubility (sometimes called VP/AS), and HSDB (2015) where the data were calculated with the quantitative structure-property relationship (QSPR) or a similar theoretical method. Curve 3 includes data from Reichl (1995) and Abraham et al. (2001)-observed, which are both measured values from original publications. Considering that the data which were based on measurements match with our results (Fig. S2e) calculated by Method II (only based on the physical properties of compounds), **Curve 3 (the curve in the bottom) is chosen** as the water solubility fit.**

In Deeds (2008), freshwater solubility functions in Bunsen solubility unit ( $\alpha$ , in  $L L^{-1}$ , at standard temperature and pressure, STP) were converted to the Ostwald solubility unit for comparison. The freshwater solubility function in Ostwald solubility unit for PFC-14 (Fig. S2h) was compared with the results from Clever (2005) and Deeds (2008). The fit for water solubility functions agrees to within 4.0%, 7.8%, 2.5%, 6.8%, 5.9%, 2.3%, 0.95% and 3.5% with majority (two-thirds) of the data for HCFC-22, HCFC-141b, HCFC-142b, HFC-134a, HFC-125, HFC-23, PFC-14 and PFC-116, respectively. The constants  $a_1$ ,  $a_2$ ,  $a_3$  for solubility functions of the target compounds in water are given in Table 5.

- Deleted: phase
- Field Code Changed
- Deleted: as ozone depleting substance
- Deleted: is consistent with the
- Deleted: accelerated
- Deleted: phase
- Deleted: bank
- Deleted: ,
- Deleted: exponential
- Moved up [7]: As for HCFCs, global
- Deleted: As for HCFCs, global and
- Moved (insertion) [1]
- Moved up [1]: (Ashford et al.,
- Deleted: solubility
- Formatted: Heading 3
- Deleted: of
- Deleted: all species
- Deleted: collected and
- Deleted: The freshwater solubility data
- Deleted: for all species
- Deleted: build
- Deleted: (
- Deleted: 1-S8)
- Deleted: values
- Deleted: involved
- Deleted: 1, S4-S6, S8
- Deleted: were
- Deleted: there are
- Deleted: S5
- Deleted: .
- Deleted: the
- Deleted: Table S2,
- Deleted: 1-S8
- Deleted: the Revised
- Deleted: the
- Deleted: the
- Deleted: in
- Deleted: (
- Deleted: )
- Deleted: S7
- Deleted:
- Deleted: 4

In order to validate the calculation method of water solubility, the solubility for CFC-12 in water calculated by the Combined Method and by the method from Warner and Weiss (1985) were compared. Warner and Weiss (1985) estimated the freshwater and seawater solubility function of CFC-12 by experiments and a different model fit without using a salting-out coefficient. The freshwater solubility function of CFC-12 calculated by the Combined Method was constructed by collecting freshwater solubility data from the literature (Fig. S2i). The freshwater solubility of CFC-12 from Warner and Weiss (1985) match data from other studies very well (the root-mean-square of misfit is 0.006). Moreover, the fits based on the function in Warner and Weiss (1985) and the CGW model in this study match very well (Fig. S2i). The average Relative Standard Deviation (RSD) of water solubility estimated by the two methods for CFC-12 in the range of 273.15-313.15 K (0-40 °C) is 0.17%. This means that our method for estimating the freshwater solubility is valid.

Deleted: (Fig. S9) ...as constructed by

Deleted: fit...in this study match very

### 3.3.2 Salting-out coefficient

The salting-out coefficient  $K_S$  is independent of salinity and is a function only of temperature, which can be obtained from Method I and Method II in Sect. 2.7. In order to validate this,  $K_S$  was calculated by Eq. (16) (Method II) based on the experimental results of the freshwater and seawater solubility of CFC-12 from Warner and Weiss (1985). The average of  $K_S$  is  $0.229 \pm (1.41 \cdot 10^{-15}) \text{ L g}^{-1}$  at 298.15 K when the salinity is in the range of 0-40. The RSD is  $6.16 \cdot 10^{-13}\%$ , which is minor enough to be neglected. Thus  $K_S$  is independent of salinity. In Fig. S3, a quadratic relationship between the salting-out coefficient and temperature was found.  $K_S$  is in the range of 0.229-0.249  $\text{L g}^{-1}$  (at a mean of  $0.235 \pm 0.005 \text{ L g}^{-1}$ ) at a salinity of 35 when the temperature is in the range of 273.15-313.15 K (0-40 °C). The RSD is 2.3%. This means that the effect of temperature on the salting-out coefficient is also very small.

Deleted: Based on the experimental results of the freshwater and seawater solubility of CFC-12 from Warner and Weiss (1985), t

Deleted: (calculated by the Combined Method)...is independent of salinity and

Deleted: In the study of Warner and Weiss (1985), t

Deleted: ..., which is minor enough t

In order to estimate the solubility functions for target compounds in seawater, their salting-out coefficients ( $K_S$ ) should be estimated. As shown in Eq. (17),  $K_S$  is estimated based on the descriptors of all target compounds. With the exception of PFC-116,  $E$ ,  $S$ ,  $A$ ,  $B$ ,  $V_e$  values for the target compounds were obtained from studies (Abraham et al., 2001; 2012). For PFC-116, the excess molar refraction ( $E$ ) was calculated by Eq. (15). The dipolarity/polarizability ( $S$ ) for PFC-116 ( $\text{C}_2\text{F}_6$ ) was estimated as -0.350 based on the  $S$  of PFC-14 ( $\text{CF}_4$ , -0.250) and PFC-218 ( $\text{C}_3\text{F}_8$ , -0.450) (Abraham et al., 2001) and the error for the estimate of  $S$  is estimated to be 0.02 based on the error propagation.  $A$  and  $B$  for PFC-116 ( $\text{C}_2\text{F}_6$ ) are both zero since it includes only carbon-halogen atom bonds and no carbon-hydrogen bonds.  $V_e$  of PFC-116 was obtained from studies (Abraham and McGowan, 1987; Goss et al., 2006). The values of all descriptors for the target compounds are shown in Table 4. The errors in calculating the descriptors were estimated as 0.088, 0.047, 0.128, 0.081, 0.095, 0.051, 0.071 and 0.088 for HCFC-22, HCFC-141b, HCFC-142b, HFC-134a, HFC-125, HFC-23, PFC-14 and PFC-116, respectively (Abraham et al., 2001). On the basis of the  $E$ ,  $S$ ,  $A$ ,  $B$ ,  $V_e$  descriptors,  $K_S$  was estimated at  $298.15 \pm 2 \text{ K}$  and are also shown in Table 5.

Deleted: also ...e estimated. As showr

Deleted: 11...5). The

Deleted: C...halogen atom bonds and

Deleted: 5

Deleted: V...descriptors,  $K_S$  was

Deleted: we know from the...hown in

Formatted: Not Superscript/ Subscript

Deleted: , so here...we assume that the

As shown in Sect. 2.7.2,  $K_S$  changes with temperature are described by the coefficients  $c$ ,  $e$ ,  $s$ ,  $a$ ,  $b$ , and  $v$  in Eq. (17). The salting-out coefficient is a second-order polynomial function of temperature as we described in Method I in Sect. 2.7.1 and discussed above for CFC-12 based on Method II. Based on the discussion of CFC-12, the effect of temperature on the salting-out coefficient is small. Also, very limited studies of  $K_S$  have been reported and we assume that the salting-out coefficient  $K_S$  does not change with temperature (i.e. it is a constant). Thus the final salting-out coefficient are calculated using Eq. (17) at 298.15 K for the target compounds and shown in Table 5.

### 3.3.3 Solubility in seawater based on Combined Method

Following the calculation method shown in Sect. 2.7.3, seawater solubility functions for HCFC-22, HCFC-141b, HCFC-142b, HFC-134a, HFC-125, HFC-23, PFC-14 and PFC-116 were constructed in the corresponding temperature range (Table 5) based on Eq. (19). Ostwald solubility coefficients in seawater at 1 atm, 25 °C and 35  $\text{g kg}^{-1}$  were estimated to be 0.669  $\text{L L}^{-1}$  for HCFC-22, 0.537 (HCFC-141b), 0.268 (HCFC-142b), 0.292 (HFC-134a), 0.063 (HFC-125), 0.249 (HFC-23), 0.00388 (PFC-14) and 0.00102 (PFC-116), respectively (Table 5). For comparison, the solubilities of CFC-12, CFC-11, CFC-113,

Deleted: ¶  
Based on ...following the

CCl<sub>4</sub> and SF<sub>6</sub> in seawater are converted to the Ostwald solubility unit at 1 atm, 25°C and 35 g kg<sup>-1</sup>. They are 0.0504, 0.177, 0.0518, 0.568 and 0.00401 L L<sup>-1</sup>, respectively. In previous studies, Mackay et al. (2006) reported that many hydrocarbons have solubility in seawater of ~75% of their solubility in distilled water. Moore et al. (1995) reported that the solubility of short-lived halocarbons (e.g. CH<sub>3</sub>I, CHBr<sub>3</sub>, CH<sub>2</sub>Br<sub>2</sub>, CHBr<sub>2</sub>Cl, and CHCl<sub>3</sub>) in seawater is 80% of their solubility in freshwater. For comparison, the solubility of CFC-12 in seawater is 73% of its solubility in freshwater (Warner and Weiss, 1985). The percentages are 72% for CFC-11 (Warner and Weiss, 1985), 74% for CFC-113 (Bu and Warner, 1995), 78% for CCl<sub>4</sub> (Bullister and Wisegarver, 1998) and 73% for SF<sub>6</sub> (Bullister et al., 2002). For our target compounds, the percentages of the seawater solubility on the freshwater solubility at 298.15 K and salinity of 35 are 79% for HCFC-22 and HFC-23, 77% for HFC-134a, 76% for HCFC-141b, HCFC-142b and PFC-14, 73% for HFC-125, and 71% for PFC-116. Similar to the CFCs and SF<sub>6</sub>, the percentages for HCFCs, HFCs and PFCs are also in the range of around 70-80%.

The temperature dependence of the Ostwald solubility coefficients of the target compounds in seawater at a salinity of 35 is shown in Fig. 3. The dependence on salinity at 298.15 K is shown in Fig. 4. Seawater solubilities fall monotonically, with increasing temperature and salinity. The latter shows a near linear decline.

Overall uncertainties of water solubility estimates for target compounds are calculated as the root-mean-square of the misfit between the measurements and the fitted values. They are 0.0352 L L<sup>-1</sup> for HCFC-22, 0.0283 (HCFC-141b), 0.0065 (HCFC-142b), 0.0141 (HFC-134a), 0.0016 (HFC-125), 0.0132 (HFC-23),  $9.0695 \times 10^{-5}$  (PFC-14) and  $9.1858 \times 10^{-5}$  (PFC-116). The uncertainties of seawater solubility of target compounds at different salinities (0-40) and a temperature of 298.15 K are estimated by the propagation of uncertainty from water solubility and salting-out coefficients. They are 0.034 L L<sup>-1</sup> for HCFC-22, 0.032 (HCFC-141b), 0.031 (HCFC-142b), 0.031 (HFC-134a), 0.030 (HFC-125), 0.031 (HFC-23), 0.030 (PFC-14) and 0.029 (PFC-116). The uncertainties of seawater solubility at different temperatures (273.15-313.15 K) and a salinity of 35 are also estimated by the same method. They are 0.041 L L<sup>-1</sup> for HCFC-22, 0.037 (HCFC-141b), 0.029 (HCFC-142b), 0.030 (HFC-134a), 0.026 (HFC-125), 0.029 (HFC-23), 0.027 for (PFC-14) and 0.025 (PFC-116).

In order to evaluate the effectiveness of the Combined Method, the Ostwald solubility coefficients of PFC-14 in seawater estimated by the Combined Method were compared with the observed values (Table 6) because only seawater solubilities of PFC-14 have been measured (Scharlin and Battino, 1995). The estimated solubility of PFC-14 in seawater at 293.15 K is the closest to the measured values. The RSD of calculated value and the measured value is only 0.79%.

### 3.3.4 Comparison of solubility in seawater based on three methods

In order to validate the possibility of Method I and Method II, and to find out the advantages of the Combined Method, we estimated seawater solubilities of the target compounds based on Method I and Method II and compared them to the results from the Combined Method.

For Method I, only the seawater solubility function of PFC-14 was constructed (Table S3) as only the seawater solubility of PFC-14 has been measured (Scharlin and Battino, 1995). The advantage of the constructed seawater solubility function is that it can be used over a greater temperature range rather than only for a few selected temperatures.

The only difference between Method II and the Combined Method is the difference in estimating water solubility. For water solubility calculations, Method II uses the pp-LFERs, based only on the physical properties of compounds, whereas the Combined Method uses the CGW model based on measurements. For water solubility based on the pp-LFERs, the water solubilities  $L_0$  estimated by Eqs. (12), (13) and (14) based on  $V$ ,  $\log L^{16}$  and  $V_c$  were compared to the observed values (Table S4). As shown in Table S4, the water solubilities of most compounds calculated based on  $V_c$  (Revised Method II) are closer to both the observed values (Abraham et al., 2001) and the CGW fitted values than when they are calculated based on  $V$  or  $\log L^{16}$  (Method II). So Revised Method II is more suitable for target compounds except for HFC-125 for which the pp-LFER model method is used. The calculated water solubilities based on the (Revised) Method II are shown in Fig. S2a-i for comparison. Small differences in water solubility calculated by the (Revised) Method II and the Combined Method (CGW

Deleted: L L<sup>-1</sup>... 0.177 L L<sup>-1</sup>... 0.0518

Deleted: about ...f ~75

Deleted: ... of their solubility in

Deleted: 1.7

Deleted: 3.5

Deleted: .4

Deleted: 2.7

Deleted: .2 ... for HCFC-22 and HFC

Deleted: in the available temperature range ...t the permanent... salinity of 35

Deleted: The o...verall uncertainties of

Moved (insertion) [6]

Deleted: Comparison of...the Ostwald

Deleted: is shown in Table 6... The

Deleted: We also used Method I to build the...ly the seawater solubility function

Deleted: Whereas

Moved up [6]: Comparison of the Ostwald solubility coefficients ( $L$ , L L<sup>-1</sup>) of PFC-14 in seawater estimated by the Combined Method with the measured results from Scharlin and Battino (1995) is shown in Table 6. The estimated solubility of PFC-14 in seawater at 293.15 K is the closest to the measured values. The RSD of calculated value and measured value is only 0.79%.

Deleted: T...he only difference

Deleted: S2...4, with the exception of

Deleted: Based on the above discussio

model) verifies the reliability of both methods. Compared with the pp-LFERs model method, the water solubility estimated by the CGW model method is closer to the observed values (Table S4). This is also the reason why the CGW model method from Method I is chosen for the Combined Method in estimating water solubility coefficients. The final seawater solubility functions of target compounds and CFC-12 based on (Revised) Method II are shown in Table S5.

Until now, seawater solubility functions for target compounds and CFC-12 based on (Revised) Method II and the Combined Method were constructed. In order to better understand the difference between experimental results and model estimations, we compared the seawater solubility of CFC-12 calculated from Warner and Weiss (1985), from Revised Method II and from the Combined Method. The results are shown in Fig. 5. The RSDs of the seawater solubility for CFC-12 estimated by the Revised Method II and by Warner and Weiss (1985) are 3.4% at 298.15 K and 13.5% at 310.15 K. The average RSDs of the seawater solubilities estimated by Warner and Weiss (1985) and by the Combined Method are  $1.4 \pm 0.9\%$  in the coincidental temperature range of 278.15-313.15 K at the same salinity of 35, and  $2.9 \pm 0.4\%$  in the coincidental salinity range of 0-40 at the same temperature of 298.15 K. These results show that the seawater solubility estimated by the Combined Method is very close to measured values in Warner and Weiss (1985). Without measurements of seawater solubility of these compounds, the Combined Method is a good way to estimate the seawater solubility.

Based on the discussion above we make the following recommendation with respect to the calculation of seawater solubilities of halogenated compounds:

(i) The (Revised) Method II could be used to estimate the seawater solubilities of compounds when neither water solubility data nor seawater solubility data have been measured. This method is only based on the physical properties of compounds. The water solubility values and the salting-out coefficients are both estimated using the pp-LFERs.

(ii) The Combined Method is a better way to estimate the seawater solubility of compounds when water solubility but not seawater solubility has been measured. This is the case for the current study. The water solubility function is constructed based on the CGW fit and the salting-out coefficient is estimated using the pp-LFERs.

(iii) The Method in published studies (Warner and Weiss, 1985; Bu and Warner, 1995; Bullister and Wisegarver, 1998; Bullister et al., 2002) is the best way to estimate the seawater solubilities. Here, both the water solubility values and seawater solubility values are experimentally determined.

It is worth noting that these methods can potentially be applied to many more compounds.

### 3.4 Transient Tracer potential and comparison with CFC-12

The production and consumption history of CFC-12 is shown in Fig. 1. The history of CFC-12 use as an oceanic transient tracer is also presented here. In 1973, Lovelock et al. (1973) first proposed that CFC-12 can be used as a transient tracer to study water masses in the ocean. Subsequently, large numbers of studies (Gammon et al., 1982; Weiss et al., 1985; Smethie et al., 1988; Körtzinger et al., 1999; Tanhua et al., 2008; Smith et al., 2016; Fine et al., 2017) using CFC-12 as an oceanic transient tracer have been published. In the 1990s, the World Ocean Circulation Experiments (WOCE) used CFC-12 as the normal tracer to investigate global ocean circulation and mixing. CFC-12 is still used as a tracer, although its production was prohibited in 1996 and its atmospheric mole fraction subsequently peaked in the early-2000s and is now in slow decline.

As one of the requirements to be a useful oceanic tracer, well-established and transient source functions (i.e. atmospheric abundance histories), have been established for HCFC-22, HCFC-141b, HCFC-142b, HFC-134a, HFC-125, HFC-23, PFC-14, and PFC-116 here. With the exception of HCFC-141b (Fig. S1b) and HCFC-142b (Fig. S1c), the discussed compounds are still steadily increasing in the atmosphere. Therefore, they have the potential to be used as oceanic transient tracers if only considering their source functions.

For HCFCs, only mole fractions of HCFC-22 are continuing to increase in the global atmosphere. All three HCFCs show declining growth rates since 2007. Combined with the ban on HCFCs in 2007, with freezing in 1996 (developed)/2013 (developing) and phase-out in 2020/30 (Fig. 1), HCFCs can likely be used as oceanic transient tracers for the next several dec-

Deleted: For comparison, with the exception of ...he seawater solubility

Deleted: the functions were also constructed by...rom the ...evised Method I

Deleted: are...3.41 ... at 298.15 K and

Deleted: is ...re 1.40...± 0.85 ...% in

Deleted: 4...± 0.44 ... in the coincident

Deleted: on ...f seawater solubility of

Deleted: , some conclusions on the methods...to the calculation estimate the...of

Moved down [5]: It is worth noting that these methods can potentially be applied to many more compounds.

Deleted: 1...i)...The (Revised) Meth

Deleted: 2...The Combined Method if

Deleted: 3...The Method in

Deleted: solubility...olubilities. Here,

Moved (insertion) [5]

Deleted: CFC-12 was first synthesized by the Belgian scientist Frédéric Swartz during 1890s (Jacobson, 2012). In 1931, CFC-12 was produced by the DuPont manufacturer under the trade name Freon. In 1974, Molina and Rowland (1974) proposed that CFC-12 could destroy the stratospheric ozone. In 1984, the "ozone hole" was discovered by the British Antarctic Survey (Farman et al., 1985). The culprit is the Chlorine injected into the stratosphere by the CFCs. In 1987, governments negotiated the Montreal Protocol. Following revisions mandated the freezing of CFC-12 in 1989 for developed countries and in 1999 for developing countries. Following revisions also mandated the complete phase-out of CFC-12. For developed countries, CFC-12 production and consumption ban was advanced to 1 January 1996. For developing countries, its ban was mandated in 2010 (UNEP, 2006).¶

Deleted: d...as an oceanic transient tra

Deleted: Afterwards...ubsequently, la

Deleted: extensively ...sed as a tracer,

Deleted: 3a... and HCFC-142b (Fig.

Deleted: Although ...CFCs, except ...

ades for recently ventilated waters. Due to a fall in emissions of HCFC-141b and HCFC-142b, the use of these two compounds will be more limited than HCFC-22 considering that atmospheric mole fractions of HCFC-141b have already begun to decrease and atmospheric mole fractions of HCFC-142b are likely to decrease quite soon. Therefore, atmospheric lifetimes of compounds are quite important particularly once emissions have fallen. When atmospheric mole fractions of a given compound start to decrease, it is obviously not monotonically increasing anymore, and the resultant calculated equilibrium atmospheric mole fraction in the ocean is no longer unique. Consequently, there will be two possible apparent ages for water masses so that this compound will have limited use as an oceanic tracer.

Deleted: and its relatively short atmospheric lifetime compared to HCFC-22 and HCFC-142b... the use of HCFC-

The mole fractions of HFCs are continuously increasing in the atmosphere, as are their growth rates. Restrictions on HFC consumption in the 2016 Kigali Amendment with freezing of consumption in 2019 and phase-out in 2024/28 (Fig. 1), mean that HFCs can likely be used as oceanic transient tracers for young waters for the next several decades. Moreover, HFCs have a higher potential to be oceanic transient tracers than HCFCs considering the increasing growth rates in the background atmosphere.

Deleted: concentration...ole fractions

PFCs are increasing in the atmosphere over a well-known natural background mole fraction. Combined with an atmospheric lifetime of over 50,000 years for PFC-14 and 10,000 years for PFC-116, PFCs have greater potential than HCFCs and HFCs to be oceanic transient tracers. PFC-14 has the potential to be a tracer for a longer period thanks to its longer lifetime, steady atmospheric growth rate and no current ban, as discussed by Deeds et al. (2008). However, PFC-14 is difficult to measure because it is extremely volatile and difficult to trap and separate chromatographically. PFC-116 can also be used as a transient tracer similar to PFC-14. The challenges for PFC-116 as an oceanic tracer are that it is a significant analytical challenge (low mole fractions in the atmosphere) and a low solubility in the seawater.

Deleted: concentration...ole fraction.

Deleted: But ...owever, PFC-14 is ver

Well-established source functions and the solubility functions in seawater are only two of the many requirements for an oceanic tracer. To be an oceanic transient tracer, the compound should also be conservative in the marine environment and be capable of rapid, relatively inexpensive and accurate measurement. The conservative nature of target compounds is briefly discussed in Sect. 1.2 by estimating the oceanic partial lifetimes of compounds with respect to hydrolysis in seawater. As we discussed for CFC-12, it is still used as an oceanic transient tracer though its production was phased-out in 1990s. For our target compounds, they have opportunities to be tracers once they are stable in seawater, can be measured in the ocean and have potential while atmospheric mole fractions continue to increase. This work provides two of the requirements for potential new oceanic transient tracers, whilst additional studies on compound conservation in seawater (comprehensive and detailed discussion) and measurement methods of target compounds are needed to qualify these compounds as suitable tracers.

Deleted: Well ...ell-established source

#### 4 Conclusions

This work has established the source functions for HCFC-22, HCFC-141b, HCFC-142b, HFC-134a, HFC-125, HFC-23, PFC-14 and PFC-116 based on a synthesis of available data and models optimized for transient tracer work in two ways: 1) the atmospheric mole fractions are calculated at the time of water masses formation (late winter in each hemisphere) and 2) the seawater solubility of these compounds are reviewed for the first time. In general, the mole fractions of most compounds have been continuously rising over the past three decades and still increasing today (though HCFC-141b and 142b rise rates have slowed down significantly). For HCFC-141b and HCFC-142b the annual mean mole fractions show sigmoidal growth and the growth rates have the shape of a normal distribution. For HFC-134a and HFC-23, the annual mean mole fractions show initial exponential growth followed by linear increase and the growth rates show a sigmoidal pattern. For HFC-125, the annual mean mole fractions and growth rates both show an exponential increase. To a certain extent, these growth patterns could predict the trends of annual mole fractions in the near future. The source functions and natural background mole fractions for all compounds show that HCFC-22, HCFC-141b, HCFC-142b, HFC-134a, HFC-125 and HFC-23 have the potential to be oceanic transient tracers for the next few decades, though their growth rates are expected to reverse, particularly for

Deleted: in a way that is ...ptimized fr

the HCFCs, due to the restriction on production and consumption imposed by the Montreal Protocol. HFCs have a higher potential to be oceanic transient tracers than HCFCs due to the increasing growth rates in the atmosphere, though these are likely to fall as a result of the recent Kigali Amendment. PFC-14 and PFC-116 have potential to be the tracers for a longer period due to their longer lifetimes, more consistent atmospheric growth rates and because no direct production or emission bans are currently in place, though they are listed in the Kyoto Protocol and industrial practices are changing to try to reduce/minimise emissions. In addition, we have used three different methods to estimate the seawater solubilities of the compounds of interest based on available theoretical concepts and experimental data. The seawater solubility functions of these compounds were subsequently constructed, completing the input function of these potentially useful oceanic transient tracers.

Deleted: is

Deleted: were

Deleted: solubility

## Acknowledgments

We acknowledge the Advanced Global Atmospheric Gases Experiment (AGAGE) programs, the Scripps Institution of Oceanography (SIO), the Commonwealth Scientific and Industrial Research Organization (CSIRO) Oceans and Atmosphere, the National Oceanic and Atmospheric Administration Earth System Research Laboratory Global Monitoring Division (NOAA/ESRL/GMD) and the University of East Anglia (UEA) for making their atmospheric data available. We thank the station operators, managers and support staff at the different monitoring sites of the AGAGE, the NOAA, the UEA, and the CSIRO/Bureau of Meteorology, especially Gerry Spain, Randy Dickau, Paul Krummel, Paul Steele, Martin K. Vollmer, C. Siso, B. Hall, J. Elkins, and Ray Wang. In particular, we thank SIO, Diane Ivy (MIT), and Ray Langenfelds (CSIRO), for measuring and supplying the archived air samples. We are especially thankful to Simon O'Doherty (University of Bristol) and Johannes Laube (UEA) for providing data. The author is greatly indebted to Matthew Taliaferro for providing useful Matlab code. We also thank financial support from the China Scholarship Council (CSC). We dedicate this work to John Bullister whose tireless work in updating and establishing the source functions for the more traditional transient tracer was a great inspiration to us and served as a role model for our work.

Deleted: and

Deleted:

Deleted: efforts of the

Deleted: and

Deleted: University of East Anglia (

Deleted: )

Deleted: Ray Weiss,

Deleted: and Paul Fraser

Deleted: from the Commonwealth Scientific and Industrial Research Organization (

Deleted: , UK

Deleted: , UK

**Table 1.** Atmospheric lifetimes, ocean partial lifetimes, Ozone Depletion and Global Warming Potentials of HCFC-22, HCFC-141b, HCFC-142b, HFC-134a, HFC-125, HFC-23, PFC-14 and PFC-116

Compound	Molecular formula	Atmospheric lifetimes <sup>a</sup> (years)	Ocean partial lifetimes <sup>b</sup> (years)	ODP <sup>c</sup>	GWP <sup>d</sup> 100-yr horizon
HCFC-22	CHClF <sub>2</sub>	12	1174	0.025	1,765
HCFC-141b	C <sub>2</sub> H <sub>3</sub> Cl <sub>2</sub> F	9.4	9190	0.082	782
HCFC-142b	C <sub>2</sub> H <sub>3</sub> ClF <sub>2</sub>	18	122,200	0.025	1,982
HFC-134a	CH <sub>2</sub> FCF <sub>3</sub>	14	5909	0	1,301
HFC-125	C <sub>2</sub> HF <sub>5</sub>	31	10,650	0	3,169
HFC-23	CHF <sub>3</sub>	228	-	0	12,398
PFC-14	CF <sub>4</sub>	> 50,000	-	0	6,626
PFC-116	C <sub>2</sub> F <sub>6</sub>	> 10,000	-	0	11,123

<sup>a</sup> See SPARC (2013).

<sup>b</sup> Partial atmospheric lifetimes with respect to oceanic uptake, see studies (Yvon-Lewis and Butler, 2002; Carpenter et al., 2014).

<sup>c</sup> ODP: Ozone Depletion Potential, see Laube et al. (2013).

<sup>d</sup> GWP: Global Warming Potential, see Hodnebrog et al. (2013).

Deleted: Metrics

Deleted: c

Formatted Table

Deleted: b

5

Deleted: b

Deleted: depletion

Deleted: potential

Deleted: c

Deleted: warming

Deleted: potential

**Table 2.** Primary calibration scale conversion factors for HCFC-22, HCFC-141b, HCFC-142b, HFC-134a, HFC-125 and HFC-23 between AGAGE (UB and SIO) and NOAA <sup>a</sup>

HCFC-22	SIO-93	SIO-98	SIO-05	NOAA-1992
SIO-98	1.0053 <sup>b</sup>	-	-	-
NOAA-1992	0.997 ± 0.004 <sup>c</sup>	0.993 ± 0.007 <sup>b</sup>	-	-
NOAA-2006	-	-	0.9971 ± 0.0027 <sup>d</sup>	1.005 <sup>e</sup>
HCFC-141b		UB-98	SIO-05	
NOAA-1994		1.006 ± 0.003 <sup>b</sup>	0.9941 ± 0.0049 <sup>d</sup>	
HCFC-142b		UB-98	SIO-05	
NOAA-1994		0.937 ± 0.003 <sup>b</sup>	0.9743 ± 0.0052 <sup>d</sup>	
HFC-134a		UB-98	SIO-05	
NOAA-1995		1.035 ± 0.004 <sup>b</sup>	1.0015 ± 0.0048 <sup>d</sup>	
HFC-125		UB-98	SIO-14	
SIO-14		1.0826 <sup>f</sup>	-	
NOAA-2008		-	0.946 ± 0.008 <sup>g</sup>	

<sup>a</sup> Example: for HCFC-22 measurement results reported on the SIO-98 scale, multiply 1.0053 to convert to the SIO-93 scale. AGAGE: Advanced Global Atmospheric Gases Experiment, UB: University of Bristol, SIO: Scripps Institution of Oceanography, NOAA: National Oceanic and Atmospheric Administration.

<sup>b</sup> (Prinn et al., 2000).

<sup>c</sup> (Miller et al., 1998).

<sup>d</sup> (Prinn et al., 2018a).

<sup>e</sup> NOAA calibration scales for various trace gases (<https://www.esrl.noaa.gov/gmd/ccl/scales.html>).

<sup>f</sup> The AGAGE calibration scale ([http://agage.eas.gatech.edu/data\\_archive/agage/AGAGE\\_scale\\_2018\\_v1.pdf](http://agage.eas.gatech.edu/data_archive/agage/AGAGE_scale_2018_v1.pdf)).

<sup>g</sup> (Simmonds et al., 2017).

Deleted: 3

Deleted: 003

Deleted: 005

Deleted: 005

Deleted: <sup>d</sup>

Deleted: using conversion factor:

Deleted: equal their results reported on

Deleted: <sup>d</sup> (Simmonds et al., 2017a).<sup>¶</sup>

Field Code Changed

Deleted: 2017

**Table 3. Regression coefficients in equations for partition**

Equation	Coefficient	Process	$T$ (K)	$c$	$e$	$s$	$a$	$b$	$v$	$n^a$	$r^b$	$S.D.^c$	$F^d$
Eqs. (12), (14)	$L_0$	Water to gas	298.15	-0.994	0.577	2.549	3.813	4.841	-0.869	408	0.9976	0.151	16810
Eqs. (12), (14)	$L_0$	Water to gas	310.15	-0.966	0.698	2.412	3.393	4.577	-1.072	82	0.9945	0.156	1270.8
Eq. (13)	$L_0$	Gas to water	298.15	-1.271	0.822	2.743	3.904	4.814	-0.213	392	0.9962	0.185	10229
Eq. (13)	$L_0$	Gas to water	310.15	-1.328	1.058	2.568	3.658	4.533	-0.248	84	0.9920	0.188	863
Eq. (17)	$K_s$	Salting-out	298.15 $\pm$ 2	0.112 $\pm$ 0.021	-0.020 $\pm$ 0.013	-0.042 $\pm$ 0.020	-0.047 $\pm$ 0.018	-0.060 $\pm$ 0.022	0.171 $\pm$ 0.017	43	0.83	0.031	-

<sup>a</sup>  $n$  is the number of data points.

<sup>b</sup>  $r$  is the correlation coefficient.

<sup>c</sup>  $S.D.$  is the standard deviation.

<sup>d</sup>  $F$  is the  $F$ -statistic.

**Table 4.** *E*, *S*, *A*, *B*, *V*, *V<sub>c</sub>*, and *log L<sup>16</sup>* descriptors of HCFC-22, HCFC-141b, HCFC-142b, HFC-134a, HFC-125, HFC-23, PFC-14, PFC-116 and CFC-12 [for the pp-LFER model](#)

Species	Chemical Formula	<i>E</i>	<i>S</i>	<i>A</i>	<i>B</i>	<i>V</i>	<i>V<sub>c</sub></i>	<i>log L<sup>16</sup></i>
HCFC-22	CHClF <sub>2</sub>	-0.056	0.380	0.040	0.050	0.4073	0.4473	<u>0.692</u>
HCFC-141b	C <sub>2</sub> H <sub>3</sub> Cl <sub>2</sub> F	0.084	0.430	0.005	0.054	0.6530	0.6729	<u>1.920</u>
HCFC-142b	C <sub>2</sub> H <sub>3</sub> ClF <sub>2</sub>	-0.080	0.240	0.060	0.056	0.5482	0.5882	<u>1.081</u>
HFC-134a	CH <sub>2</sub> FCF <sub>3</sub>	-0.410	0.342	0.060	0.040	0.4612	0.5412	<u>0.318</u>
HFC-125	C <sub>2</sub> HF <sub>5</sub>	-0.510	-0.019	0.105	0.064	0.4789	0.6445	<u>0.100</u>
HFC-23	CHF <sub>3</sub>	-0.427	0.183	0.110	0.034	0.3026	0.3626	<u>-0.274</u>
PFC-14	CF <sub>4</sub>	-0.550	-0.250	0.000	0.000	0.3203	0.4003	<u>-0.819</u>
PFC-116	C <sub>2</sub> F <sub>6</sub>	-0.590	-0.350	0.000	0.000	0.4966	0.6166	=
CFC-12	CCl <sub>2</sub> F <sub>2</sub>	0.027	0.125	0.000	0.000	0.5297	0.5697	<u>1.124</u>

Deleted: 5

Formatted Table

Deleted: Corrected

**Table 5.** Ostwald solubility coefficients of HCFC-22, HCFC-141b, HCFC-142b, HFC-134a, HFC-125, HFC-23, PFC-14, PFC-116 and CFC-12 in seawater estimated based on Combined Method

Compound	$a_1$	$a_2$	$a_3$	$K_S$	$T_{min}$ (K)	$T_{max}$ (K)	$L_0$ at 1 atm, 25 °C (L L <sup>-1</sup> )	$L$ at 1 atm, 25 °C, 35.0 ‰ (L L <sup>-1</sup> )
HCFC-22	-66.9256	109.8625	27.3778	$0.169 \pm 0.022$	278.15	353.15	0.844	0.669
HCFC-141b	-85.6439	138.0940	35.6875	$0.204 \pm 0.023$	278.15	353.15	0.711	0.537
HCFC-142b	-73.3682	118.3104	29.8797	$0.198 \pm 0.022$	278.15	353.15	0.352	0.268
HFC-134a	-67.1680	109.1227	27.0984	$0.193 \pm 0.022$	278.15	353.15	0.381	0.292
HFC-125	-51.8823	84.5045	19.3067	$0.224 \pm 0.021$	283.15	343.15	0.086	0.063
HFC-23	30.0046	-31.6631	-18.8072	$0.168 \pm 0.021$	278.15	348.15	0.313	0.249
PFC-14	-113.8218	162.6686	49.4215	$0.202 \pm 0.022$	273.15	328.15	0.00513	0.00388
PFC-116	-102.0437	147.9210	41.9999	$0.244 \pm 0.022$	278.15	328.15	0.00143	0.00102
CFC-12	-101.3445	156.4709	42.2833	$0.204 \pm 0.021$	273.15	348.15	0.069	0.052

$$L = 10^{-K_S \cdot S / M_{NaCl}} \cdot \exp \left[ a_1 + a_2 \cdot \left( \frac{100}{T} \right) + a_3 \cdot \ln \left( \frac{T}{100} \right) \right]$$

Deleted: 3

Deleted: 37

Deleted: 43

Deleted: 37

Deleted: 34

Deleted: 28

Deleted: 8

Deleted: 16

Deleted: 17

Deleted: 34

**Table 6.** Comparison of the Ostwald solubility coefficients ( $L$ ,  $L L^{-1}$ ) of PFC-14 in seawater with previous results.

$T$ (K)	$t$ ( $^{\circ}C$ )	$S$ (‰)	$L$ , this study	$L$ , (Scharlin and Battino, 1995)	$RSD^a$ (%)
288.15	15	35.086	0.005052	0.005169	1.62
293.15	20	35.086	0.004578	0.004527	0.79
298.15	25	35.086	0.004217	0.004027	3.26
303.15	30	35.086	0.003944	0.003635	5.77

<sup>a</sup> Relative standard deviation (RSD) of the Ostwald solubility coefficients estimated by the Combined Method and measured in Scharlin and Battino (1995).

Deleted: 6

Deleted: in this study

Deleted: the

Deleted: from the literature

Formatted: Left

Formatted Table

Deleted: in this study

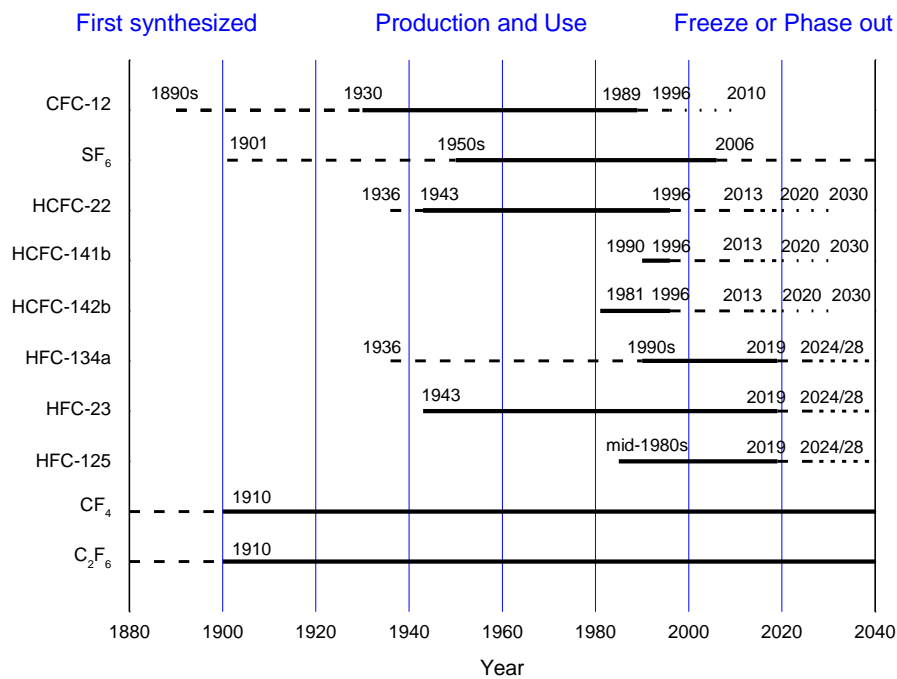
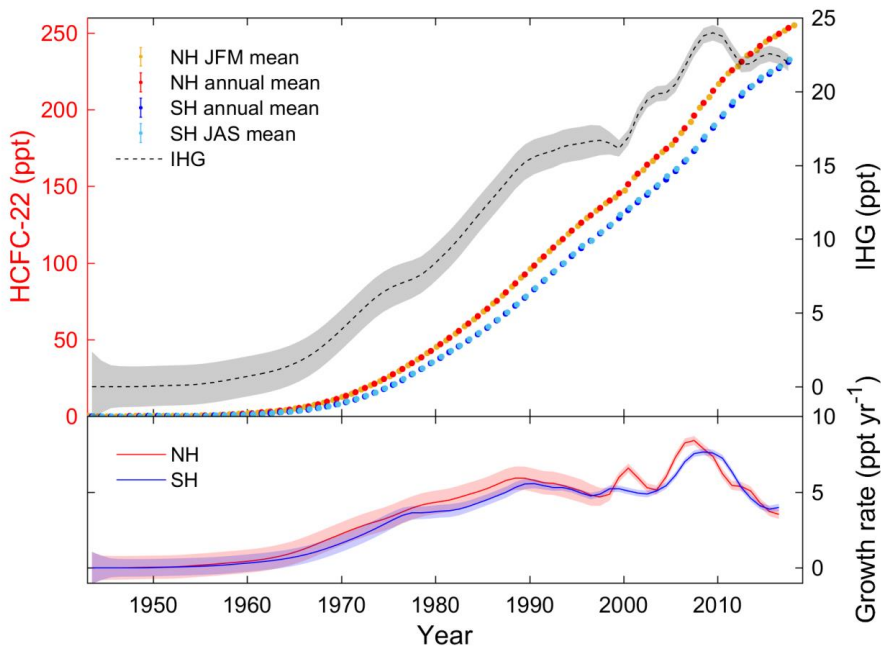


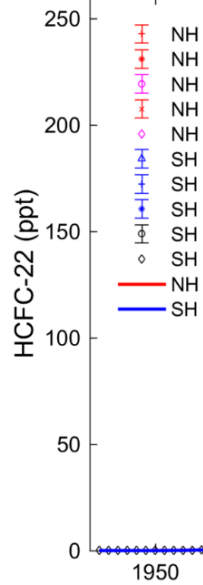
Fig. 1. Comparison of production and use histories of CFC-12, SF<sub>6</sub>, HCFCs, HFCs and PFCs.

Deleted: ure



**Fig. 2a. HCFC-22:** The top panel shows the JFM means (NH), annual means (NH and SH), and JAS means (SH) of atmospheric mole fractions for HCFC-22 and the inter-hemispheric gradients (IHG, in black), using the right axes. The lower panel shows the annual growth rates in ppt yr<sup>-1</sup>. Shadings in the figure reflect the uncertainties.

5



Deleted: ...

Deleted: ure

Deleted: (a) The northern hemisphere (NH) and southern hemisphere (SH) monthly means atmospheric history for HCFC-22 obtained from the smoothing spline fit on all collected data. The data includes the AGAGE in situ measurements at MHD and THD for NH and at CGO for SH, NOAA flask air measurements (MHD and CGO) and 2-D box model mole fractions

Deleted: reconstructed

Deleted: mid-February, mid-year and mid-August annual mean

Deleted: in the NH and SH

Deleted: mid-year

Deleted: y

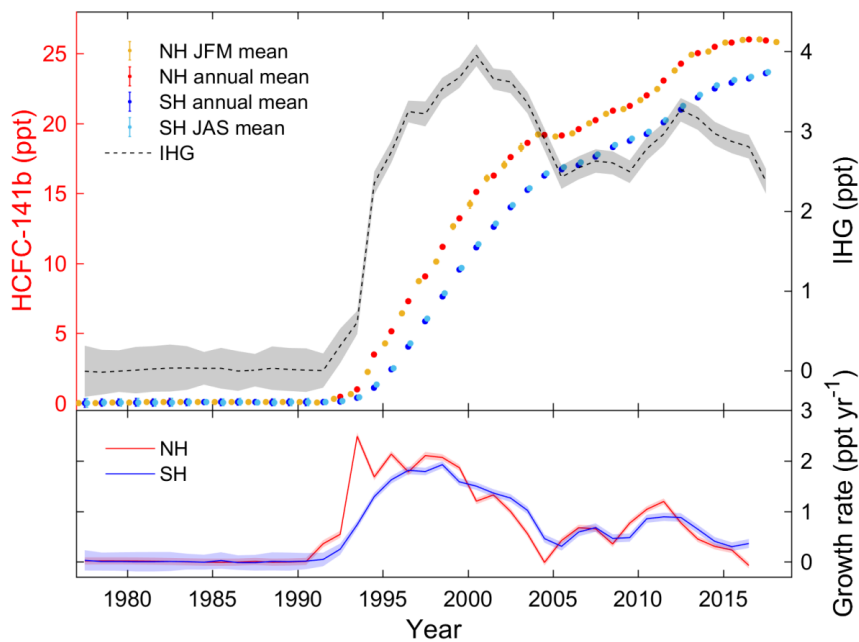
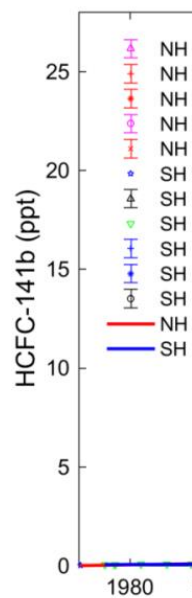


Fig. 2b. Similar to Fig. 2a, but for HCFC-141b.



Deleted: ...

Deleted: ure

Deleted: 3

Deleted: (a) The northern hemisphere (NH) and southern hemisphere (SH) monthly means atmospheric history for HCFC-141b obtained from the smoothing spline fit on all collected data. The data includes the AGAGE in situ measurements at MHD and THD for NH and at CGO for SH, NOAA flask (MHD and CGO) and archived air measurements for both hemispheres. The SH firm air record (Sturrock et al., 2002) is also included. (b) The top panel shows the reconstructed mid-February, mid-year and mid-August annual mean atmospheric mole fractions for HCFC-141b in the NH and SH and the inter-hemispheric gradients (IHG, in black using the right axes). The low panel shows the mid-year annual growth

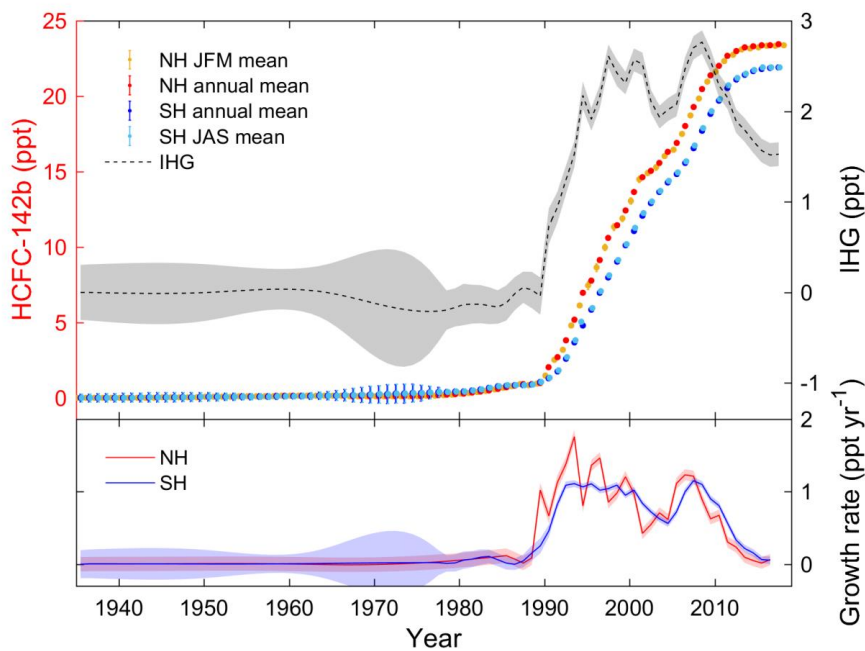
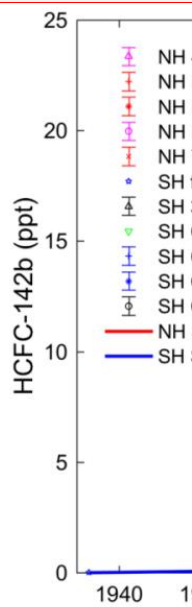


Fig. 2c. Similar to Fig. 2a, but for HCFC-142b



Deleted: ...

Deleted: ure

Deleted: 4

Deleted: (a) The northern hemisphere (NH) and southern hemisphere (SH) monthly means atmospheric history for HCFC-142b obtained from the smoothing spline fit on all collected data. The data includes the AGAGE in situ measurements at MHD and THD for NH and at CGO for SH, NOAA flask (MHD and CGO) and archived air measurements for both hemispheres. The SH firm air record (Sturrock et al., 2002) is also included. (b) The top panel shows the reconstructed mid-February, mid-year and mid-August annual mean atmospheric mole fractions for HCFC-142b in the NH and SH and the inter-hemispheric gradients (IHG, in black using the right axes). The low panel shows the mid-year annual growth

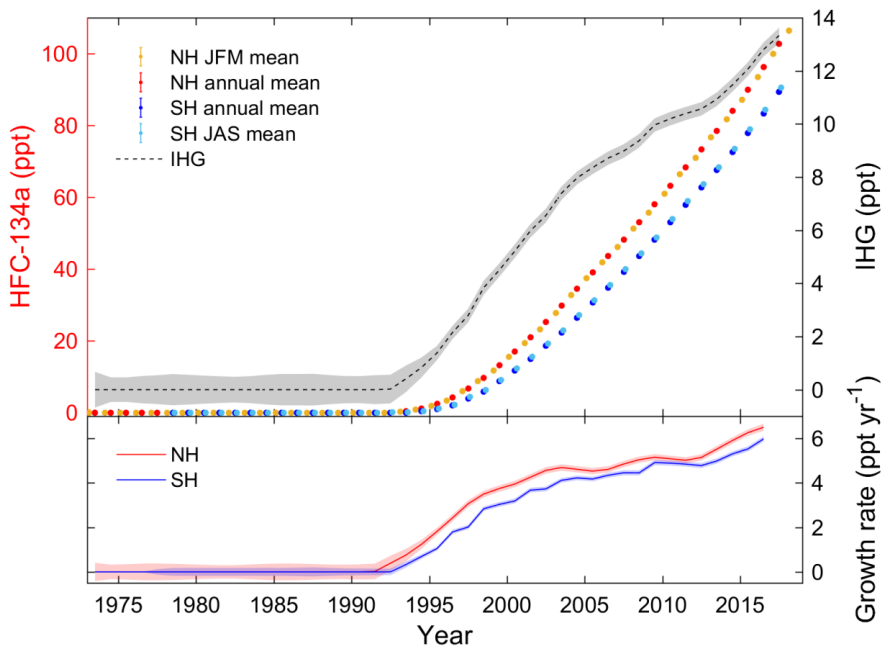
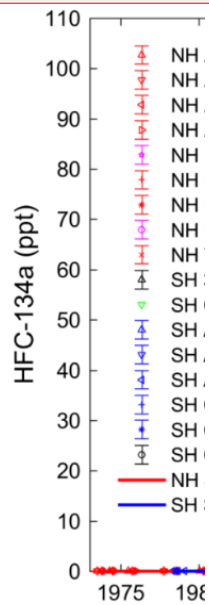


Fig. 2d. Similar to Fig. 2a, but for HFC-134a.



Deleted: ...

Deleted: ure

Deleted: 5

Deleted: (a) The northern hemisphere (NH) and southern hemisphere (SH) monthly means atmospheric history for HFC-134a obtained from the smoothing spline fit on all collected data. The data includes the AGAGE in situ measurements at MHD and THD for NH and at CGO for SH, NOAA flask (MHD and CGO) and archived air measurements for both hemispheres. The AGAGE air archive measurements for both hemispheres and UEA CGAA data are also included. (b) The top panel shows the reconstructed mid-February, mid-year and mid-August annual mean atmospheric mole fractions for HFC-134a in the NH and SH and the inter-hemispheric gradients (IHG, in black using the right axes). The low panel shows the mid-year annual growth

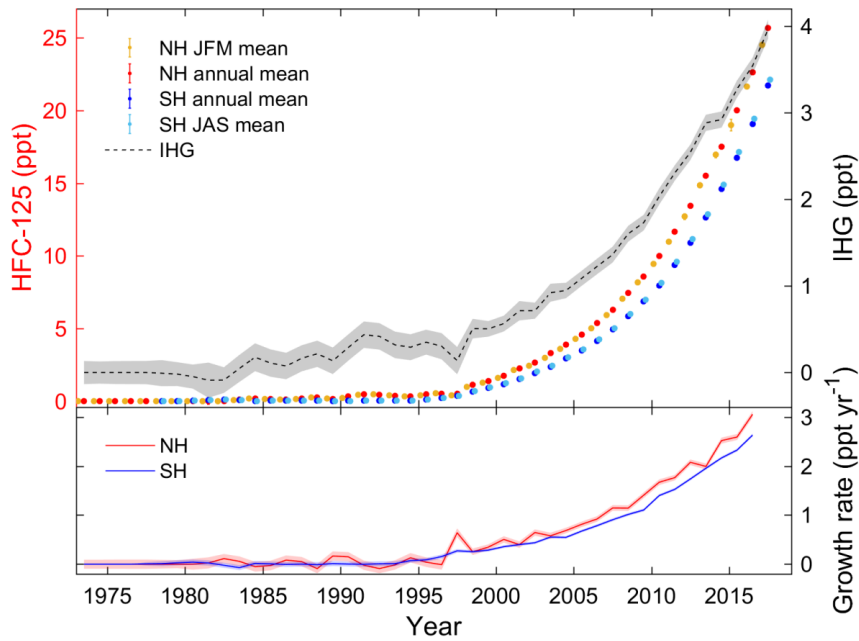
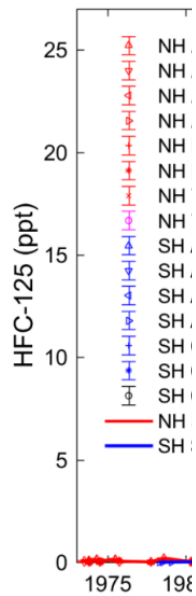


Fig. 2e. Similar to Fig. 2a, but for HFC-125.



Deleted: ...

Deleted: ure

Deleted: 6

Deleted: (a) The northern hemisphere (NH) and southern hemisphere (SH) monthly means atmospheric history for HFC-125 obtained from the smoothing spline fit on all collected data. The data includes the AGAGE in situ measurements at MHD and THD for NH and at CGO for SH, NOAA flask (MHD and CGO) and archived air measurements for both hemispheres. The AGAGE air archive measurements for both hemispheres and UEA CGAA data are also included. (b) The top panel shows the reconstructed mid-February, mid-year and mid-August annual mean atmospheric mole fractions for HFC-125 in the NH and SH and the inter-hemispheric gradients (IHG, in black using the right axes). The low panel shows the mid-year annual growth

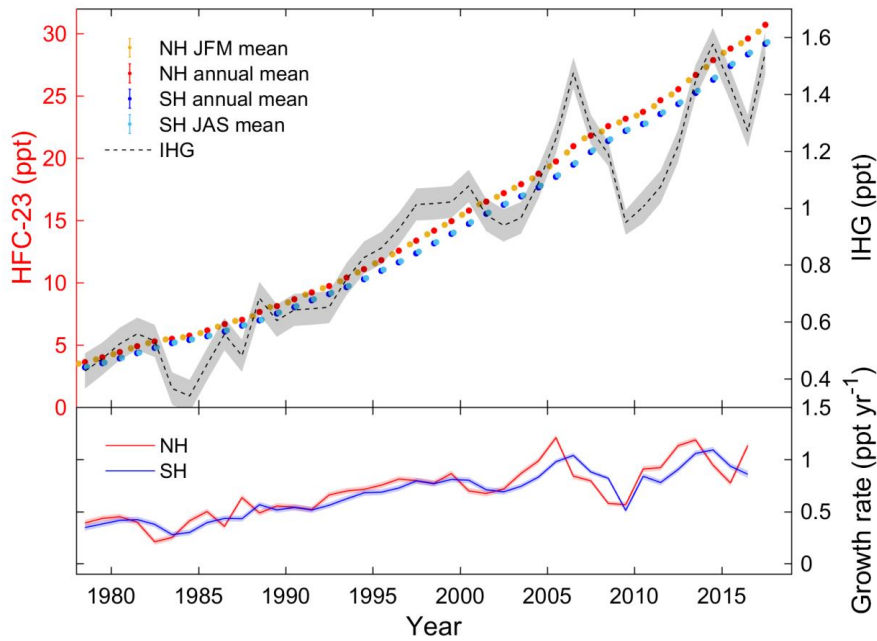
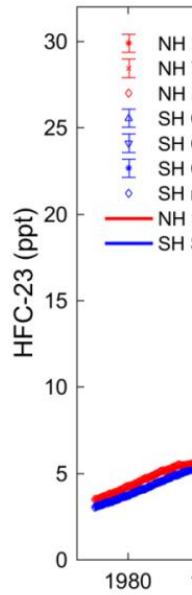


Fig. 2f. Similar to Fig. 2a, but for HFC-23.



Deleted: ...

Deleted: ure

Deleted: 7

Deleted: (a) The northern hemisphere (NH) and southern hemisphere (SH) monthly means atmospheric history for HFC-23 obtained from the smoothing spline fit on all collected data. The data includes the AGAGE in situ measurements at MHD and THD for NH and at CGO for SH, 2-D 12-box model data (Miller et al., 2010) for both hemispheres. The AGAGE CGAA measurements are also included. (b) The top panel shows the reconstructed mid-February, mid-year and mid-August annual mean atmospheric mole fractions for HFC-23 in the NH and SH and the inter-hemispheric gradients (IHG, in black using the right axes). The low panel shows the mid-year annual growth rates in ppt yr<sup>-1</sup>.

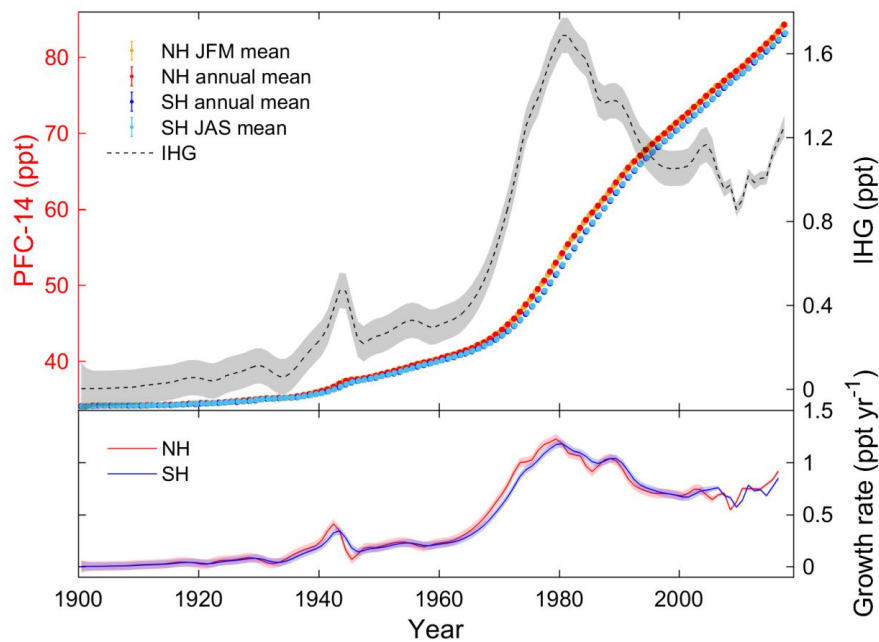
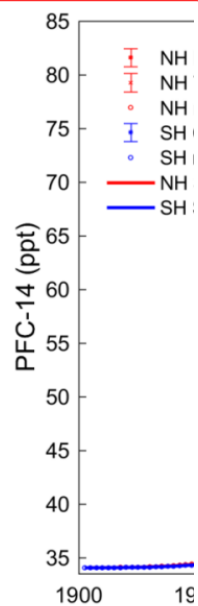


Fig. 2g. Similar to Fig. 2a, but for PFC-14.



Deleted: 1

Deleted: ure

Deleted: 8

Deleted: (a) The northern hemisphere (NH) and southern hemisphere (SH) monthly means atmospheric history for PFC-14 obtained from the smoothing spline fit on all collected data. The data includes the AGAGE in situ measurements at MHD and THD for NH and at CGO for SH, model data (Trudinger et al., 2016) for both hemispheres. (b) The top panel shows the reconstructed mid-February, mid-year and mid-August annual mean atmospheric mole fractions for PFC-14 in the NH and SH and the inter-hemispheric gradients (IHG, in black using the right axes). The low pan...

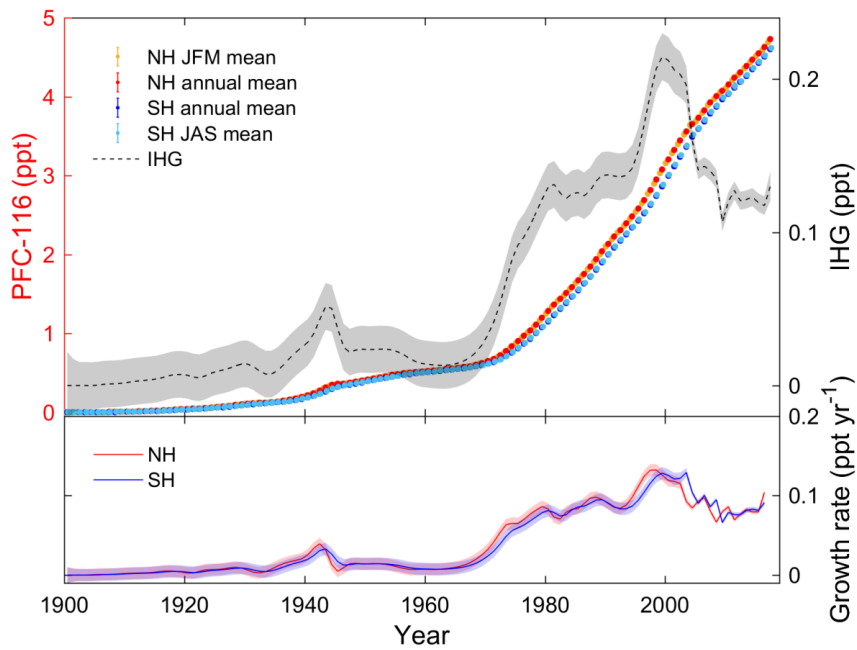
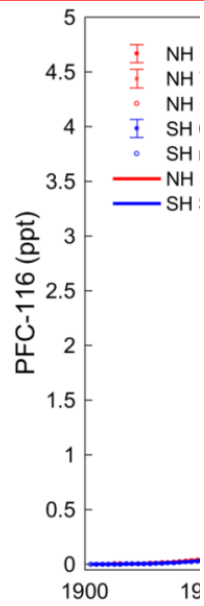


Fig. 2h. Similar to Fig. 2a, but for PFC-116.



Deleted: 1

Deleted: ure

Deleted: 9

Deleted: (a) The northern hemisphere (NH) and southern hemisphere (SH) monthly means atmospheric history for PFC-116 obtained from the smoothing spline fit on all collected data. The data includes the AGAGE in situ measurements at MHD and THD for NH and at CGO for SH, model data (Trudinger et al., 2016) for both hemispheres. (b) The top panel shows the reconstructed mid-February, mid-year and mid-August annual mean atmospheric mole fractions for PFC-116 in the NH and SH and the inter-hemispheric gradients (IHG, in black using the right axes). The low

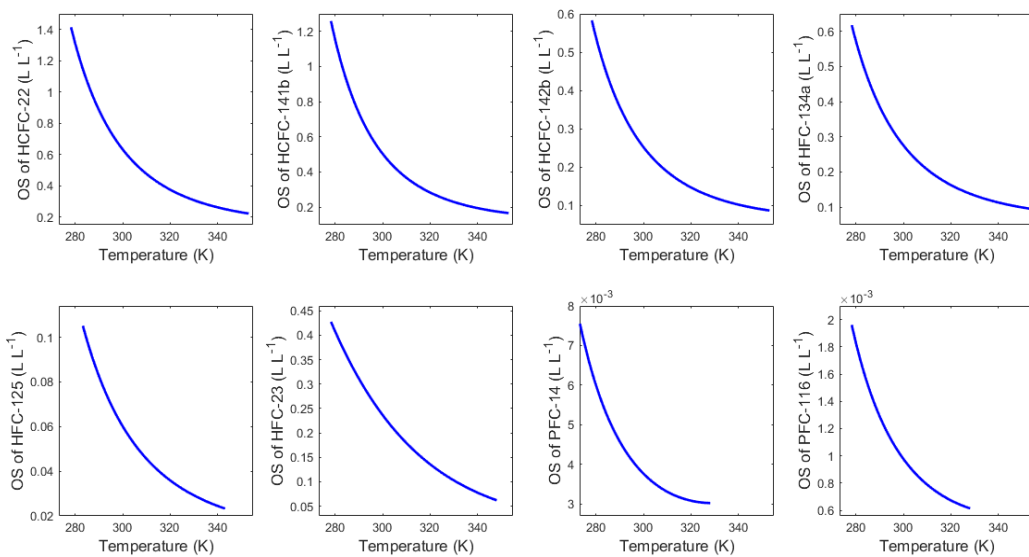


**Fig. 3.** Temperature dependence of the Ostwald solubility (OS) coefficients in seawater for HCFC-22, HCFC-141b, HCFC-142b, HFC-134a, HFC-125, HFC-23, PFC-14 and PFC-116 at a salinity of 35.

Deleted: ure  
 Deleted: 10  
 Deleted: T  
 Deleted: in the available temperature range  
 Deleted: in seawater for each compound. The  
 Deleted: is set at

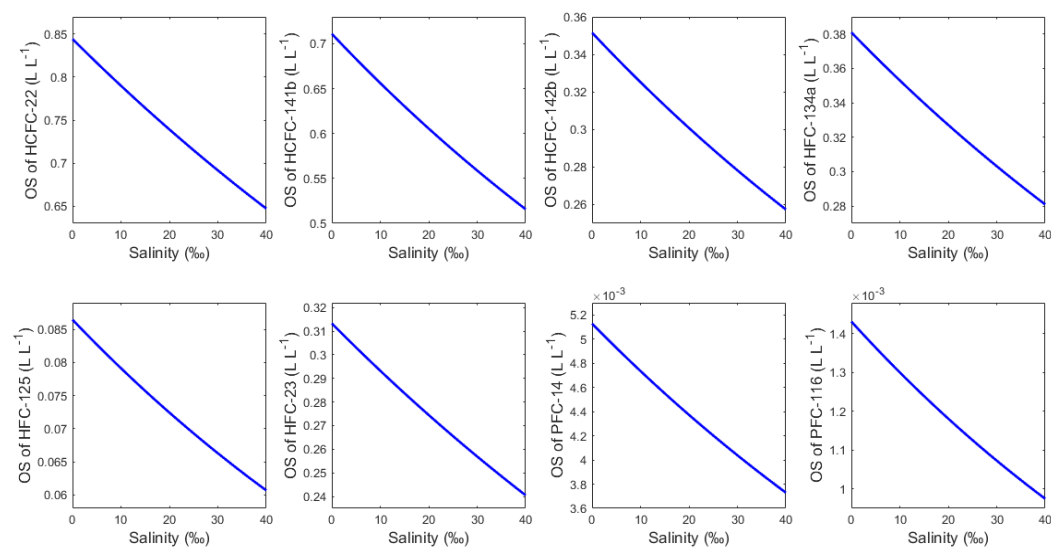


**Fig. 4.** Salinity dependence of the Ostwald solubility (OS) coefficients in seawater for HCFC-22, HCFC-141b, HCFC-142b, HFC-134a, HFC-125, HFC-23, PFC-14 and PFC-116 at a temperature of 298.15 K.

Deleted: ure  
 Deleted: 11  
 Deleted: T  
 Deleted: in the salinity range of 0-40 in seawater for each compound. The  
 Deleted: is set at

5

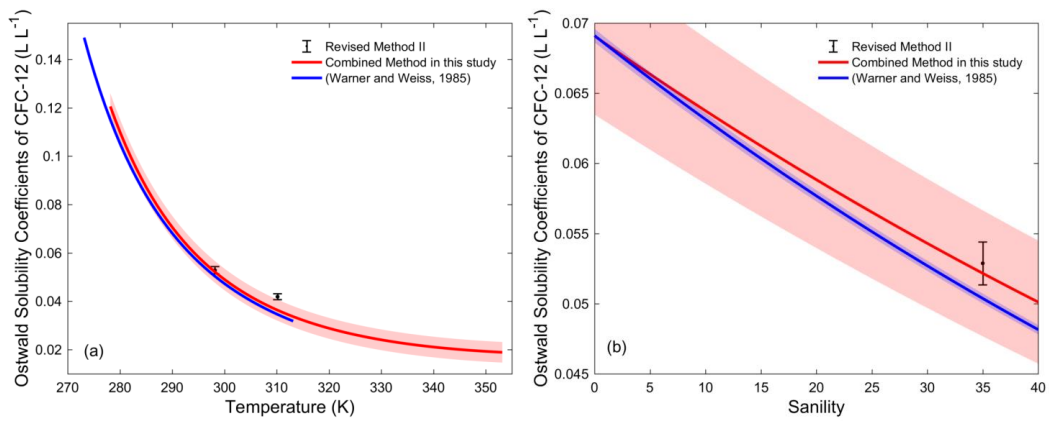
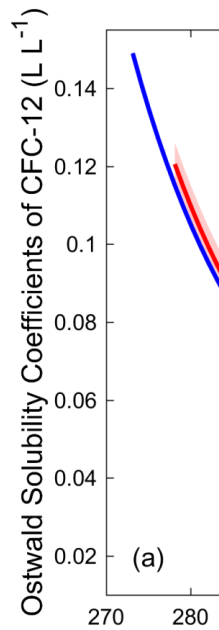


**Fig. 5.** Comparison of the Ostwald solubility coefficients in seawater for CFC-12 (a) in the available temperature range at a salinity of 35 and (b) in the salinity range of 0-40 at a temperature of 298.15 K calculated from Revised Method II, from Combined Method and from Warner and Weiss (1985). Error bars and shadings in the figure reflect the uncertainties.

5



- Deleted: ...
- Deleted: ure
- Deleted: 12
- Deleted: (a)
- Deleted: the permanent
- Deleted: comparison of the Ostwald solubility coefficients
- Deleted: permanent
- Deleted: for CFC-12 from the seawater solubility functions constructed by
- Deleted: the
- Deleted: the
- Deleted: in this study
- Deleted: uncertainty

## References

- Abraham, M., Enrique Cometto-Mu, J., Cain, W., and D'Yaz, M.: The determination of solvation descriptors for terpenes, and the prediction of nasal pungency thresholds, *J. Chem. Soc., Perkin Trans. 2*, 2405-2412, 1998.
- 5 Abraham, M. H., Grellier, P. L., and McGill, R. A.: Determination of olive oil-gas and hexadecane-gas partition coefficients, and calculation of the corresponding olive oil-water and hexadecane-water partition coefficients, *J. Chem. Soc., Perkin Trans. 2*, 797-803, 1987.
- Abraham, M. H., and McGowan, J. C.: The use of characteristic volumes to measure cavity terms in reversed phase liquid chromatography, *Chromatographia*, 23, 243-246, doi:10.1007/bf02311772, 1987.
- 10 Abraham, M. H., Grellier, P. L., Prior, D. V., Duce, P. P., Morris, J. J., and Taylor, P. J.: Hydrogen bonding. Part 7. A scale of solute hydrogen-bond acidity based on logK values for complexation in tetrachloromethane, *J. Chem. Soc., Perkin Trans. 2*, 699-711, doi:10.1039/P29890000699, 1989.
- Abraham, M. H., Whiting, G. S., Doherty, R. M., and Shuely, W. J.: Hydrogen bonding: XVI. A new solute solvation parameter,  $\pi 2H$ , from gas chromatographic data, *J. Chromatogr. A*, 587, 213-228, doi:10.1016/0021-9673(91)85158-C, 1991.
- 15 Abraham, M. H.: Scales of solute hydrogen-bonding: their construction and application to physicochemical and biochemical processes, *Chem. Soc. Rev.*, 22, 73-83, doi:10.1039/CS9932200073, 1993.
- Abraham, M. H., Andonian-Haftivan, J., Whiting, G. S., Leo, A., and Taft, R. S.: Hydrogen bonding. Part 34. The factors that influence the solubility of gases and vapours in water at 298 K, and a new method for its determination, *J. Chem. Soc., Perkin Trans. 2*, 1777-1791, doi:10.1039/P29940001777, 1994.
- 20 Abraham, M. H., Gola, J. M., Cometto-Muñiz, J. E., and Cain, W. S.: Solvation properties of refrigerants, and the estimation of their water-solvent and gas-solvent partitions, *Fluid Phase Equilib.*, 180, 41-58, doi:10.1016/S0378-3812(00)00511-2, 2001.
- Abraham, M. H., Ibrahim, A., and Zissimos, A. M.: Determination of sets of solute descriptors from chromatographic measurements, *J. Chromatogr. A*, 1037, 29-47, doi:10.1016/j.chroma.2003.12.004, 2004.
- Abraham, M. H., Gil-Lostes, J., Corr, S., and Acree, W. E.: Determination of partition coefficients of refrigerants by gas liquid chromatographic headspace analysis, *J. Chromatogr. A*, 1265, 144-148, doi:10.1016/j.chroma.2012.09.085, 2012.
- 25 Arnold, T., Mühle, J., Salameh, P. K., Harth, C. M., Ivy, D. J., and Weiss, R. F.: Automated Measurement of Nitrogen Trifluoride in Ambient Air, *Anal. Chem.*, 84, 4798-4804, doi:10.1021/ac300373e, 2012.
- Barber, M., and Tabereaux, A. T.: The Evolution of Søderberg Aluminum Cell Technology in North and South America, *JOM*, 66, 223-234, doi:10.1007/s11837-013-0855-1, 2014.
- 30 Battino, R., Seybold, P. G., and Campanell, F. C.: Correlations Involving the Solubility of Gases in Water at 298.15 K and 101325 Pa, *Journal of Chemical & Engineering Data*, 56, 727-732, doi:10.1021/jc101070h, 2011.
- Bu, X., and Warner, M. J.: Solubility of chlorofluorocarbon 113 in water and seawater, *Deep-Sea Res. Pt. I*, 42, 11, doi:10.1016/0967-0637(95)00052-8, 1995.
- Bullister, J. L., and Wisegarver, D. P.: The solubility of carbon tetrachloride in water and seawater, *Deep-Sea Res. Pt. I*, 45, 1285-1302, doi:10.1016/S0967-0637(98)00017-X, 1998.
- 35 Bullister, J. L., Wisegarver, D. P., and Menzia, F. A.: The solubility of sulfur hexafluoride in water and seawater, *Deep-Sea Res. Pt. I*, 49, 175-187, doi:10.1016/S0967-0637(01)00051-6, 2002.
- Bullister, J. L., Wisegarver, D. P., and Sonnerup, R. E.: Sulfur hexafluoride as a transient tracer in the North Pacific Ocean, *Geophys. Res. Lett.*, 33, doi:10.1029/2006GL026514, 2006.
- 40 Bullister, J. L.: Atmospheric Histories (1765-2015) for CFC-11, CFC-12, CFC-113, CCl<sub>4</sub>, SF<sub>6</sub> and N<sub>2</sub>O, NDP-095, 2015.
- Butler, J. H., Battle, M., Bender, M. L., Montzka, S. A., Clarke, A. D., Saltzman, E. S., Sucher, C. M., Severinghaus, J. P., and Elkins, J. W.: A record of atmospheric halocarbons during the twentieth century from polar firn air, *Nature*, 399, 749-755, doi:10.1038/21586, 1999.
- Calm, J. M., and Domanski, P. A.: R-22 replacement status, *ASHRAE J.*, 46, 29, 2004.
- Carpenter, L. J., Reimann, S., Burkholder, J. B., Clerbaux, C., Hall, B. D., Hossaini, R., Laube, J. C., and Yvon-Lewis, S. A.: Scientific Assessment of Ozone Depletion: 2014, 2014.
- 45 Cicerone, R. J.: Atmospheric carbon tetrafluoride: A nearly inert gas, *Science*, 206, 1979.
- Clever, H. L.: IUPAC-NIST Solubility Data Series. 80. Gaseous Fluorides of Boron, Nitrogen, Sulfur, Carbon, and Silicon and Solid Xenon Fluorides in all Solvents, *J. Phys. Chem. Ref. Data*, 34, 201, doi:10.1063/1.1794762, 2005.
- Craven, P., and Wahba, G.: Smoothing noisy data with spline functions: Estimating the Correct Degree of Smoothing by the Method of Generalized Cross-Validation, *Numer. Math.*, 31, 377-403, doi:10.1007/BF01404567, 1978.
- 50 Cunnold, D. M., Prinn, R. G., Rasmussen, R. A., Simmonds, P. G., Alyea, F. N., Cardelino, C. A., Crawford, A. J., Fraser, P. J., and Rosen, R. D.: The Atmospheric Lifetime Experiment: 3. Lifetime methodology and application to three years of CFCl<sub>3</sub> data, *J. Geophys. Res.*, 88, 8379, doi:10.1029/JC088iC13p08379, 1983.
- Cunnold, D. M., Fraser, P. J., Weiss, R. F., Prinn, R. G., Simmonds, P. G., Miller, B. R., Alyea, F. N., and Crawford, A. J.: Global trends and annual releases of CCl<sub>3</sub>F and CCl<sub>2</sub>F<sub>2</sub> estimated from ALE/GAGE and other measurements from July 1978 to June 1991, *J. Geophys. Res.*, 99, 1107-1126, doi:10.1029/93JD02715, 1994.
- 55 Deeds, D. A.: The Natural Geochemistry of Tetrafluoromethane and Sulfur Hexafluoride : Studies of Ancient Mojave Desert Groundwaters, North Pacific Seawaters and the Summit Emissions of Kilauea Volcano, PhD thesis, 2008.
- Deeds, D. A., Mühle, J., and Weiss, R. F.: Tetrafluoromethane in the deep North Pacific Ocean, *Geophys. Res. Lett.*, 35, doi:10.1029/2008gl034355, 2008.
- 60 Deeds, D. A., Kulongoski, J. T., Mühle, J., and Weiss, R. F.: Tectonic activity as a significant source of crustal tetrafluoromethane emissions to the atmosphere: Observations in groundwaters along the San Andreas Fault, *Earth. Planet. Sci. Lett.*, 412, 163-172, doi:10.1016/j.epsl.2014.12.016, 2015.
- Derwent, R. G., Simmonds, P. G., Grealley, B. R., O'doherty, S., McCulloch, A., Manning, A., Reimann, S., Folini, D., and Vollmer, M. K.: The phase-in and phase-out of European emissions of HCFC-141b and HCFC-142b under the Montreal Protocol: Evidence from observations at Mace Head, Ireland and Jungfraujoch, Switzerland from 1994 to 2004, *Atmos. Environ.*, 41, 757-767, doi:10.1016/j.atmosenv.2006.09.009, 2007.
- Endo, S., Pfennigsdorff, A., and Goss, K.-U.: Salting-out effect in aqueous NaCl solutions: Trends with size and polarity of solute molecules, *Environ. Sci. Technol.*, 46, 1496-1503, doi:10.1021/es203183z, 2012.

- Fine, R. A.: Observations of CFCs and SF<sub>6</sub> as ocean tracers, *Annu. Rev. Mar. Sci.*, 3, 173-195, doi:10.1146/annurev.marine.010908.163933, 2011.
- Fine, R. A., Peacock, S., Maltrud, M. E., and Bryan, F. O.: A new look at ocean ventilation time scales and their uncertainties, *J. Geophys. Res.: Oceans*, 10.1002/2016JC012529, 2017.
- 5 Fraser, P., Steele, P., and Cooksey, M.: PFC and carbon dioxide emissions from an Australian aluminium smelter using time-integrated stack sampling and GC-MS, GC-FID analysis, in: *Light Metals 2013*, Springer, 871-876, 2013.
- Fraser, P. J., Pearman, G. I., and Derek, N.: CSIRO Non-carbon Dioxide Greenhouse Gas Research. Part 1: 1975–90, *Historical Records of Australian Science*, 29, 1-13, 2017.
- 10 Gammon, R. H., Cline, J., and Wisegarver, D.: Chlorofluoromethanes in the northeast Pacific Ocean: Measured vertical distributions and application as transient tracers of upper ocean mixing, *J. Geophys. Res.: Oceans*, 87, 9441-9454, doi:10.1029/JC087iC12p09441, 1982.
- Gamsjäger, H., Lorimer, J. W., Scharlin, P., and Shaw, D. G.: Glossary of terms related to solubility (IUPAC Recommendations 2008), *Pure Appl. Chem.*, 80, 233-276, doi:10.1351/pac200880020233, 2008.
- Gamsjäger, H., Lorimer, J. W., Salomon, M., Shaw, D. G., and Tomkins, R.: The IUPAC-NIST Solubility Data Series: A guide to preparation and use of compilations and evaluations (IUPAC Technical Report), *Pure Appl. Chem.*, 82, 1137-1159, doi:10.1351/PAC-REP-09-10-33, 2010.
- 15 Gassmann, M.: Freon 14 im „Krypton reinst“ und in der Atmosphäre, *Naturwissenschaften*, 61, 127-127, doi:10.1007/BF00606286, 1974.
- Goss, K.-U., Bronner, G., Harner, T., Hertel, M., and Schmidt, T. C.: The partition behavior of fluorotelomer alcohols and olefins, *Environ. Sci. Technol.*, 40, 3572-3577, doi:10.1021/es060004p, 2006.
- 20 Graziosi, F., Arduini, J., Furlani, F., Giostra, U., Kuijpers, L. J. M., Montzka, S. A., Miller, B. R., O'Doherty, S. J., Stohl, A., Bonasoni, P., and Maione, M.: European emissions of HCFC-22 based on eleven years of high frequency atmospheric measurements and a Bayesian inversion method, *Atmos. Environ.*, 112, 196-207, doi:10.1016/j.atmosenv.2015.04.042, 2015.
- Hodnebrog, Ø., Etminan, M., Fuglested, J. S., Marston, G., Myhre, G., Nielsen, C. J., Shine, K. P., and Wallington, T. J.: Global warming potentials and radiative efficiencies of halocarbons and related compounds: A comprehensive review, *Rev. Geophys.*, 51, 300-378, doi:10.1002/rog.20013, 2013.
- 25 HSDB: Hazardous Substances Data Bank, TOXicology data NETwork (TOXNET), National Library of Medicine (US), available at: <http://toxnet.nlm.nih.gov/newtoxnet/hsdb.htm> (last access: 10 April 2015), 2015.
- Hutchinson, M. F., and De Hoog, F.: Smoothing noisy data with spline functions, *Numer. Math.*, 47, 99-106, doi:10.1007/BF01404567, 1985.
- Jacobson, M. Z.: *Air pollution and global warming: history, science, and solutions*, Cambridge University Press, 2012.
- 30 Khalil, M. A. K., Rasmussen, R. A., Culbertson, J. A., Prins, J. M., Grimsrud, E. P., and Shearer, M. J.: Atmospheric perfluorocarbons, *Environ. Sci. Technol.*, 37, 4358-4361, doi:10.1021/es030327a, 2003.
- Kim, J., Fraser, P. J., Li, S., Mühle, J., Ganesan, A. L., Krummel, P. B., Steele, L. P., Park, S., Kim, S. K., and Park, M. K.: Quantifying aluminum and semiconductor industry perfluorocarbon emissions from atmospheric measurements, *Geophys. Res. Lett.*, 41, 4787-4794, 2014.
- 35 Körtzinger, A., Rhein, M., and Mintrop, L.: Anthropogenic CO<sub>2</sub> and CFCs in the North Atlantic Ocean - A comparison of man-made tracers, *Geophys. Res. Lett.*, 26, 2065-2068, doi:10.1029/1999GL900432, 1999.
- Langenfelds, R., Steele, P. F. R. F. L., and Allison, L. P. C.: The Cape Grim Air Archive: the first seventeen years, 1978-1995, *Baseline Atmospheric Program (Australia) 1994-95*, 53-70, 1996.
- 40 Laube, J. C., Keil, A., Bönnisch, H., Engel, A., Röckmann, T., Volk, C. M., and Sturges, W. T.: Observation-based assessment of stratospheric fractional/newline release, lifetimes, and ozone depletion potentials of ten important source gases, *Atmos. Chem. Phys.*, 13, 2779-2791, doi:10.5194/acp-13-2779-2013, 2013.
- Lovelock, J. E., Maggs, R. J., and Wade, R. J.: Halogenated Hydrocarbons in and over the Atlantic, *Nature*, 241, 194-196, doi:10.1038/241194a0, 1973.
- 45 Mackay, D., Shiu, W., Ma, K., and Lee, S. C.: *Handbook of physical-chemical properties and environmental fate for organic chemicals*, CRC press, 2006.
- Masterton, W. L.: Salting coefficients for gases in seawater from scaled-particle theory, *J. Solution Chem.*, 4, 523-534, doi:10.1007/BF00650690, 1975.
- Matsunaga, K. O.: *Comparison of Environmental Impacts and Physical Properties of Refrigerants*, in, New York: Columbia University, 2002.
- 50 McCulloch, A., Midgley, P. M., and Ashford, P.: Releases of refrigerant gases (CFC-12, HCFC-22 and HFC-134a) to the atmosphere, *Atmos. Environ.*, 37, 889-902, doi:10.1016/s1352-2310(02)00975-5, 2003.
- McCulloch, A., and Lindley, A. A.: Global emissions of HFC-23 estimated to year 2015, *Atmos. Environ.*, 41, 1560-1566, doi:10.1016/j.atmosenv.2006.02.021, 2007.
- McGowan, J. C., and Mellors, A.: *Molecular volumes in chemistry and biology*, E. Horwood, 1986.
- 55 Mclinden, M. O.: Physical properties of alternatives to the fully halogenated chlorofluorocarbons, *Scientific assessment of stratospheric ozone*, 2, 1990.
- Meinshausen, M., Vogel, E., Nauels, A., Lorbacher, K., Meinshausen, N., Etheridge, D. M., Fraser, P. J., Montzka, S. A., Rayner, P. J., and Trudinger, C. M.: Historical greenhouse gas concentrations for climate modelling (CMIP6), *Geosci. Model Dev.*, 10, 2057, doi:10.5194/gmd-10-2057-2017, 2017.
- 60 Miguel, A. A. F., Ferreira, A. G. M., and Fonseca, I. M. A.: Solubilities of some new refrigerants in water, *Fluid Phase Equilib.*, 173, 97-107, doi:10.1016/s0378-3812(00)00390-3, 2000.
- Miller, B. R., Huang, J., Weiss, R. F., Prinn, R. G., and Fraser, P. J.: Atmospheric trend and lifetime of chlorodifluoromethane (HCFC-22) and the global tropospheric OH concentration, *J. Geophys. Res.*, 103, 13237, doi:10.1029/98jd00771, 1998.
- 65 Miller, B. R., Weiss, R. F., Salameh, P. K., Tanhua, T., Grealley, B. R., Mühle, J., and Simmonds, P. G.: Medusa: A sample preconcentration and GC/MS detector system for in situ measurements of atmospheric trace halocarbons, hydrocarbons, and sulfur compounds, *Anal. Chem.*, 80, 1536-1545, doi:10.1021/ac702084k, 2008.
- Miller, B. R., Rigby, M., Kuijpers, L. J. M., Krummel, P. B., Steele, L. P., Leist, M., Fraser, P. J., McCulloch, A., Harth, C., Salameh, P., Mühle, J., Weiss, R. F., Prinn, R. G., Wang, R. H. J., O'Doherty, S., Grealley, B. R., and Simmonds, P. G.: HFC-23 (CHF<sub>3</sub>) emission trend response to HCFC-22 (CHClF<sub>2</sub>) production and recent HFC-23 emission abatement measures, *Atmos. Chem. Phys.*, 10, 7875-7890, doi:10.5194/acp-10-7875-2010, 2010.
- 70 Miller, B. R., and Kuijpers, L. J. M.: Projecting future HFC-23 emissions, *Atmos. Chem. Phys.*, 11, 13259-13267, doi:10.5194/acp-11-13259-2011, 2011.

Field Code Changed

- Millero, F. J., and Poisson, A.: International one-atmosphere equation of state of seawater, *Deep Sea Res. Part A. Oceanogr. Res. Pap.*, 28, 625-629, doi:10.1016/0198-0149(81)90122-9, 1981.
- Molina, M. J., and Rowland, F. S.: Stratospheric sink for chlorofluoromethanes: chlorine atom-catalysed destruction of ozone, *Nature*, 249, 810-812, doi:10.1038/249810a0, 1974.
- 5 Montzka, S. A., Myers, R. C., Butler, J. H., Elkins, J. W., and Cummings, S. O.: Global tropospheric distribution and calibration scale of HCFC-22, *Geophys. Res. Lett.*, 20, 703-706, doi:10.1029/93GL00753, 1993.
- Montzka, S. A., Myers, R. C., Butler, J. H., and Elkins, J. W.: Early trends in the global tropospheric abundance of hydrochlorofluorocarbon-141b and 142b, *Geophys. Res. Lett.*, 21, 2483-2486, doi:10.1029/94GL02342, 1994.
- 10 Montzka, S. A., Myers, R. C., Butler, J. H., Elkins, J. W., Lock, L. T., Clarke, A. D., and Goldstein, A. H.: Observations of HFC-134a in the remote troposphere, *Geophys. Res. Lett.*, 23, 169-172, doi:10.1029/95gl03590, 1996.
- Montzka, S. A., Hall, B. D., and Elkins, J. W.: Accelerated increases observed for hydrochlorofluorocarbons since 2004 in the global atmosphere, *Geophys. Res. Lett.*, 36, doi:10.1029/2008gl036475, 2009.
- Montzka, S. A., Kuijpers, L., Battle, M. O., Aydin, M., Verhulst, K. R., Saltzman, E. S., and Fahey, D. W.: Recent increases in global HFC-23 emissions, *Geophys. Res. Lett.*, 37, L02808, doi:10.1029/2009gl041195, 2010a.
- 15 Montzka, S. A., Reimann, S. C. L. A., O'Doherty, S., Engel, A., Krüger, K., and Sturges, W. T.: Ozone-Depleting Substances (ODSs) and Related Chemicals, Chapter 1, 2010b.
- Montzka, S. A., McFarland, M., Andersen, S. O., Miller, B. R., Fahey, D. W., Hall, B. D., Hu, L., Siso, C., and Elkins, J. W.: Recent trends in global emissions of hydrochlorofluorocarbons and hydrofluorocarbons: Reflecting on the 2007 adjustments to the Montreal Protocol, *J. Phys. Chem. A*, 119, 4439-4449, doi:10.1021/jp5097376, 2015.
- 20 Moore, R. M., Geen, C. E., and Tait, V. K.: Determination of Henry's law constants for a suite of naturally occurring halogenated methanes in seawater, *Chemosphere*, 30, 1183-1191, doi:10.1016/0045-6535(95)00009-W, 1995.
- Morris, R. A., Miller, T. M., Viggiano, A., Paulson, J. F., Solomon, S., and Reid, G.: Effects of electron and ion reactions on atmospheric lifetimes of fully fluorinated compounds, *J. Geophys. Res.: Atmos.*, 100, 1287-1294, 1995.
- Mühle, J., Ganesan, A. L., Miller, B. R., Salameh, P. K., Harth, C. M., Grealley, B. R., Rigby, M., Porter, L. W., Steele, L. P., Trudinger, C. M., Krummel, P. B., O'Doherty, S., Fraser, P. J., Simmonds, P. G., Prinn, R. G., and Weiss, R. F.: Perfluorocarbons in the global atmosphere: tetrafluoromethane, hexafluoroethane, and octafluoropropane, *Atmos. Chem. Phys.*, 10, 5145-5164, doi:10.5194/acp-10-5145-2010, 2010.
- O'Doherty, S., Cunnold, D. M., Manning, A. J., Miller, B. R., Wang, R. H. J., Krummel, P. B., Fraser, P. J., Simmonds, P. G., McCulloch, A., and Weiss, R. F.: Rapid growth of hydrofluorocarbon 134a and hydrochlorofluorocarbons 141b, 142b, and 22 from Advanced Global Atmospheric Gases Experiment (AGAGE) observations at Cape Grim, Tasmania, and Mace Head, Ireland, *J. Geophys. Res.*, 109, doi:10.1029/2003jd004277, 2004.
- 30 O'Doherty, S., Cunnold, D. M., Miller, B. R., Mühle, J., McCulloch, A., Simmonds, P. G., Manning, A. J., Reimann, S., Vollmer, M. K., Grealley, B. R., Prinn, R. G., Fraser, P. J., Steele, L. P., Krummel, P. B., Dunse, B. L., Porter, L. W., Lunder, C. R., Schmidbauer, N., Hermansen, O., Salameh, P. K., Harth, C. M., Wang, R. H. J., and Weiss, R. F.: Global and regional emissions of HFC-125 (CHF<sub>2</sub>CF<sub>3</sub>) from in situ and air archive atmospheric observations at AGAGE and SOGE observatories, *J. Geophys. Res.*, 114, doi:10.1029/2009jd012184, 2009.
- 35 Oram, D. E., Reeves, C. E., Penkett, S. A., and Fraser, P. J.: Measurements of HCFC-142b and HCFC-141b in the Cape Grim Air Archive: 1978-1993, *Geophys. Res. Lett.*, 22, 2741-2744, doi:10.1029/2003JD004277, 1995.
- Oram, D. E., Reeves, C. E., Sturges, W. T., Penkett, S. A., Fraser, P. J., and Langenfelds, R. L.: Recent tropospheric growth rate and distribution of HFC-134a (CF<sub>3</sub>CH<sub>2</sub>F), *Geophys. Res. Lett.*, 23, 1949-1952, doi:10.1029/96gl01862, 1996.
- 40 Oram, D. E., Sturges, W. T., Penkett, S. A., McCulloch, A., and Fraser, P. J.: Growth of fluorocarbon (CHF<sub>3</sub>, HFC-23) in the background atmosphere, *Geophys. Res. Lett.*, 25, 35-38, doi:10.1029/97gl03483, 1998.
- Penkett, S. A., Prosser, N. J. D., Rasmussen, R. A., and Khalil, M. A. K.: Atmospheric measurements of CF<sub>4</sub> and other fluorocarbons containing the CF<sub>3</sub> grouping, *J. Geophys. Res.: Oceans*, 86, 5172-5178, doi:10.1029/JC086iC06p05172, 1981.
- 45 Prinn, R., Cunnold, D., Simmonds, P., Aleya, F., Boldi, R., Crawford, A., Fraser, P., Gutzler, D., Hartley, D., and Rosen, R.: Global average concentration and trend for hydroxyl radicals deduced from ALE/GAGE trichloroethane (methyl chloroform) data for 1978-1990, *J. Geophys. Res.: Atmos.*, 97, 2445-2461, 1992.
- Prinn, R. G., Weiss, R. F., Fraser, P. J., Simmonds, P. G., Cunnold, D. M., Aleya, F. N., O'Doherty, S., Salameh, P., Miller, B. R., Huang, J., Wang, R. H. J., Hartley, D. E., Harth, C., Steele, L. P., Sturrock, G., Midgley, P. M., and McCulloch, A.: A history of chemically and radiatively important gases in air deduced from ALE/GAGE/AGAGE, *J. Geophys. Res.*, 105, 17751, doi:10.1029/2000jd900141, 2000.
- 50 Prinn, R. G., Weiss, R. F., Arduini, J., Arnold, T., DeWitt, H. L., Fraser, P. J., Ganesan, A. L., Gasore, J., Harth, C. M., and Hermansen, O.: History of chemically and radiatively important atmospheric gases from the Advanced Global Atmospheric Gases Experiment (AGAGE), *Earth System Science Data*, 10, 985, 2018a.
- Prinn, R. G., Weiss, R. F., Arduini, J., Arnold, T., Fraser, P. J., Ganesan, A. L., Gasore, J., Harth, C. M., Hermansen, O., Kim, J., Krummel, P. B., Li, S., Loh, Z. M., Lunder, C. R., Maione, M., Manning, A. J., Miller, B. R., Mitrevski, B., Mühle, J., O'Doherty, S., Park, S., Reimann, S., Rigby, M., Salameh, P. K., Schmidt, R., Simmonds, P. G., Steele, L. P., Vollmer, M. K., Wang, R. H., and Young, D.: The ALE/GAGE/AGAGE Network (DB 1001), <http://cdiac.essdive.lbl.gov/ndps/alegagage.html> doi:10.3334/CDIAC/atg.db1001, 2018b.
- 55 Rasmussen, R. A., Penkett, S. A., and Prosser, N.: Measurement of carbon tetrafluoride in the atmosphere, *Nature*, 277, 549-551, doi:10.1038/277549a0, 1979.
- 60 Rasmussen, R. A., Khalil, M. A. K., Penkett, S. A., and Prosser, N. J. D.: CHClF<sub>2</sub> (F-22) in the Earth's atmosphere, *Geophys. Res. Lett.*, 7, 809-812, doi:10.1029/GL007i010p00809, 1980.
- Ravishankara, A., Solomon, S., Turnipseed, A. A., and Warren, R.: Atmospheric lifetimes of long-lived halogenated species, *Science*, 194-199, 1993.
- Reichl, A.: Messung und Korrelierung von Gaslöslichkeiten halogener Kohlenwasserstoffe, Shaker, 1995.
- 65 Reinsch, C. H.: Smoothing by spline functions, *Numer. Math.*, 10, 177-183, doi:10.1007/BF02162161, 1967.
- Rigby, M., Ganesan, A. L., and Prinn, R. G.: Deriving emissions time series from sparse atmospheric mole fractions, *J. Geophys. Res.: Atmos.*, 116, doi:10.1029/2010JD015401, 2011.
- Rigby, M., Prinn, R., O'Doherty, S., Miller, B., Ivy, D., Mühle, J., Harth, C., Salameh, P., Arnold, T., and Weiss, R.: Recent and future trends in synthetic greenhouse gas radiative forcing, *Geophys. Res. Lett.*, 41, 2623-2630, 2014.
- 70 Rowland, F. S., and Molina, M. J.: Chlorofluoromethanes in the environment, *Rev. Geophys.*, 13, 1-35, 1975.
- Saikawa, E., Rigby, M., Prinn, R. G., Montzka, S. A., Miller, B. R., Kuijpers, L. J. M., Fraser, P. J. B., Vollmer, M. K., Saito, T., Yokouchi, Y., Harth, C. M., Mühle, J., Weiss, R. F., Salameh, P. K., Kim, J., Li, S., Park, S., Kim, K. R., Young, D., O'Doherty, S.,

Field Code Changed

- Simmonds, P. G., McCulloch, A., Krummel, P. B., Steele, L. P., Lunder, C., Hermansen, O., Maione, M., Arduini, J., Yao, B., Zhou, L. X., Wang, H. J., Elkins, J. W., and Hall, B.: Global and regional emission estimates for HCFC-22, *Atmos. Chem. Phys.*, 12, 10033-10050, doi:10.5194/acp-12-10033-2012, 2012.
- 5 Sander, R.: Modeling atmospheric chemistry: Interactions between gas-phase species and liquid cloud/aerosol particles, *Surveys in Geophysics*, 20, 1-31, doi:10.1023/A:1006501706704, 1999.
- Scharlin, P., and Battino, R.: Solubility of  $\text{CCl}_2\text{F}_2$ ,  $\text{CClF}_3$ ,  $\text{CF}_4$ , and  $\text{CH}_4$  in Water and Seawater at 288.15-303.15 K and 101.325 kPa, *J. Chem. Eng. Data*, 40, 167-169, doi:10.1021/je00017a036, 1995.
- Schneider, A., Tanhua, T., Körtzinger, A., and Wallace, D. W. R.: An evaluation of tracer fields and anthropogenic carbon in the equatorial and the tropical North Atlantic, *Deep-Sea Res. Pt. I*, 67, 85-97, doi:10.1016/j.dsr.2012.05.007, 2012.
- 10 Schwarzenbach, R. P., Gschwend, P. M., and Imboden, D. M.: *Environmental Organic Chemistry*, 2. ed, John Wiley & Sons: Hoboken, NJ, 2003.
- Simmonds, P. G., O'Doherty, S., Nickless, G., Sturrock, G. A., Swaby, R., Knight, P., Ricketts, J., Woffendin, G., and Smith, R.: Automated gas chromatograph/mass spectrometer for routine atmospheric field measurements of the CFC replacement compounds, the hydrofluorocarbons and hydrochlorofluorocarbons, *Anal. Chem.*, 67, 717-723, doi:10.1021/ac00100a005, 1995.
- 15 Simmonds, P. G., O'Doherty, S., Huang, J., Prinn, R., Derwent, R. G., Ryall, D., Nickless, G., and Cunnold, D.: Calculated trends and the atmospheric abundance of 1, 1, 1, 2-tetrafluoroethane, 1, 1-dichloro-1-fluoroethane, and 1-chloro-1, 1-difluoroethane using automated in-situ gas chromatography-mass spectrometry measurements recorded at Mace Head, Ireland, from October 1994 to March 1997, *J. Geophys. Res.: Atmos.*, 103, 16029-16037, doi:10.1029/98JD00774, 1998.
- 20 Simmonds, P. G., Derwent, R. G., Manning, A. J., McCulloch, A., and O'Doherty, S.: USA emissions estimates of  $\text{CH}_3\text{CHF}_2$ ,  $\text{CH}_2\text{FCF}_3$ ,  $\text{CH}_3\text{CF}_3$  and  $\text{CH}_2\text{F}_2$  based on in situ observations at Mace Head, *Atmos. Environ.*, 104, 27-38, doi:10.1016/j.atmosenv.2015.01.010, 2015.
- Simmonds, P. G., Rigby, M., McCulloch, A., O'Doherty, S., Young, D., Mühle, J., Krummel, P. B., Steele, P., Fraser, P. J., and Manning, A. J.: Changing trends and emissions of hydrochlorofluorocarbons (HCFCs) and their hydrofluorocarbon (HFCs) replacements, *Atmos. Chem. Phys.*, 17, 4641-4655, doi:10.5194/acp-17-4641-2017, 2017.
- 25 Simmonds, P. G., Rigby, M., McCulloch, A., Vollmer, M. K., Henne, S., Mühle, J., O'Doherty, S., Manning, A. J., Krummel, P. B., Fraser, P. J., Young, D., Weiss, R. F., Salameh, P. K., Harth, C. M., Reimann, S., Trudinger, C. M., Steele, P., Wang, R. H. J., Ivy, D. J., Prinn, R. G., Mitrevski, B., and Etheridge, D. M.: Recent increases in the atmospheric growth rate and emissions of HFC-23 ( $\text{CHF}_3$ ) and the link to HCFC-22 ( $\text{CHClF}_2$ ) production, *Atmos. Chem. Phys.*, 2018, 4153-4169, doi:10.5194/acp-18-4153-2018, 2018.
- 30 Smethie, W., Chipman, D., Swift, J., and Koltermann, K.: Chlorofluoromethanes in the Arctic Mediterranean seas: evidence for formation of bottom water in the Eurasian Basin and deep-water exchange through Fram Strait, *Deep Sea Res. Part A. Oceanogr. Res. Pap.*, 35, 347-369, doi:10.1016/0198-0149(88)90015-5, 1988.
- Smith, J. N., Smethie, W. M., Yashayev, I., Curry, R., and Azetsu-Scott, K.: Time series measurements of transient tracers and tracer-derived transport in the Deep Western Boundary Current between the Labrador Sea and the subtropical Atlantic Ocean at Line W, *J. Geophys. Res.: Oceans*, 121, 8115-8138, doi:10.1002/2016JC011759, 2016.
- 35 SPARC: Lifetimes of Stratospheric Ozone-Depleting Substances, Their Replacements, and Related Species, AGU Fall Meeting Abstracts, 2013.
- Stöven, T., Tanhua, T., Hoppema, M., and Bullister, J. L.: Perspectives of transient tracer applications and limiting cases, *Ocean Sci.*, 11, 699-718, doi:10.5194/os-11-699-2015, 2015.
- Stöven, T., Tanhua, T., Hoppema, M., and von Appen, W. J.: Transient tracer distributions in the Fram Strait in 2012 and inferred anthropogenic carbon content and transport, *Ocean Sci.*, 12, 319-333, doi:10.5194/os-12-319-2016, 2016.
- 40 Sturrock, G. A., Etheridge, D. M., Trudinger, C. M., Fraser, P. J., and Smith, A. M.: Atmospheric histories of halocarbons from analysis of Antarctic firn air: Major Montreal Protocol species, *J. Geophys. Res.: Atmos.*, 107, doi:10.1029/2002JD002548, 2002.
- Tanhua, T., Anders Olsson, K., and Fogelqvist, E.: A first study of  $\text{SF}_6$  as a transient tracer in the Southern Ocean, *Deep-Sea Res. Pt. II*, 51, 2683-2699, doi:10.1016/j.dsr2.2001.02.001, 2004.
- 45 Tanhua, T., Olsson, K. A., and Jeansson, E.: Tracer evidence of the origin and variability of Denmark Strait Overflow Water, in: *Arctic-Subarctic Ocean Fluxes*, Springer, 475-503, 2008.
- TEAP: Report of the Technology and Economic Assessment Panel. HCFC Task Force Report, United Nations Environment Programme, Ozone Secretariat, P.O. Box 30552, Nairobi, Kenya, 2003.
- Thompson, T. M., Butler, J. H., Daube, B. C., Dutton, G. S., Elkins, J. W., Hall, B. D., Hurst, D. F., King, D. B., Kline, E. S., and Lafleur, B. G.: Halocarbons and other atmospheric trace species, *Climate Monitoring Diagnostics Laboratory Summary Report*, 27, 115-135, 2004.
- 50 Trudinger, C. M., Fraser, P. J., Etheridge, D. M., Sturges, W. T., Vollmer, M. K., Rigby, M., Martinerie, P., Mühle, J., Worton, D. R., and Krummel, P. B.: Atmospheric abundance and global emissions of perfluorocarbons  $\text{CF}_4$ ,  $\text{C}_2\text{F}_6$  and  $\text{C}_3\text{F}_8$  since 1800 inferred from ice core, firn, air archive and in situ measurements, *Atmos. Chem. Phys.*, 16, 11733-11754, doi:10.5194/acp-16-11733-2016, 2016.
- UNEP: United Nations Environment Programme, ozone.unep.org/countries/data, 2018.
- 55 Vogel, H., and Friedrich, B.: An Estimation of PFC Emission by Rare Earth Electrolysis, TMS Annual Meeting & Exhibition, 2018, 1507-1517.
- Vollmer, M. K., Mühle, J., Trudinger, C. M., Rigby, M., Montzka, S. A., Harth, C. M., Miller, B. R., Henne, S., Krummel, P. B., and Hall, B. D.: Atmospheric histories and global emissions of halons H-1211 ( $\text{CBrClF}_2$ ), H-1301 ( $\text{CBrF}_3$ ), and H-2402 ( $\text{CBr}_2\text{CBrF}_2$ ), *J. Geophys. Res.: Atmos.*, 121, 3663-3686, 2016.
- 60 Wahba, G.: Bayesian "confidence intervals" for the cross-validated smoothing spline, *Journal of the Royal Statistical Society. Series B (Methodological)*, 133-150, 1983.
- Wahba, G.: Spline models for observational data, *Siam*, 1990.
- Walker, S. J., Weiss, R. F., and Salameh, P. K.: Reconstructed histories of the annual mean atmospheric mole fractions for the halocarbons CFC-11, CFC-12, CFC-113, and carbon tetrachloride, *J. Geophys. Res.*, 105, 14285, doi:10.1029/1999jc900273, 2000.
- 70 Warner, M. J., and Weiss, R. F.: Solubilities of chlorofluorocarbons 11 and 12 in water and seawater, *Deep Sea Res. Part A. Oceanogr. Res. Pap.*, 32, 13, doi:10.1016/0198-0149(85)90099-8, 1985.
- 65 Waugh, D. W., Vollmer, M. K., Weiss, R. F., Haine, T. W., and Hall, T. M.: Transit time distributions in Lake Issyk-Kul, *Geophys. Res. Lett.*, 29, doi:10.1029/2002GL016201, 2002.
- Waugh, D. W., Abraham, E. R., and Bowen, M. M.: Spatial variations of stirring in the surface ocean: A case study of the Tasman Sea, *J. Phys. Oceanogr.*, 36, 526-542, doi:10.1175/jpo2865.1, 2006.
- 70 Weiss, R. F.: The solubility of nitrogen, oxygen and argon in water and seawater, *Deep-Sea Res. Oceanogr. Abstr.*, 17, 721-735, doi:10.1016/0011-7471(70)90037-9, 1970.

- Weiss, R. F.: Carbon Dioxide in Water and Seawater: the Solubility of a Non-ideal Gas, *Mar. Chem.*, 2, 13, doi:10.1016/0304-4203(74)90015-2, 1974.
- Weiss, R. F., Bullister, J. L., Gammon, R. H., and Warner, M. J.: Atmospheric chlorofluoromethanes in the deep equatorial Atlantic, *Nature*, doi:10.1038/314608a0, 1985.
- 5 Xiang, B., Patra, P. K., Montzka, S. A., Miller, S. M., Elkins, J. W., Moore, F. L., Atlas, E. L., Miller, B. R., Weiss, R. F., Prinn, R. G., and Wofsy, S. C.: Global emissions of refrigerants HCFC-22 and HFC-134a: Unforeseen seasonal contributions, *Proc. Natl. Acad. Sci. USA*, 111, 17379-17384, doi:10.1073/pnas.1417372111, 2014.
- Young, C. L., Battino, R., and Clever, H. L.: *The Solubility of Gases in Liquids: Introductory Information*, IUPAC SDS, 27/28, 1987.
- 10 Yvon-Lewis, S. A., and Butler, J. H.: Effect of oceanic uptake on atmospheric lifetimes of selected trace gases, *J. Geophys. Res.: Atmos.*, 107, 2002.

Supplement of

# **Atmospheric Histories, Growth Rates and Solubilities in Seawater and other Natural Water of the Potential Transient Tracers HCFC-22, HCFC-141b, HCFC-142b, HFC-134a, HFC-125, HFC-23, PFC-14 and PFC-116**

Pingyang Li <sup>1</sup>, Jens Mühle <sup>2</sup>, Stephen A. Montzka <sup>3</sup>, David E. Oram <sup>4</sup>, Benjamin R. Miller <sup>3</sup>, Ray F. Weiss <sup>2</sup>, Paul J. Fraser <sup>5</sup> and Toste Tanhua <sup>1</sup>

<sup>1</sup>GEOMAR Helmholtz Centre for Ocean Research Kiel, Kiel, [24105](#), Germany

<sup>2</sup>Scripps Institution of Oceanography, University of California, [San Diego](#), La Jolla, California, [92093](#), USA

<sup>3</sup>Earth System Research Laboratory, National Oceanic and Atmospheric Administration, Boulder, Colorado, 80305, USA

<sup>4</sup>National Centre for Atmospheric Science, [Centre for Ocean and Atmospheric Sciences](#), School of Environmental Sciences, University of East Anglia, Norwich, NR4 7TJ, UK

<sup>5</sup>[Climate Science Centre, Commonwealth Scientific and Industrial Research Organization Oceans and Atmosphere](#), Aspendale, Victoria, 3195, Australia

Correspondence to: [Toste Tanhua](mailto:ttanhua@geomar.de) ([ttanhua@geomar.de](mailto:ttanhua@geomar.de))

## **Content:**

### **Section S1. Smoothing spline fit method**

**Table S1 (a-h).** Collected data used for HCFC-22, HCFC-141b, HCFC-142b, HFC-134a, HFC-125, HFC-23, PFC-14 and PFC-116

**Table S2.** Atmospheric mole fractions for HCFC-22, HCFC-141b, HCFC-142b, HFC-134a, HFC-125, HFC-23, PFC-14 and PFC-116 (See Excel file)

**Table S3.** Ostwald solubility function of PFC-14 in seawater estimated by Method I

**Table S4.** Comparison among the calculated Ostwald solubility coefficients ( $L_0$ ,  $L$   $L^{-1}$ ) by the poly-parameter linear free energy relationships (pp-LFERs) based on  $V$ ,  $V_c$  and  $\log L^{16}$ , observed ones and calculated ones by the Clark-Glew-Weiss (CGW) model fit of target compounds and CFC-12 in water at 298.15 K and 310.15 K

**Table S5.** Ostwald solubility functions of target compounds and CFC-12 in water estimated by (Revised) Method II at 298.15 K and 310.15 K

**Fig. S1 (a-h).** HCFC-22, HCFC-141b, HCFC-142b, HFC-134a, HFC-125, HFC-23, PFC-14 and PFC-116: Atmospheric mole fractions in the NH and SH estimated from collected data (Table S1a-h)

**Fig. S2 (a-i).** HCFC-22, HCFC-141b, HCFC-142b, HFC-134a, HFC-125, HFC-23, PFC-14, PFC-116 and CFC-12 freshwater solubility (Ostwald solubility coefficients) as a function of temperature based on previous studies

**Fig. S3.** The relationship between salting-out coefficients (SOC) and temperature calculated by Eq. (16) for CFC-12 based on the data from Warner and Weiss (1985).

Deleted: Global Annual Mean

Deleted: Solubility Estimations

Deleted: Halogenated Compounds

Deleted: <sup>5</sup>

Deleted: San Diego,

Deleted: nited States

Deleted: <sup>5</sup>Centre for Ocean and Atmospheric Sciences, School of Environmental Sciences, University of East Anglia, Norwich, NR4 7TJ, UK

Deleted: Pingyang Li

Deleted: pli

Deleted: ¶

## Section S1. Smoothing spline fit method

After the database containing replicate times have been converted into a value at each replicate time, the data is sorted as  $x_1 < x_2 < \dots < x_i < \dots < x_n$ .

Set  $x_i, y_i, \delta y_i$  ( $i = 1, 2, \dots, n$ ) to be the decimal time, the corresponding atmospheric mole fractions and the standard deviation.

Normalize the  $x$  vector

$$t_i = (x_i - \min(x_i)) / (\max(x_i) - \min(x_i)) \quad (1)$$

The smoothing function  $f(t)$  to be constructed shall

$$\text{Minimize } p \sum_{i=1}^n \left[ \frac{g(t_i) - y_i}{\delta y_i} \right]^2 + \int g''(t)^2 dt \quad (2)$$

The solution of the minimum principle is a cubic spline. By introducing the auxiliary variable  $z$  together with the Lagrangian parameter  $p$ , we have to look for the minimum of the functional

$$\int_{t_1}^{t_n} g''(t)^2 dt + p \left[ \sum_{i=1}^n \left( \frac{g(t_i) - y_i}{\delta y_i} \right)^2 + z^2 \right] \quad (3)$$

From the corresponding Euler-Lagrange equations, we determine the optimal function  $f(t)$ .

$$f(t) = a_i + b_i(t - t_i) + c_i(t - t_i)^2 + d_i(t - t_i)^3, \quad t_i \leq t < t_{i+1} \quad (4)$$

We obtain the spline coefficients (Reinsch, 1967).

$$c_i = \frac{pQ^T y}{B}, \quad c = [0; c_i; 0]^T \quad (5)$$

$$a = y - W^2 Q c / p \quad (6)$$

$$d_i = (c_{i+1} - c_i) / (3h_i) \quad (7)$$

$$b_i = (a_{i+1} - a_i) / h_i - c_i h_i - d_i h_i^2 \quad (8)$$

$$\text{coeffs} = [d, c, b, a] \quad (9)$$

Here, the following notation is used:

$$h_i = t_{i+1} - t_i, \quad (10)$$

$$W = \text{diag}(\delta y_1, \dots, \delta y_n), \quad (11)$$

T is the  $(n-1) \times (n-1)$  dimensional positive tridiagonal matrix with entries  $t_{ij}$  ( $i, j = 1, 2, \dots, n-1$ ) given by

$$t_{ii} = 2(h_{i-1} + h_i) / 3, \quad t_{i,i+1} = t_{i+1,i} = h_i / 3 \quad (12)$$

Q is the  $(n) \times (n-2)$  dimensional tridiagonal matrix with entries  $q_{ij}$  ( $i = 1, 2, \dots, n; j = 1, 2, \dots, n-2$ ) given by

$$q_{i-1,i} = 1/h_{i-1}, \quad q_{i,i} = -1/h_{i-1} - 1/h_i, \quad q_{i+1,i} = 1/h_i \quad (13)$$

The elements in the  $i^{\text{th}}$  column of  $Q$  given by the coefficients of the 2<sup>th</sup> order divided differences based on  $t_i, \dots, t_{i+2}$ . Let the coefficient matrix be denoted by

$$B_p = Q^T W^2 Q + pT \quad (14)$$

The influence matrix associated with the smoothing spline is the unique  $n \times n$  symmetric matrix  $A_p$  satisfying

$$a = A_p y \quad (15)$$

The error

Deleted: We collected data from in situ, flask, archived air, firm air measurements. Database containing replicate times have been converted into a value without such replicates by using the mean of values at each replicate time. The error of the means will be the root-mean-square (RMS) of standard deviation values of replicate values. Then

$$error = y - a = W^2 Q B_p^{-1} Q^T y \quad (16)$$

So that

$$I - A_p = W^2 Q B_p^{-1} Q^T \quad (17)$$

The weighted residual sum of squares

$$RSS = \|(I - A_p)y/W\|^2 = \|W^2 Q B_p^{-1} Q^T y\|^2 \quad (18)$$

The estimate value of the generalized cross-validation (GCV) minimization function  $V$  of  $p$  used in the experiments below is the minimizer of the GCV function  $V_p$  defined

$$V_p = \frac{n \|(I - A_p)y/W\|^2}{[Tr(I - A_p)]^2} \quad (19)$$

The estimated degrees of freedom (Hutchinson and De Hoog, 1985)

$$Tr(I - A_p) = n - 2 - pTr(T/B) \quad (20)$$

The estimated variance

$$VAR = RSS/Tr(I - A_p) \quad (21)$$

The estimated 95 % Bayesian confidence intervals (CI) for the Cross-validated Smoothing Spline (Wahba, 1983) are given by

$$CI = 1.96 \sqrt{VAR * diag(A_p)} \quad (22)$$

**Table S1a. Collected data** used for HCFC-22

Data	Network	Station	Latitude °N	Longitude °E	Instrument	Data availability	Scale	Reference
NH								
<i>In situ</i>	AGAGE	Mace Head	53.3	-9.9	ADS	1999.01-2004.12	SIO-05	(Prinn et al., 2018a; Prinn et al., 2018b)
<i>In situ</i>	AGAGE	Mace Head	53.3	-9.9	Medusa	2003.11-2017.09	SIO-05	(Prinn et al., 2018a; Prinn et al., 2018b)
Flask	NOAA	Mace Head	53.3	-9.9	GC-MS	1998.10-2018.08	NOAA-2006	(Montzka et al., 1996a; Montzka et al., 2015)
<i>In situ</i>	AGAGE	Trinidad Head	41.0	-124.1	Medusa	2005.05-2017.09	SIO-05	(Prinn et al., 2018a; Prinn et al., 2018b)
<b>Flask</b>	<b>NOAA</b>	<b>Trinidad Head</b>	<b>41.0</b>	<b>-124.1</b>	<b>GC-MS</b>	<b>2002.03-2018.08</b>	<b>NOAA-2006</b>	(Montzka et al., 1996a; Montzka et al., 2015)
Model	NOAA	NH	30-90	-	2-D box	1944-2009	NOAA-2006	(Montzka et al., 2010)
SH								
<i>In situ</i>	AGAGE	Cape Grim	-40.7	144.7	ADS	1998.03-2004.12	SIO-05	(Prinn et al., 2018a; Prinn et al., 2018b)
<i>In situ</i>	AGAGE	Cape Grim	-40.7	144.7	Medusa	2004.01-2017.09	SIO-05	(Prinn et al., 2018a; Prinn et al., 2018b)
Flask	NOAA	Cape Grim	-40.7	144.7	GC-MS	1991.11-2018.08	NOAA-2006	(Montzka et al., 1996a; Montzka et al., 2015)
Archived air	AGAGE	Cape Grim	-40.7	144.7	Medusa	1978.04-1996.12	SIO-93	(Miller et al., 1998)
Model	NOAA	SH	-30 ~ -90	-	2-D box	1944-2009	NOAA-2006	(Montzka et al., 2010)

Deleted: 2a...1a. Data ...

Formatted Table

Field Code Changed

Deleted: 03

Formatted ...

Formatted ...

Field Code Changed

Deleted: (Prinn et al., 2000;Prinn et al., 2018b)

Formatted ...

Deleted: 2017.07

Deleted: 03

Field Code Changed

Deleted: (Prinn et al., 2000;Prinn et al., 2018b)

Formatted ...

Formatted ...

Formatted ...

Field Code Changed

Deleted: (Prinn et al., 2000;Prinn et al., 2018b)

Formatted ...

Formatted ...

Formatted ...

Deleted: 03

Field Code Changed

Deleted: (Prinn et al., 2000;Prinn et al., 2018b)

Formatted ...

Formatted ...

Formatted ...

Deleted: 2017.07

Deleted: (Montzka et al., 1996a)

**Table S1b. Collected data** used for HCFC-141b

Data	Network	Station	Latitude °N	Longitude °E	Instrument	Data availability	Scale	Reference
NH								
Archived air	NOAA	Niwot Ridge	40.0	-	GC <sub>2</sub> MS	1987.01-1994.03	NOAA-1994	(Thompson et al., 2004)
<i>In situ</i>	AGAGE	Mace Head	53.3	-9.9	ADS	1994.11-2004.12	SIO-05	(Prinn et al., 2018a; Prinn et al., 2018b)
<i>In situ</i>	AGAGE	Mace Head	53.3	-9.9	Medusa	2003.11-2017.09	SIO-05	(Prinn et al., 2018a; Prinn et al., 2018b)
Flask	NOAA	Mace Head	53.3	-9.9	GC <sub>2</sub> MS	1998.10-2018.08	NOAA-1994	(Montzka et al., 1996a; Montzka et al., 2015)
<i>In situ</i>	AGAGE	Trinidad Head	41.0	-124.1	Medusa	2005.03-2017.09	SIO-05	(Prinn et al., 2018a; Prinn et al., 2018b)
<u>Flask</u>	<u>NOAA</u>	<u>Trinidad Head</u>	<u>41.0</u>	<u>-124.1</u>	<u>GC-MS</u>	<u>2002.02-2018.08</u>	<u>NOAA-1994</u>	(Montzka et al., 1996a; Montzka et al., 2015)
SH								
Firn air	AGAGE	Antarctic	-90.0	-4.8	ADS	1935.06-1991.11	UB-98	(Sturrock et al., 2002)
Archived air	NOAA	-	-29.4	-	GC <sub>2</sub> MS	1987.06	NOAA-1994	(Thompson et al., 2004)
Archived air	UEA	Cape Grim	-40.7	144.7	GC <sub>2</sub> MS	1978.04-2011.06	NOAA-1994	(Oram et al., 1995);
<i>In situ</i>	AGAGE	Cape Grim	-40.7	144.7	ADS	1998.03-2004.12	SIO-05	(Prinn et al., 2018a; Prinn et al., 2018b)
<i>In situ</i>	AGAGE	Cape Grim	-40.7	144.7	Medusa	2004.01-2017.09	SIO-05	(Prinn et al., 2018a; Prinn et al., 2018b)
Flask	NOAA	Cape Grim	-40.7	144.7	GC <sub>2</sub> MS	1994.10-2018.08	NOAA-1994	(Montzka et al., 1996a; Montzka et al., 2015)

Deleted: 2b...1b. Collected dataData ...

Formatted Table ...

Deleted: (Prinn et al., 2000;Prinn et al ...

Formatted ...

Formatted ...

Field Code Changed ...

Formatted ...

Deleted: 03 ...

Field Code Changed ...

Deleted: (Prinn et al., 2000;Prinn et al ...

Formatted ...

Formatted ...

Formatted ...

Deleted: 2017.07 ...

Deleted: (Montzka et al., 1996a) ...

Deleted: 03 ...

Field Code Changed ...

Deleted: (Prinn et al., 2000;Prinn et al ...

Formatted ...

Formatted ...

Formatted ...

Deleted: 02 ...

Field Code Changed ...

Deleted: (Prinn et al., 2000;Prinn et al ...

Formatted ...

Formatted ...

Formatted ...

Deleted: 03 ...

Field Code Changed ...

Deleted: (Prinn et al., 2000;Prinn et al ...

Formatted ...

Formatted ...

Formatted ...

Deleted: 2017.07 ...

Deleted: (Montzka et al., 1996a) ...

**Table S1c. Collected data** used for HCFC-142b

Data	Network	Station	Latitude °N	Longitude °E	Instrument	Data availability	Scale	Reference
NH								
Archived air	NOAA	Niwot Ridge	40.0	-	GC <sub>2</sub> MS	1987.01-1994.03	NOAA-1994	(Thompson et al., 2004)
<i>In situ</i>	AGAGE	Mace Head	53.3	-9.9	ADS	1994.10-2004.12	SIO-05	(Prinn et al., 2018a; Prinn et al., 2018b)
<i>In situ</i>	AGAGE	Mace Head	53.3	-9.9	Medusa	2003.11-2017.09	SIO-05	(Prinn et al., 2018a; Prinn et al., 2018b)
Flask	NOAA	Mace Head	53.3	-9.9	GC <sub>2</sub> MS	1998.10-2018.07	NOAA-1994	(Montzka et al., 1996a; Montzka et al., 2015)
<i>In situ</i>	AGAGE	Trinidad Head	41.0	-124.1	Medusa	2005.03-2017.09	SIO-05	(Prinn et al., 2018a; Prinn et al., 2018b)
<b>Flask</b>	<b>NOAA</b>	<b>Trinidad Head</b>	<b>41.0</b>	<b>-124.1</b>	<b>GC-MS</b>	<b>2002.02-2018.08</b>	<b>NOAA-1994</b>	(Montzka et al., 1996a; Montzka et al., 2015)
SH								
Firn air	AGAGE	Antarctic	-90.0	-4.8	ADS	1936.06-1992.05	UB-98	(Sturrock et al., 2002)
Archived air	NOAA	-	-29.4	-	GC <sub>2</sub> MS	1987.06	NOAA-1994	(Thompson et al., 2004)
Archived air	UEA	Cape Grim	-40.7	144.7	GC <sub>2</sub> MS	1978.04-2011.06	NOAA-1994	(Oram et al., 1995);
<i>In situ</i>	AGAGE	Cape Grim	-40.7	144.7	ADS	1998.03-2004.12	SIO-05	(Prinn et al., 2018a; Prinn et al., 2018b)
<i>In situ</i>	AGAGE	Cape Grim	-40.7	144.7	Medusa	2004.01-2017.09	SIO-05	(Prinn et al., 2018a; Prinn et al., 2018b)
Flask	NOAA	Cape Grim	-40.7	144.7	GC <sub>2</sub> MS	1992.01-2018.08	NOAA-1994	(Montzka et al., 1996a; Montzka et al., 2015)

Deleted: 2c...1c. Collected dataData ...

Formatted Table ...

Deleted: (Prinn et al., 2000;Prinn et al ...

Formatted ...

Formatted ...

Field Code Changed ...

Formatted ...

Deleted: 03 ...

Field Code Changed ...

Deleted: (Prinn et al., 2000;Prinn et al ...

Formatted ...

Formatted ...

Formatted ...

Deleted: 2017 ...

Deleted: (Montzka et al., 1996a) ...

Deleted: 03 ...

Field Code Changed ...

Deleted: (Prinn et al., 2000;Prinn et al ...

Formatted ...

Formatted ...

Formatted ...

Formatted ...

Deleted: 03 ...

Field Code Changed ...

Deleted: (Prinn et al., 2000;Prinn et al ...

Formatted ...

Formatted ...

Formatted ...

Deleted: 2017.07 ...

Deleted: (Montzka et al., 1996a) ...

**Table S1d. Collected data** used for HFC-134a

Data	Network	Station	Latitude °N	Longitude °E	Instrument	Data availability	Scale	Reference
NH								
Archived air	AGAGE	La Jolla <u>and other</u>	32.87	-117.25	Medusa	1973.06-2016.04	SIO-05	this study
Archived air	NOAA	Niwot Ridge	40.0	-	GC-MS	1976.01-1999.04	<u>NOAA-1995</u>	(Montzka et al., 1996b)
<i>In situ</i>	AGAGE	Mace Head	53.3	-9.9	ADS	1994.10-2004.12	SIO-05	(Prinn et al., 2018a; Prinn et al., 2018b)
<i>In situ</i>	AGAGE	Mace Head	53.3	-9.9	Medusa	2003.11-2017.09	SIO-05	(Prinn et al., 2018a; Prinn et al., 2018b)
Flask	NOAA	Mace Head	53.3	-9.9	GC-MS	1998.10- <u>2018.06</u>	<u>NOAA-1995</u>	(Montzka et al., 1996a; Montzka et al., 2015)
<i>In situ</i>	AGAGE	Trinidad Head	41.0	-124.1	Medusa	2005.03-2017.09	SIO-05	(Prinn et al., 2018a; Prinn et al., 2018b)
<u>Flask</u>	<u>NOAA</u>	<u>Trinidad Head</u>	<u>41.0</u>	<u>-124.1</u>	<u>GC-MS</u>	<u>2002.02-2018.06</u>	<u>NOAA-1995</u>	(Montzka et al., 1996a; Montzka et al., 2015)
SH								
Archived air	AGAGE	Cape Grim	-40.7	144.7	Medusa	<u>1978.04</u> -2011.06	SIO-05	this study
Archived air	NOAA	-	-29.4	-	GC-MS	1987.06	NOAA-1995	(Montzka et al., 1996b)
Archived air	UEA	Cape Grim	-40.7	144.7	GC-MS	1990.05-2012.12	NOAA-1995	(Oram et al., 1996)
<i>In situ</i>	AGAGE	Cape Grim	-40.7	144.7	ADS	1998.02-2004.12	SIO-05	(Prinn et al., 2018a; Prinn et al., 2018b)
<i>In situ</i>	AGAGE	Cape Grim	-40.7	144.7	Medusa	2004.01-2017.09	SIO-05	(Prinn et al., 2018a; Prinn et al., 2018b)
Flask	NOAA	Cape Grim	-40.7	144.7	GC-MS	1994.10- <u>2018.08</u>	NOAA-1995	(Montzka et al., 1996a; Montzka et al., 2015)

Deleted: 2d...1d. Collected dataData ...

Formatted Table ...

Deleted: 1

Deleted: Archived air ...

Deleted: SIO-05

Field Code Changed ...

Deleted: (Prinn et al., 2000;Prinn et al ...)

Formatted ...

Formatted ...

Formatted ...

Deleted: 03

Field Code Changed ...

Deleted: (Prinn et al., 2000;Prinn et al ...)

Formatted ...

Formatted ...

Formatted ...

Deleted: 2017.07

Deleted: 1994

Deleted: (Montzka et al., 1996a)

Deleted: 03

Field Code Changed ...

Deleted: (Prinn et al., 2000;Prinn et al ...)

Formatted ...

Formatted ...

Formatted ...

Deleted: 1

Deleted: 1995.02

Deleted: Archived air ...

Field Code Changed ...

Deleted: (Prinn et al., 2000;Prinn et al ...)

Formatted ...

Formatted ...

Formatted ...

Deleted: 03

Field Code Changed ...

Deleted: (Prinn et al., 2000;Prinn et al ...)

Formatted ...

Formatted ...

Formatted ...

**Table S1e. Collected data** used for HFC-125

Data	Network	Station	Latitude °N	Longitude °E	Instrument	Data availability	Scale	Reference
<b>NH</b>								
Archived air	AGAGE	La Jolla <b>and other</b>	32.87	-117.25	Medusa	1973.06-2015.11	SIO-14	(O'Doherty et al., 2009)
Archived air	AGAGE	La Jolla <b>and other</b>	32.87	-117.25	Medusa	1973.06-2011.06	UB-98	(O'Doherty et al., 2009)
<i>In situ</i>	AGAGE	Mace Head	53.3	-9.9	ADS	1998.02-2004.12	SIO-14	(Prinn et al., 2018a; Prinn et al., 2018b)
<i>In situ</i>	AGAGE	Mace Head	53.3	-9.9	Medusa	2003.11-2017.09	SIO-14	(Prinn et al., 2018a; Prinn et al., 2018b)
<i>In situ</i>	AGAGE	Trinidad Head	41.0	-124.1	Medusa	2005.03-2017.09	SIO-14	(Prinn et al., 2018a; Prinn et al., 2018b)
Flask	NOAA	Trinidad Head	41.0	-124.1	GC_MS_M2	2007.01-2015.04	NOAA-2008	(Montzka et al., 2015)
<b>SH</b>								
Archived air	AGAGE	Cape Grim	-40.7	144.7	Medusa	1978.04-2011.06	SIO-14	(O'Doherty et al., 2009)
Archived air	AGAGE	Cape Grim	-40.7	144.7	Medusa	1995.02-2001.09	UB-98	(O'Doherty et al., 2009)
<i>In situ</i>	AGAGE	Cape Grim	-40.7	144.7	ADS	1998.02-2004.12	SIO-14	(Prinn et al., 2018a; Prinn et al., 2018b)
<i>In situ</i>	AGAGE	Cape Grim	-40.7	144.7	Medusa	2004.02-2017.09	SIO-14	(Prinn et al., 2018a; Prinn et al., 2018b)
Flask	NOAA	Cape Grim	-40.7	144.7	GC_MS_M2	2007.01-2015.04	NOAA-2008	(Montzka et al., 2015)

- Deleted: 2e...1e. Collected dataData ...
- Formatted Table ...
- Deleted: 1
- Deleted: 7.Diane
- Deleted: Archived air ...
- Field Code Changed ...
- Deleted: (Prinn et al., 2000;Prinn et al ...
- Formatted ...
- Formatted ...
- Formatted ...
- Deleted: 03
- Field Code Changed ...
- Deleted: (Prinn et al., 2000;Prinn et al ...
- Formatted ...
- Formatted ...
- Formatted ...
- Deleted: 2016.08
- Field Code Changed ...
- Deleted: (Prinn et al., 2000;Prinn et al ...
- Formatted ...
- Formatted ...
- Formatted ...
- Deleted: (Montzka et al., 1996a)
- Deleted: 1
- Deleted: 1995.02
- Deleted: 7.Diane
- Deleted: Archived air ...
- Field Code Changed ...
- Deleted: (Prinn et al., 2000;Prinn et al ...
- Formatted ...
- Formatted ...
- Formatted ...
- Deleted: 03
- Field Code Changed ...
- Deleted: (Prinn et al., 2000;Prinn et al ...
- Formatted ...
- Formatted ...
- Formatted ...
- Deleted: (Montzka et al., 1996a)

**Table S1f. Collected data** used for HFC-23

Data	Network	Station	Latitude °N	Longitude °E	Instrument	Data availability	Scale	Reference
NH								
<i>In situ</i>	AGAGE	Mace Head	53.3	-9.9	Medusa	2007.10-2017 <sub>09</sub>	SIO-07	(Prinn et al., 2018a; Prinn et al., 2018b)
<i>In situ</i>	AGAGE	Trinidad Head	41.0	-124.1	Medusa	2007.09-2017 <sub>09</sub>	SIO-07	(Prinn et al., 2018a; Prinn et al., 2018b)
Model	AGAGE	NH	30-90	-	2-D 12-box	1978.01-2009.12	SIO-07	(Miller et al., 2010)
SH								
Archived air	AGAGE	Cape Grim	-40.7	144.7	Medusa3	2005.04-2009.11	SIO-07	(Miller et al., 2010)
Archived air	AGAGE	Cape Grim	-40.7	144.7	Medusa9	1978.04-2006.12	SIO-07	(Miller et al., 2010)
<i>In situ</i>	AGAGE	Cape Grim	-40.7	144.7	Medusa	2007.01-2017 <sub>09</sub>	SIO-07	(Prinn et al., 2018a; Prinn et al., 2018b)
Model	AGAGE	SH	-30 ~ -90	-	2-D 12-box	1978.01-2009.12	SIO-07	(Miller et al., 2010)

Deleted: 2f...1f. Collected dataData ...

Formatted Table

Deleted: 03

Field Code Changed

Deleted: (Prinn et al., 2000;Prinn et al., 2018b)

Formatted ...

Formatted ...

Formatted ...

Deleted: 03

Field Code Changed

Deleted: (Prinn et al., 2000;Prinn et al., 2018b)

Formatted ...

Formatted ...

Formatted ...

Deleted: 03

Field Code Changed

Deleted: (Prinn et al., 2000;Prinn et al., 2018b)

Formatted ...

Formatted ...

Formatted ...

**Table S1g. Collected data** used for PFC-14

Data	Network	Station	Latitude °N	Longitude °E	Instrument	Data availability	Scale	Reference
NH								
<i>In situ</i>	AGAGE	Mace Head	53.3	-9.9	Medusa	2006.05-2017.09	SIO-05	(Prinn et al., 2018a; Prinn et al., 2018b)
<i>In situ</i>	AGAGE	Trinidad Head	41.0	-124.1	Medusa	2006.04-2017.09	SIO-05	(Prinn et al., 2018a; Prinn et al., 2018b)
Model	AGAGE	NH	30-90	-	2-D 12-box	1900-2015	SIO-05	(Trudinger et al., 2016)
SH								
<i>In situ</i>	AGAGE	Cape Grim	-40.7	144.7	Medusa	2006.05-2017.09	SIO-05	(Prinn et al., 2018a; Prinn et al., 2018b)
Model	AGAGE	SH	-30 ~ -90	-	2-D 12-box	1900-2015	SIO-05	(Trudinger et al., 2016)

Deleted: 2g...1g. Collected dataData ...

Formatted Table

Deleted: 03

Field Code Changed

Deleted: (Prinn et al., 2000;Prinn et al., 2018b)

Formatted ...

Formatted ...

Formatted ...

Deleted: 03

Field Code Changed

Deleted: (Prinn et al., 2000;Prinn et al., 2018b)

Formatted ...

Formatted ...

Formatted ...

Deleted: 3

Field Code Changed

Deleted: (Prinn et al., 2000;Prinn et al., 2018b)

Formatted ...

Formatted ...

Formatted ...

**Table S1h. Collected data** used for PFC-116

Data	Network	Station	Latitude °N	Longitude °E	Instrument	Data availability	Scale	Reference
NH								
<i>In situ</i>	AGAGE	Mace Head	53.3	-9.9	Medusa	2003.11-2017.09	SIO-07	(Prinn et al., 2018a; Prinn et al., 2018b)
<i>In situ</i>	AGAGE	Trinidad Head	41.0	-124.1	Medusa	2005.05-2017.09	SIO-07	(Prinn et al., 2018a; Prinn et al., 2018b)
Model	AGAGE	NH	30-90	-	2-D 12-box	1900-2015	SIO-07	(Trudinger et al., 2016)
SH								
<i>In situ</i>	AGAGE	Cape Grim	-40.7	144.7	Medusa	2004.04-2017.09	SIO-07	(Prinn et al., 2018a; Prinn et al., 2018b)
Model	AGAGE	SH	-30 ~ -90	-	2-D 12-box	1900-2015	SIO-07	(Trudinger et al., 2016)

Deleted: 2h...1h. Collected dataData ...

Formatted Table

Deleted: 3

Field Code Changed

Deleted: (Prinn et al., 2000;Prinn et al., 2018b)

Formatted ...

Formatted ...

Formatted ...

Deleted: 3

Field Code Changed

Deleted: (Prinn et al., 2000;Prinn et al., 2018b)

Formatted ...

Formatted ...

Formatted ...

Deleted: 3

Field Code Changed

Deleted: (Prinn et al., 2000;Prinn et al., 2018b)

Formatted ...

Formatted ...

Formatted ...

**Table S3.** Ostwald solubility function of PFC-14 in seawater estimated by Method I

Compound	$a_1$	$a_2$	$a_3$	$c_1$	$c_2$	$c_3$	$T_{\min}$ (K)	$T_{\max}$ (K)	$L_0$ at 1 atm, 25 °C (L L <sup>-1</sup> )	$L$ at 1 atm, 25 °C, 35.0 ‰ (L L <sup>-1</sup> )
PFC-14	-113.8218	162.6686	49.4215	$6.60 \cdot 10^{-5}$	0.003341	0.21307	273.15	328.15	0.00513	0.004027

$$\ln L = \left[ a_1 + a_2 \cdot \left( \frac{100}{T} \right) + a_3 \cdot \ln \left( \frac{T}{100} \right) \right] \times \exp \left[ - (c_1 (T - 273.15)^2 + c_2 (T - 273.15) + c_3) \times \frac{0.03600}{1.80655} \times S \times \rho(T, S) \right]$$

Deleted: S3

Formatted Table

Formatted: Centered

**Table S4.** Comparison among the calculated Ostwald solubility coefficients ( $L_0$ ,  $L$  L<sup>-1</sup>) by the poly-parameter linear free energy relationships (pp-LFERs) based on  $V$ ,  $V_c$  and  $\log L^{16}$ , observed ones and calculated ones by the Clark-Glew-Weiss (CGW) model fit of target compounds and CFC-12 in water at 298.15 K and 310.15 K

Species	T (K)	Calculated $\log L_0 V$ by the pp-LFERs <sup>a</sup>	Calculated $L_0 V$ by the pp-LFERs <sup>a</sup>	Calculated $\log L_0 V_c$ by the pp-LFERs <sup>b</sup>	Calculated $L_0 V_c$ by the pp-LFERs <sup>b</sup>	Calculated $\log L_0 L^{16}$ by the pp-LFERs <sup>c</sup>	Calculated $L_0 L^{16}$ by the pp-LFERs <sup>c</sup>	Observed $\log L_0$ <sup>d</sup>	Observed $L_0$ <sup>d</sup>	Calculated $L_0$ by the CGW fit <sup>e</sup>
HCFC-22	298.15	-0.017	0.961	-0.052	0.888	-0.025	0.944	-0.091	0.811	0.844
HCFC-141b	298.15	-0.136	0.731	-0.154	0.702	-0.152	0.705	-0.148	0.711	0.711
HCFC-142b	298.15	-0.405	0.394	-0.440	0.363	-0.405	0.394	-0.449	0.356	0.352
HFC-134a	298.15	-0.326	0.472	-0.407	0.392	-0.326	0.472	-0.408	0.391	0.381
HFC-125	298.15	-1.003	0.099	-1.130	0.074	-0.989	0.103	-1.059	0.087	0.086
HFC-23	298.15	-0.453	0.352	-0.505	0.313	-0.469	0.340	-0.510	0.309	0.313
PFC-14	298.15	-2.241	0.00574	-2.296	0.00505	-0.250	0.00562	-2.306	0.00494	0.00513
PFC-116	298.15	-2.658	0.00220	-2.763	0.00173	-2.716	-	-	-	0.00143
CFC-12	298.15	-1.120	0.076	-1.155	0.070	-1.145	0.072	-1.129	0.074	0.069
HCFC-22	310.15	-0.161	0.691	-0.203	0.626	-0.210	0.617	-	-	0.598
HCFC-141b	310.15	-0.306	0.494	-0.327	0.471	-0.348	0.449	-0.336	0.461	0.484
HCFC-142b	310.15	-0.571	0.269	-0.614	0.243	-0.591	0.256	-0.605	0.248	0.246
HFC-134a	310.15	-0.563	0.274	-0.621	0.239	-0.636	0.231	-0.547	0.284	0.269
HFC-125	310.15	-1.208	0.062	-1.339	0.046	-0.241	0.057	-1.203	0.063	0.062
HFC-23	310.15	-0.618	0.241	-0.683	0.208	-0.685	0.207	-0.622	0.239	0.225
PFC-14	310.15	-2.310	0.00490	-2.382	0.00415	-2.413	0.00386	-2.386	0.00411	0.00437
PFC-116	310.15	-2.755	0.00176	-2.883	0.00131	-2.851	-	-	-	0.00110
CFC-12	310.15	-1.213	0.061	-1.256	0.055	-1.257	0.055	-1.275	0.053	0.048

<sup>a</sup> Calculated  $\log L_0 V$  and  $L_0 V$  are calculated by the pp-LFERs, which are obtained from Table 6,7,9,12-15 in Abraham et al. (2001) and Table 2 in Abraham et al. (2012)

<sup>b</sup> Calculated  $\log L_0 V_c$  and  $L_0 V_c$  are calculated by the pp-LFERs based on the  $V_c$

<sup>c</sup> Calculated  $\log L_0 L^{16}$  and  $L_0 L^{16}$  are calculated by the pp-LFERs, which are obtained from Table 6,7,9,12-15 in Abraham et al. (2001) and Table 2 in Abraham et al. (2012)

<sup>d</sup> Observed  $\log L_0$  and  $L_0$  are measured by experiments, which are also obtained from Table 6,7,9,12-15 in Abraham et al. (2001) and Table 2 in Abraham et al. (2012)

<sup>e</sup> Calculated  $L_0$  by the CGW fit are calculated based on the Combined Method for water solubility

Deleted: ¶

Deleted: S2

Deleted: ¶

Formatted Table

Deleted: c

Deleted: c

Deleted: c

Deleted: c

Deleted: d

Formatted: Font color: Auto

Formatted: Font color: Blue

Formatted: Font color: Blue

Formatted: Font color: Blue

Formatted: Font color: Blue

Formatted: Font color: Auto

Formatted: Font color: Blue

Formatted: Font color: Auto

Formatted: Font color: Blue

Formatted: Font color: Blue

Formatted: Font color: Blue

Deleted: cV

Deleted: cV

Deleted: corrected V

Deleted: c

Deleted: d

Deleted: ¶

<sup>c</sup> Relative standard deviation (RSD) of calculated  $L_0$  by the pp-LFERs and calculated  $L_0$  by the CGW fit<sup>¶</sup>

<sup>f</sup> Relative standard deviation (RSD) of calculated  $L_{0,cV}$  by the pp-LFERs and calculated  $L_0$  by the CGW fit

**Table S5.** Ostwald solubility functions of target compounds and CFC-12 in sea water estimated by (Revised) Method II at 298.15 K and 310.15 K

Species	Chemical Formula	T (K)	c	e	s	a	b	v	$K_s$	$L_0$ at 1 atm, 25 °C (L L <sup>-1</sup> )	L at 1 atm, 25 °C, 35.0 ‰ (L L <sup>-1</sup> )
HCFC-22	CHClF <sub>2</sub>	298.15	-0.994	0.577	2.549	3.813	4.841	-0.869	0.169 ± 0.022	0.888	0.703
HCFC-141b	C <sub>2</sub> H <sub>3</sub> Cl <sub>2</sub> F	298.15	-0.994	0.577	2.549	3.813	4.841	-0.869	0.204 ± 0.023	0.702	0.530
HCFC-142b	C <sub>2</sub> H <sub>3</sub> ClF <sub>2</sub>	298.15	-0.994	0.577	2.549	3.813	4.841	-0.869	0.198 ± 0.022	0.363	0.277
HFC-134a	CH <sub>2</sub> FCF <sub>3</sub>	298.15	-0.994	0.577	2.549	3.813	4.841	-0.869	0.193 ± 0.022	0.392	0.300
HFC-125	C <sub>2</sub> HF <sub>5</sub>	298.15	-0.994	0.577	2.549	3.813	4.841	-0.869	0.224 ± 0.021	0.091	0.067
HFC-23	CHF <sub>3</sub>	298.15	-0.994	0.577	2.549	3.813	4.841	-0.869	0.168 ± 0.021	0.313	0.248
PFC-14	CF <sub>4</sub>	298.15	-0.994	0.577	2.549	3.813	4.841	-0.869	0.202 ± 0.022	0.00505	0.00382
PFC-116	C <sub>2</sub> F <sub>6</sub>	298.15	-0.994	0.577	2.549	3.813	4.841	-0.869	0.244 ± 0.022	0.00173	0.00123
CFC-12	CCl <sub>2</sub> F <sub>2</sub>	298.15	-0.994	0.577	2.549	3.813	4.841	-0.869	0.204 ± 0.021	0.070	0.053
HCFC-22	CHClF <sub>2</sub>	310.15	-0.966	0.698	2.412	3.393	4.577	-1.072	0.169 ± 0.022	0.626	0.530
HCFC-141b	C <sub>2</sub> H <sub>3</sub> Cl <sub>2</sub> F	310.15	-0.966	0.698	2.412	3.393	4.577	-1.072	0.204 ± 0.023	0.471	0.385
HCFC-142b	C <sub>2</sub> H <sub>3</sub> ClF <sub>2</sub>	310.15	-0.966	0.698	2.412	3.393	4.577	-1.072	0.198 ± 0.022	0.243	0.200
HFC-134a	CH <sub>2</sub> FCF <sub>3</sub>	310.15	-0.966	0.698	2.412	3.393	4.577	-1.072	0.193 ± 0.022	0.239	0.198
HFC-125	C <sub>2</sub> HF <sub>5</sub>	310.15	-0.966	0.698	2.412	3.393	4.577	-1.072	0.224 ± 0.021	0.059	0.047
HFC-23	CHF <sub>3</sub>	310.15	-0.966	0.698	2.412	3.393	4.577	-1.072	0.168 ± 0.021	0.208	0.176
PFC-14	CF <sub>4</sub>	310.15	-0.966	0.698	2.412	3.393	4.577	-1.072	0.202 ± 0.022	0.00415	0.00340
PFC-116	C <sub>2</sub> F <sub>6</sub>	310.15	-0.966	0.698	2.412	3.393	4.577	-1.072	0.244 ± 0.022	0.00131	0.00103
CFC-12	CCl <sub>2</sub> F <sub>2</sub>	310.15	-0.966	0.698	2.412	3.393	4.577	-1.072	0.204 ± 0.021	0.055	0.045

$$L = 10^{\left[ -K_s \cdot \frac{S}{M_{NaCl}} + c + eE + sS + aA + bB + vV_c \right]}, \text{ (V for HFC-125, } V_s \text{ for other compounds)}$$

Deleted: S4

Deleted: 37

Deleted: 43

Deleted: 37

Deleted: 34

Deleted: 28

Deleted: 28

Deleted: 16

Deleted: 17

Deleted: 34

Deleted: 37

Deleted: 43

Deleted: 37

Deleted: 34

Deleted: 28

Deleted: 28

Deleted: 16

Deleted: 17

Deleted: 34

Deleted: V

Deleted: corrected

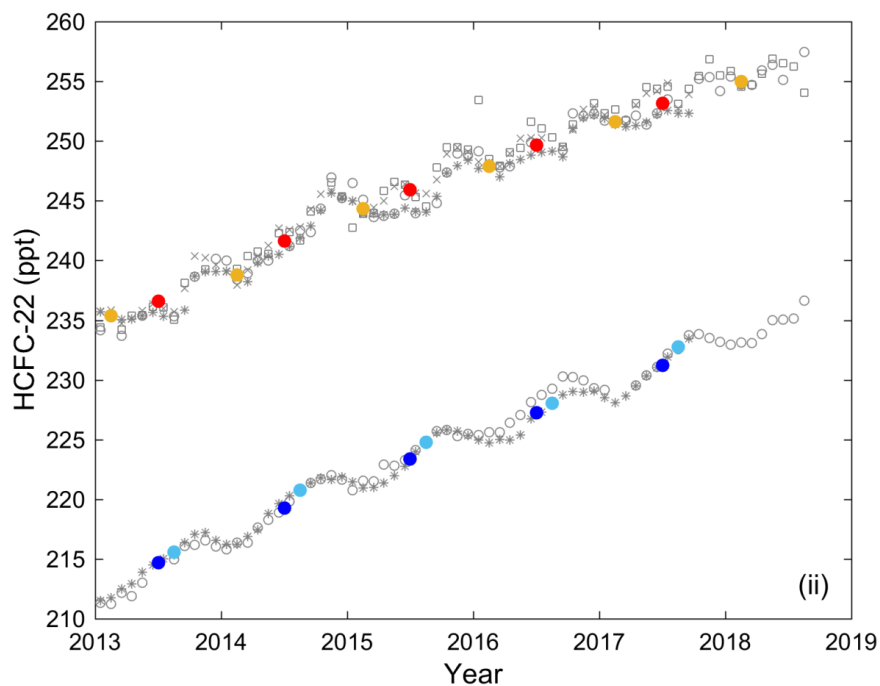
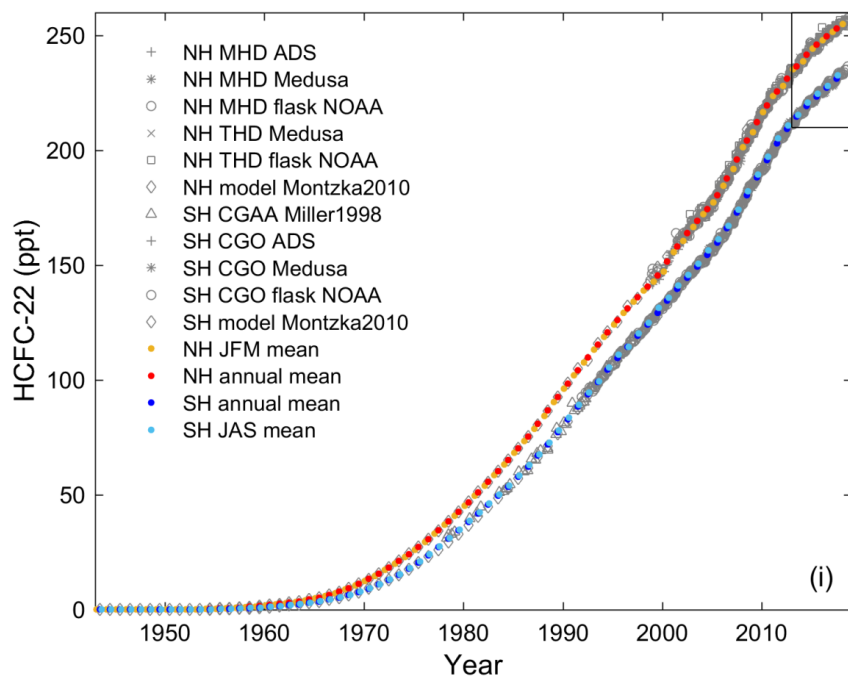


**Fig. S1a.** HCFC-22: Atmospheric mole fractions in the NH and SH based on collected data (Table S2a) in the range of (i) 1943-2019; (ii) 2013-2019. Fig. (ii) is the enlarged figure of the square in Fig. (i).

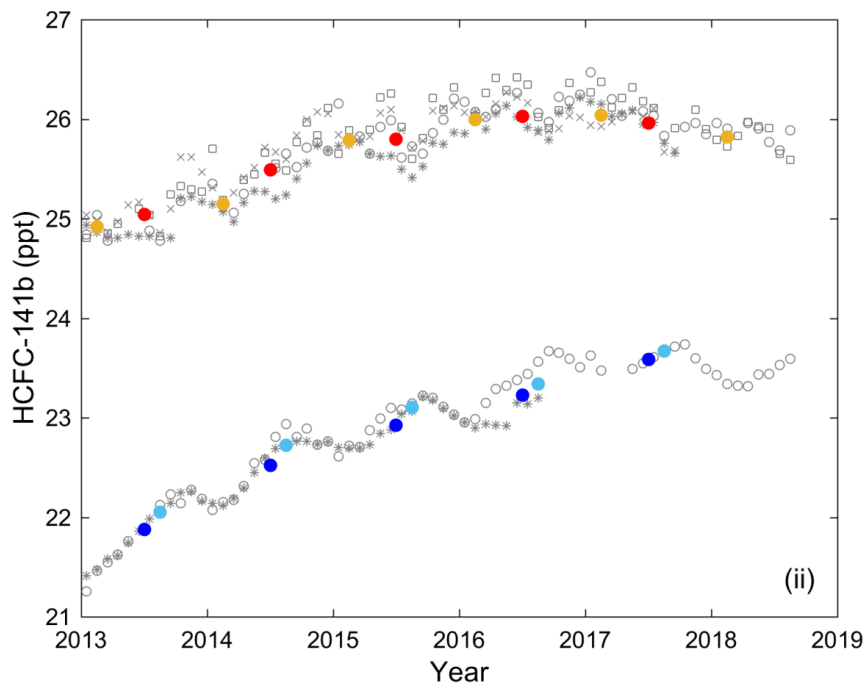
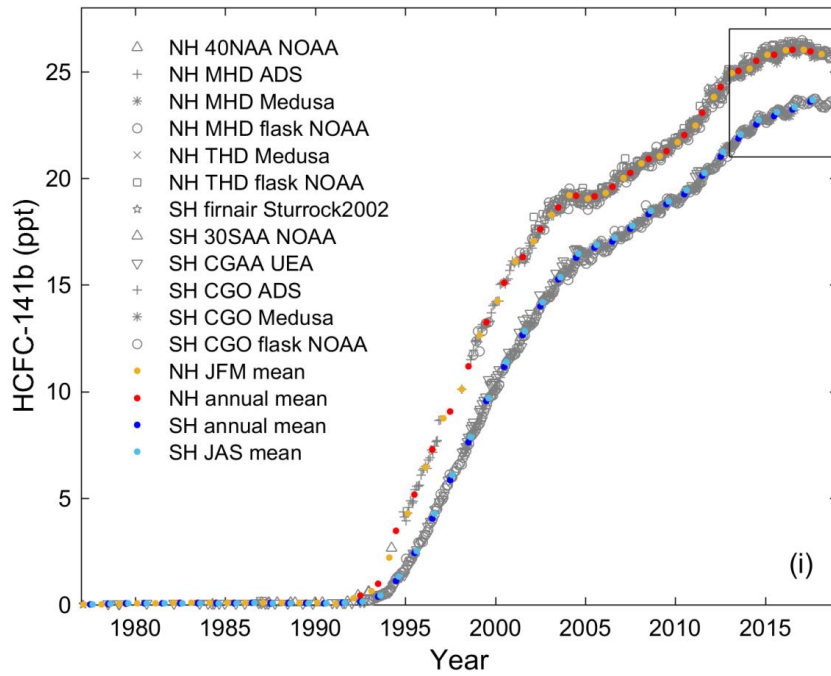


**Fig. S1b.** HCFC-141b: Atmospheric mole fractions in the NH and SH based on collected data (Table S2b) in the range of (i) 1977-2019; (ii) 2013-2019. Fig. (ii) is the enlarged figure of the square in Fig. (i).

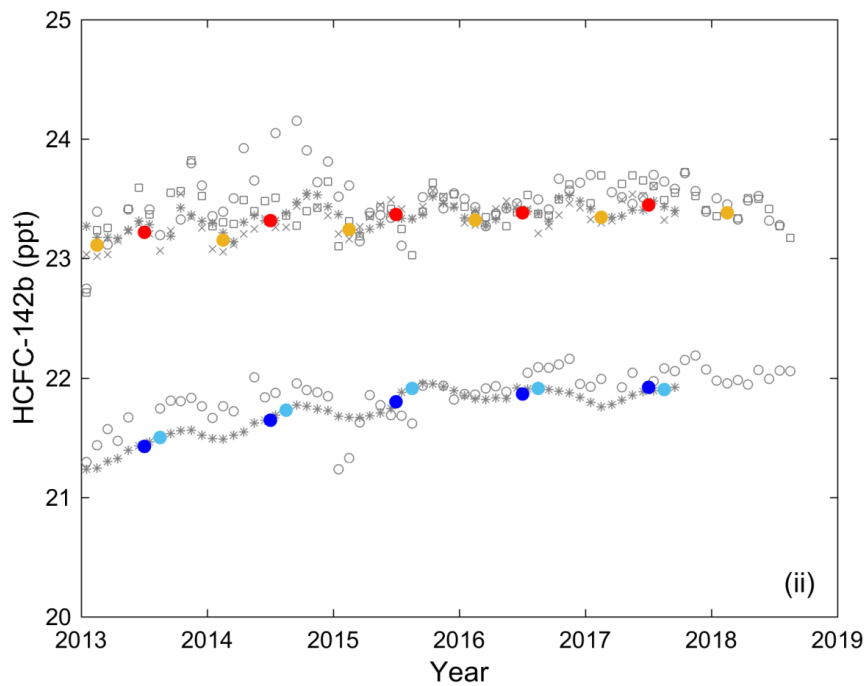
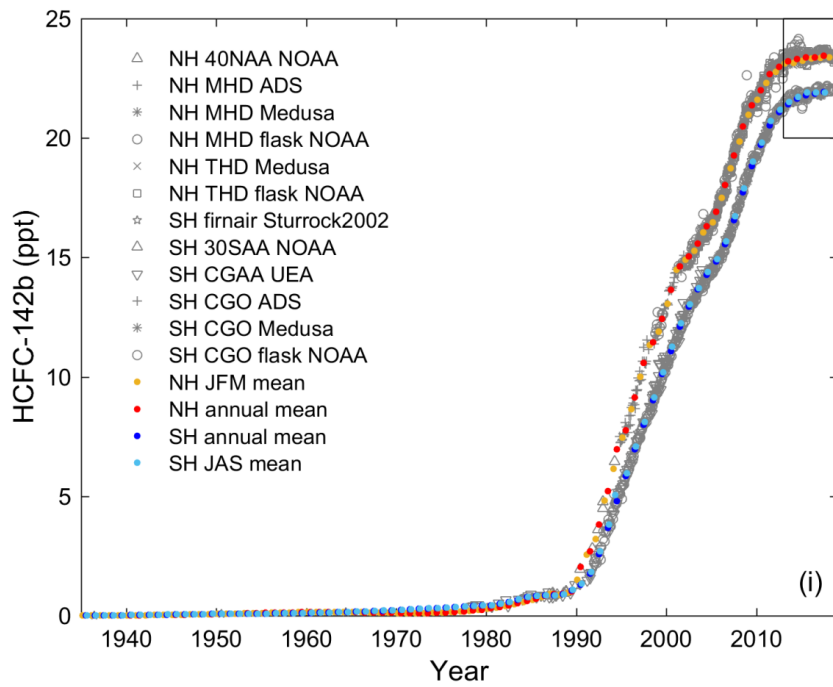


**Fig. S1c. HCFC-142b: Atmospheric mole fractions in the NH and SH based on collected data (Table S2c) in the range of (i) 1935-2019; (ii) 2013-2019. Fig. (ii) is the enlarged figure of the square in Fig. (i).**

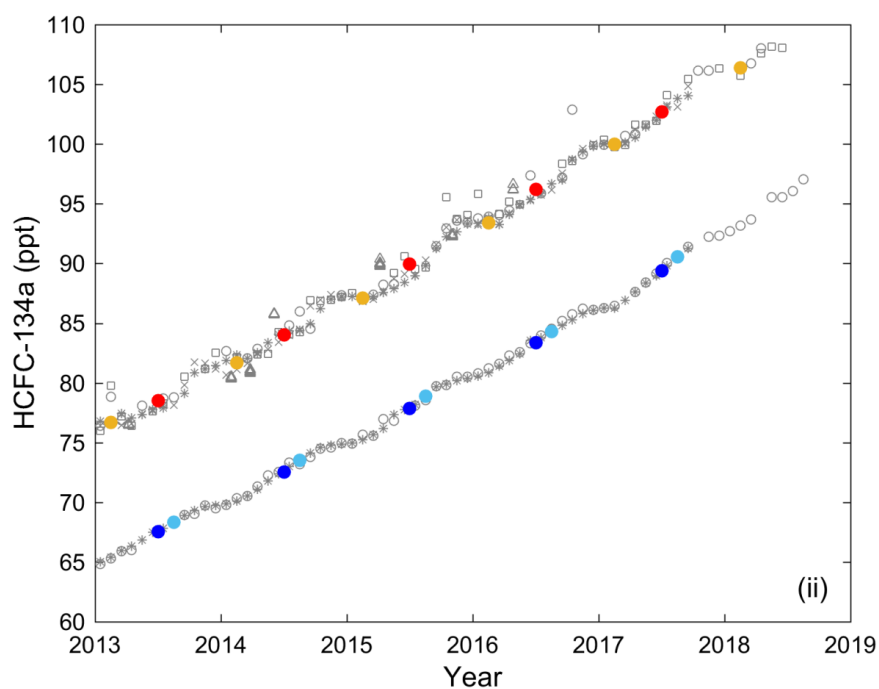
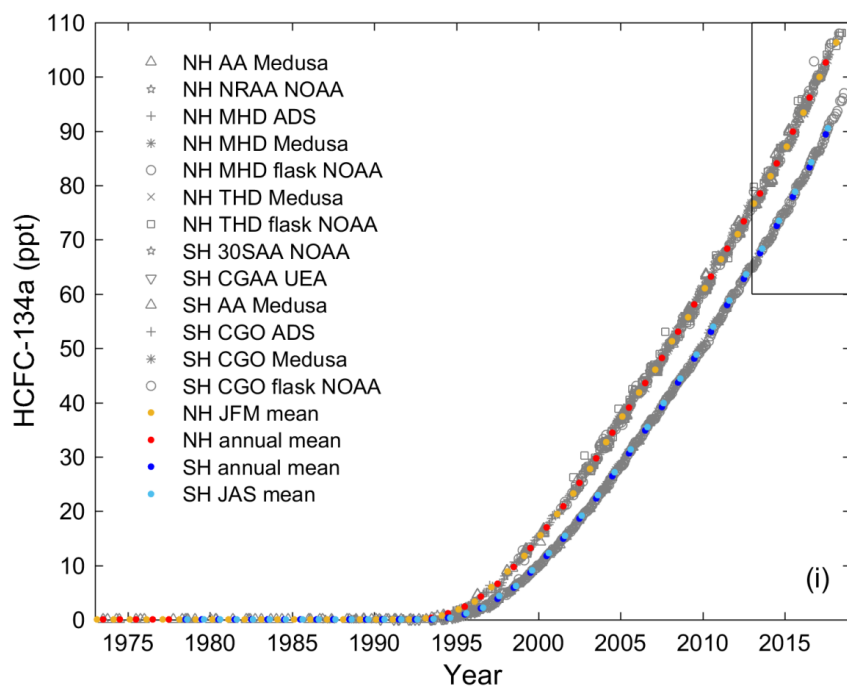


**Fig. S1d.** HFC-134a: Atmospheric mole fractions in the NH and SH based on collected data (Table S2d) in the range of (i) 1973-2019; (ii) 2013-2019. Fig. (ii) is the enlarged figure of the square in Fig. (i).

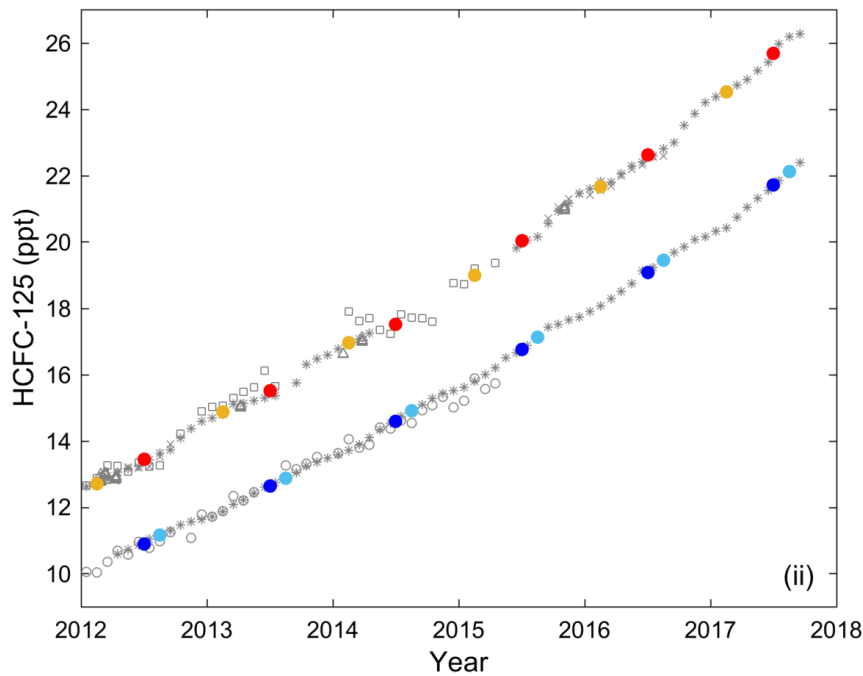
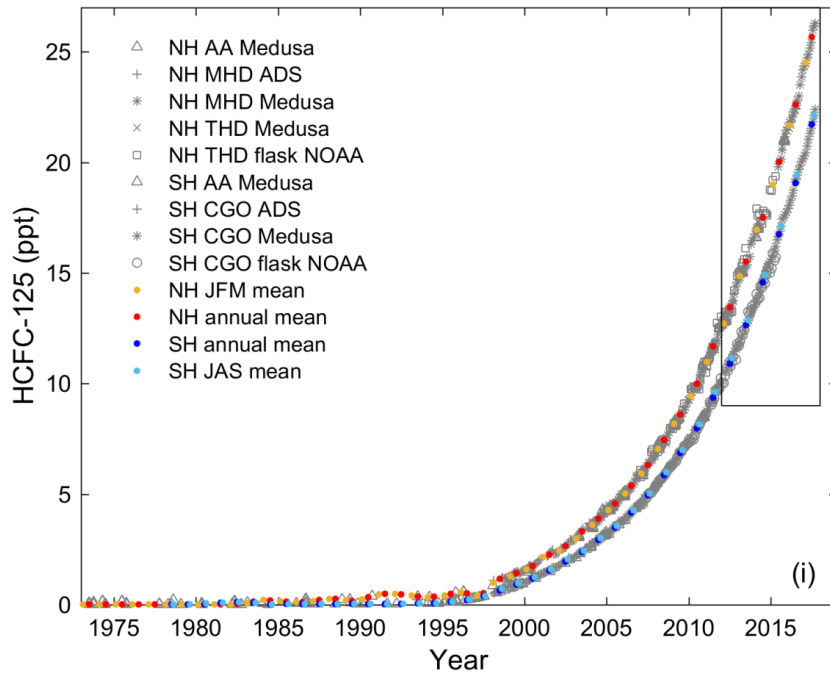


**Fig. S1e.** HCFC-125: Atmospheric mole fractions in the NH and SH based on collected data (Table S2e) in the range of (i) 1973-2018; (ii) 2012-2018. Fig. (ii) is the enlarged figure of the square in Fig. (i).

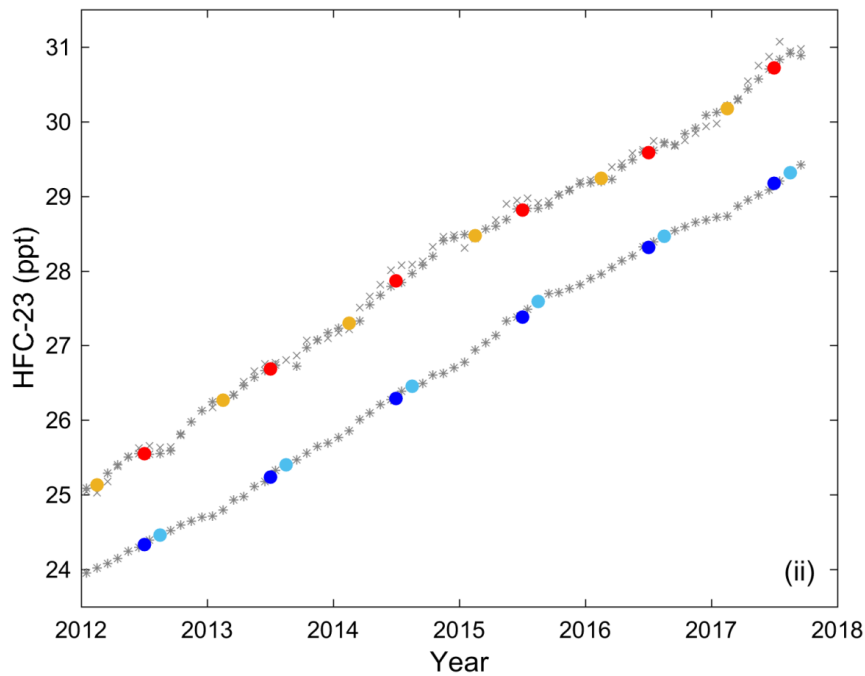
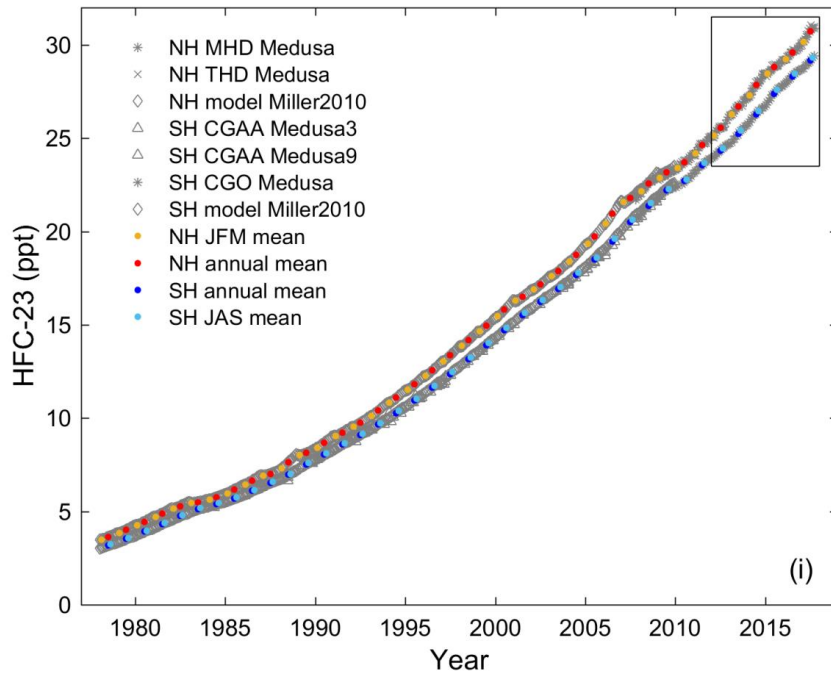


**Fig. S1f.** HFC-23: Atmospheric mole fractions in the NH and SH based on collected data (Table S2f) in the range of (i) 1978-2018; (ii) 2012-2018. Fig. (ii) is the enlarged figure of the square in Fig. (i).

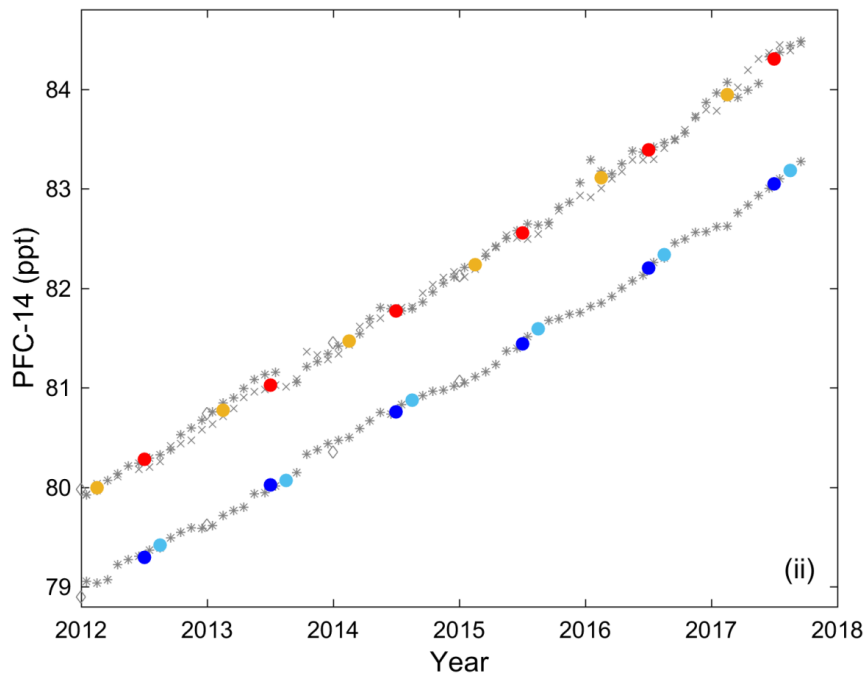
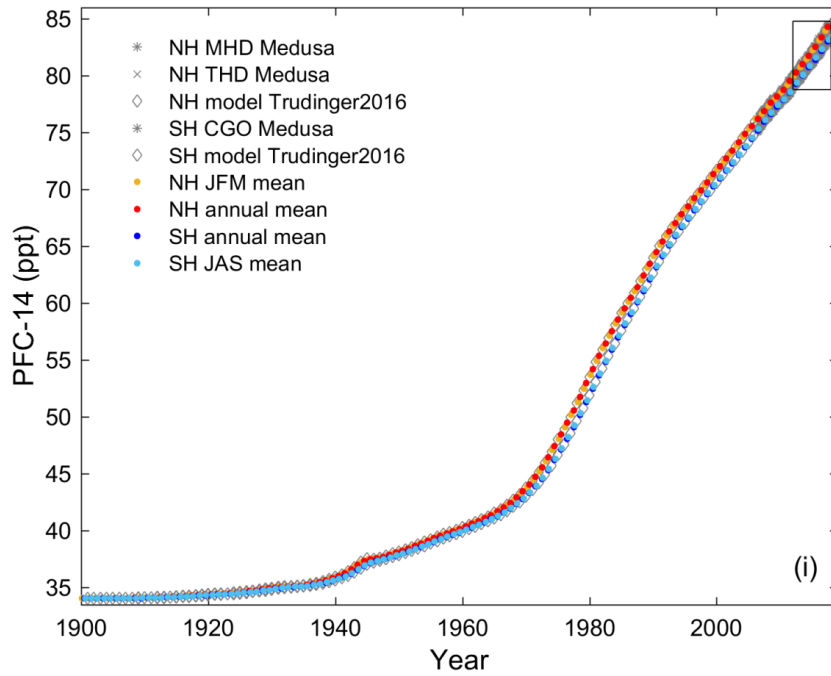


**Fig. S1g.** PFC-14: Atmospheric mole fractions in the NH and SH based on collected data (Table S2g) in the range of (i) 1900-2018; (ii) 2012-2018. Fig. (ii) is the enlarged figure of the square in Fig. (i).

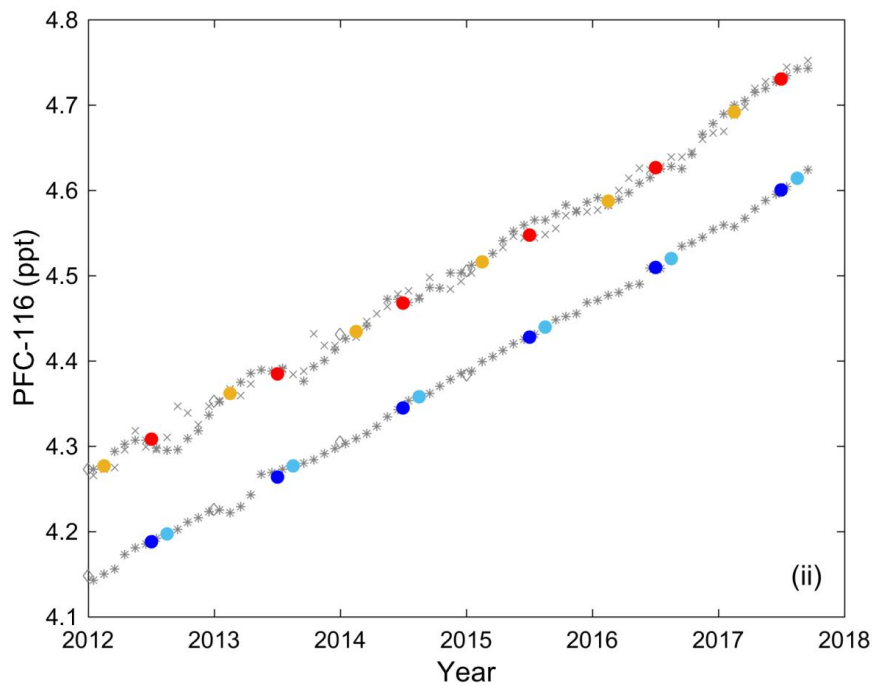
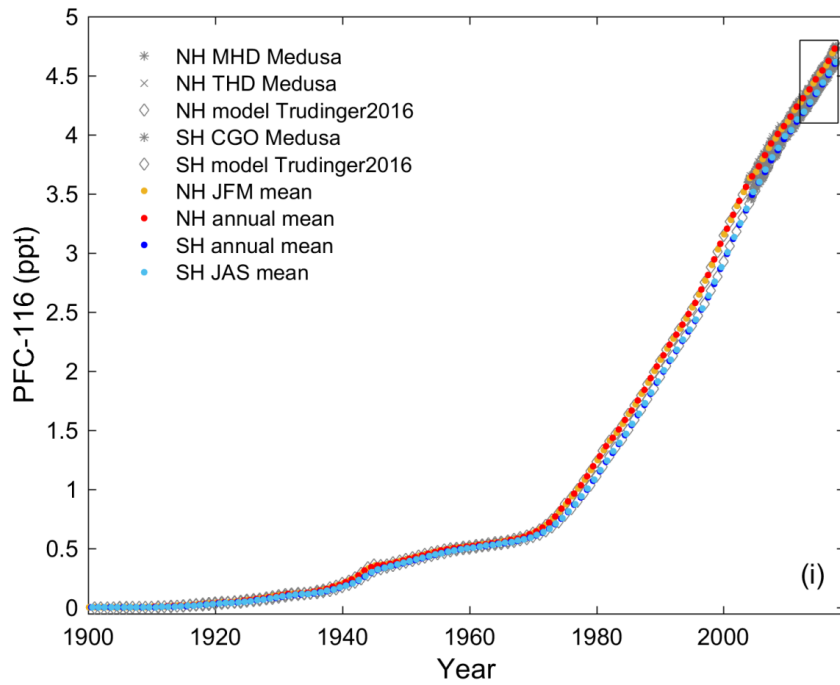


**Fig. S1h.** PFC-116: Atmospheric mole fractions in the NH and SH based on collected data (Table S2h) in the range of (i) 1900-2018; (ii) 2012-2018. Fig. (ii) is the enlarged figure of the square in Fig. (i).

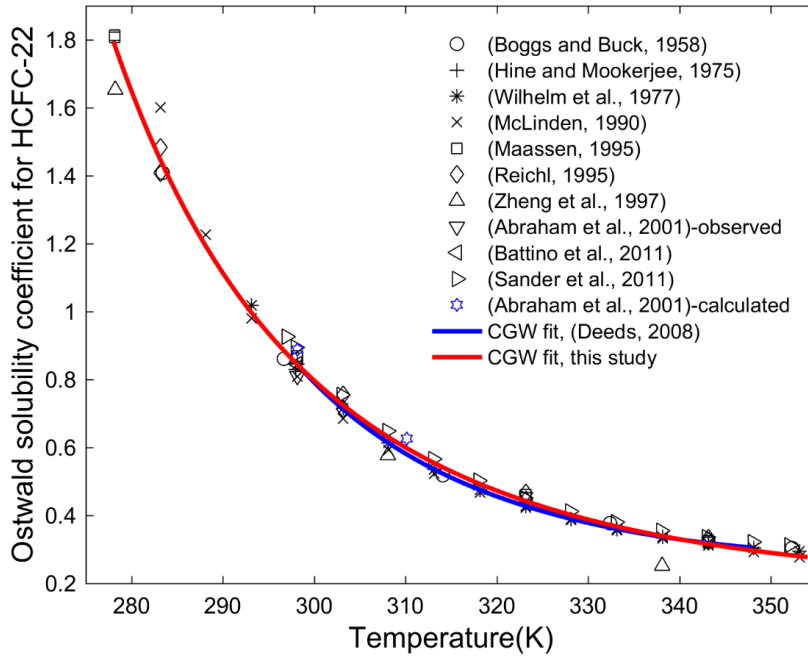


**Fig. S2a.** HCFC-22 freshwater solubility (Ostwald solubility coefficients) as a function of temperature based on previous studies (Boggs and Buck Jr, 1958; Hine and Mookerjee, 1975; Wilhelm et al., 1977; McLinden, 1990; Maaßen, 1995; Reichl, 1995; Zheng et al., 1997; Abraham et al., 2001; Battino et al., 2011; Sander et al., 2011). The Clarke-Glew-Weiss (CGW) model is used to fit the data (black markers) and compared with the results from Deeds (2008) and from (Abraham et al., 2001)-calculated (blue Hexagram, calculated by Revised Method II). The CGW fit in this study agrees to within 4.0 % with two-thirds of the data.

Deleted: ure

Deleted: S1

Deleted: The

Deleted: for HCFC-22

Deleted: by collecting data from

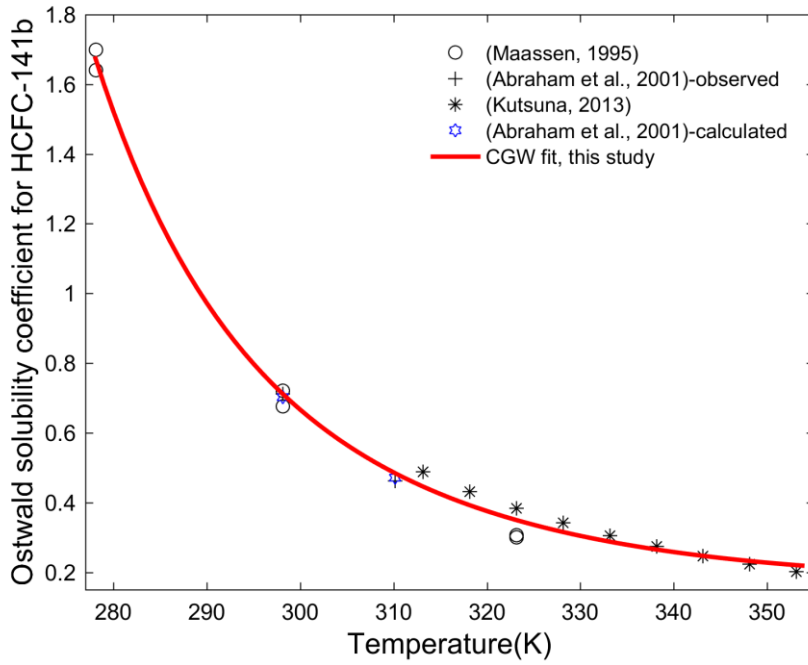


**Fig. S2b.** HCFC-141b, freshwater solubility (Ostwald solubility coefficients) as a function of temperature based on previous studies (Maassen, 1995; Abraham et al., 2001; Kutsuna, 2013). The Clarke-Glew-Weiss (CGW) model is used to fit the data (black markers) and compared with the results from (Abraham et al., 2001)-calculated (blue Hexagram, calculated by Revised Method II). The CGW fit in this study agrees to within 7.8 % with two-thirds of the data.

**Deleted:** ure

**Deleted:** The

**Deleted:** for HCFC-141b

**Deleted:** by collecting data from

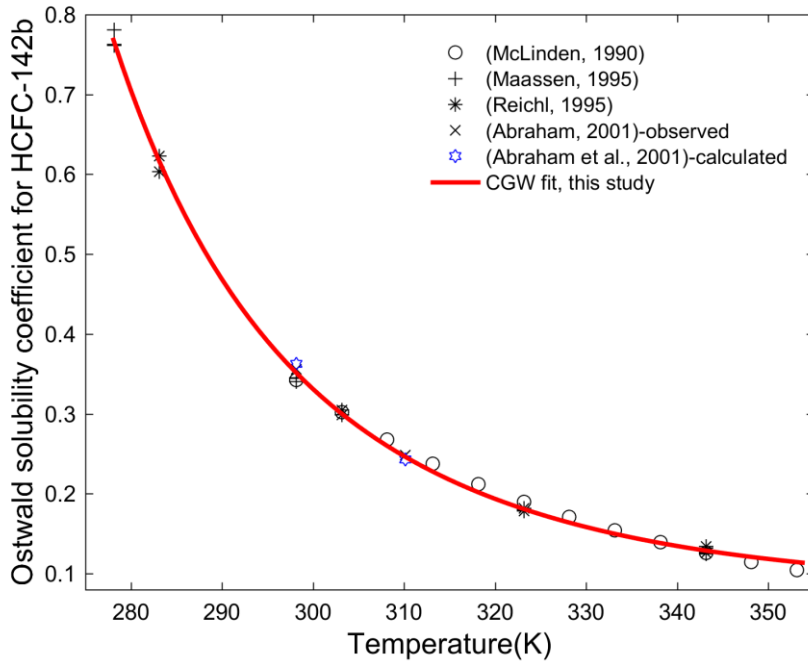


**Fig. S2c.** HCFC-142b freshwater solubility (Ostwald solubility coefficients) as a function of temperature based on previous studies (McLinden, 1990; Maaßen, 1995; Reichl, 1995; Abraham et al., 2001). The Clarke-Glew-Weiss (CGW) model is used to fit the data (black markers) and compared with the results from (Abraham et al., 2001)-calculated (blue Hexagram, calculated by Revised Method II). The CGW fit in this study agrees to within 2.5 % with two-thirds of the data.

**Deleted:** ure

**Deleted:** S3

**Deleted:** The

**Deleted:** for HCFC-142b

**Deleted:** by collecting data from

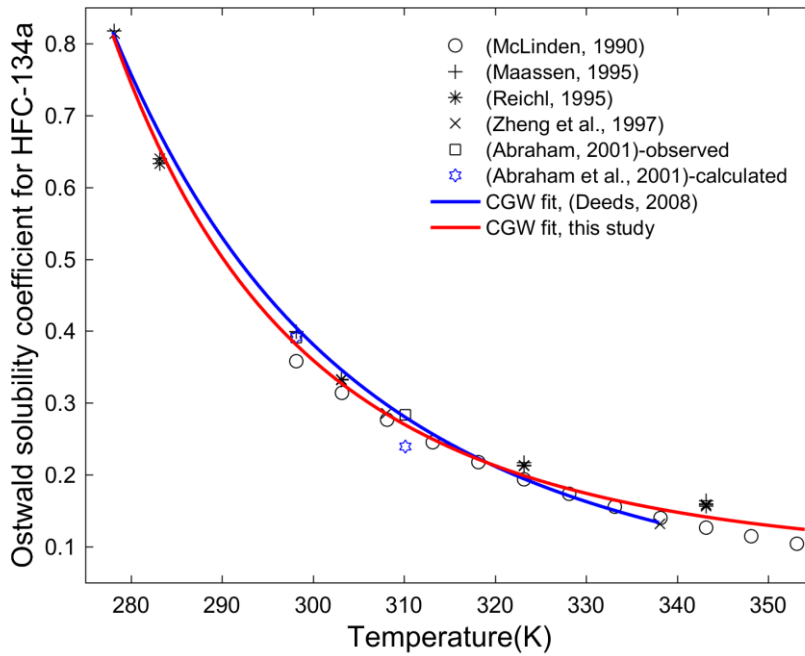


**Fig. S2d. HFC-134a**, freshwater solubility (Ostwald solubility coefficients) as a function of temperature based on previous studies (McLinden, 1990; Maaßen, 1995; Reichl, 1995; Zheng et al., 1997; Abraham et al., 2001). The Clarke-Glew-Weiss (CGW) model is used to fit the data (black markers) and compared with the results from Deeds (2008) and from (Abraham et al., 2001)-calculated (blue Hexagram, calculated by Revised Method II). The CGW fit in this study agrees to within 6.8 % with two-thirds of the data.

Deleted: ure

Deleted: S4

Deleted: The

Deleted: for HFC-134a

Deleted: by collecting data from

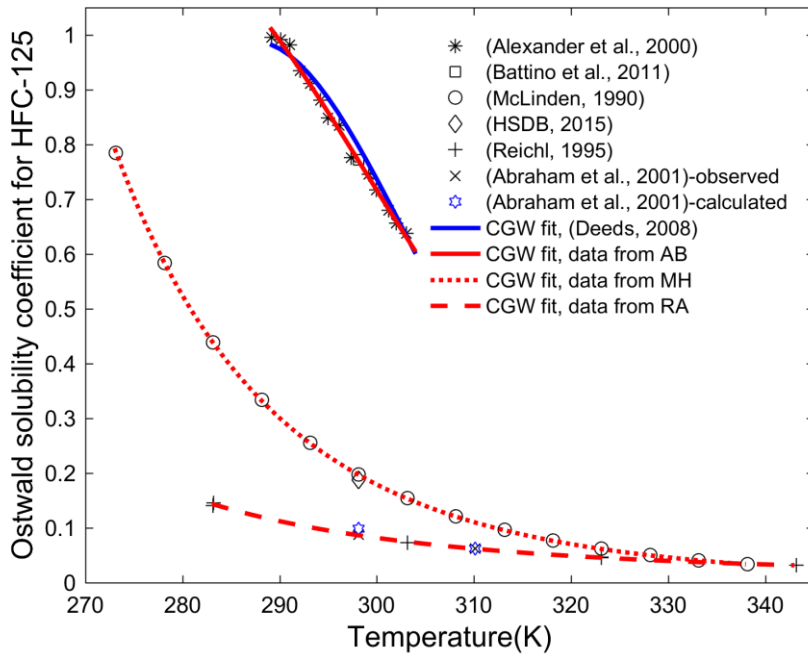


**Fig. S2e.** HFC-125 freshwater solubility (Ostwald solubility coefficients) as a function of temperature based on previous studies (Miguel et al., 2000; Battino et al., 2011; McLinden, 1990; HSDB, 2015; Reichl, 1995; Abraham et al., 2001). The Clarke-Glew-Weiss (CGW) model is used to fit the data (black markers) and compared with the results from Deeds (2008) and from Abraham et al. (2001)-calculated (blue Hexagram, calculated by Method II based on Eq. (12)). The CGW fit in this study agrees to within 2.1 % with all data. Unfortunately, the data from previous studies is not described by one CGW fit, but by three. Curve 1 is the upper and red solid line fitted the data (Miguel et al., 2000; Battino et al., 2011) in the temperature range of 289.15 K ~ 303.15 K. This fit agrees to within 1.0 % with 2/3 data. Curve 2 is the middle and red dotted line fitted the data (McLinden, 1990; HSDB, 2015) from 273.15 K to 338.15 K. This fit agrees to within 0.75 % with 2/3 data. Curve 3 is the bottom and red dashed line fitted the data (Reichl, 1995; Abraham et al., 2001) in the temperature range of 283.15 K ~ 343.15 K. This fit agrees to within 3.3 % with two-thirds of the data. The discrepancy of the three fits is discussed in the text.

Deleted: ure

Deleted: S5

Deleted: The

Deleted: for HFC-125

Deleted: by collecting data from

Deleted: There are

Deleted: CGW fit curves from these literatures

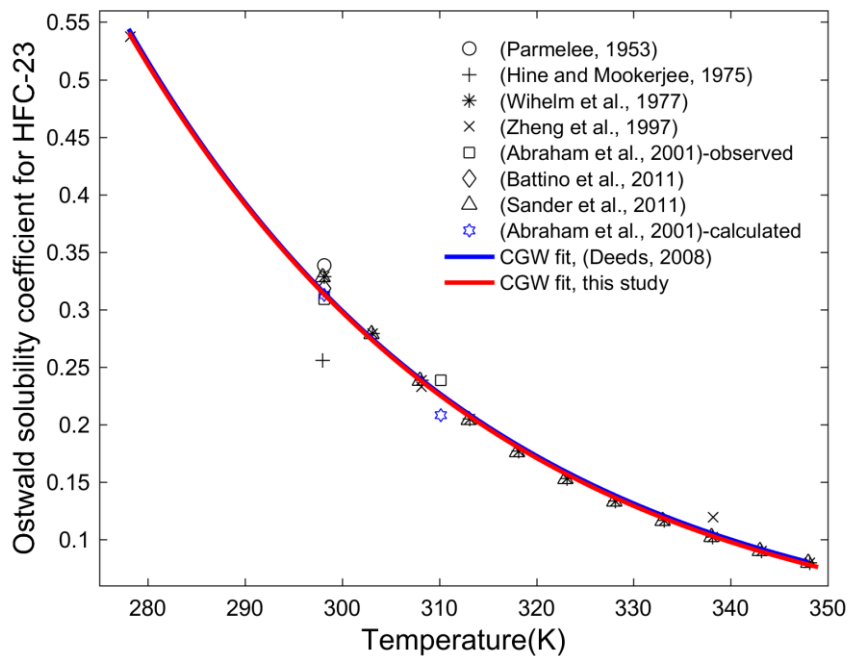


**Fig. S2f.** HFC-23 freshwater solubility (Ostwald solubility coefficients) as a function of temperature based on previous studies (Parmelee, 1953; Hine and Mookerjee, 1975; Wilhelm et al., 1977; Zheng et al., 1997; Abraham et al., 2001; Battino et al., 2011; Sander et al., 2011). The Clarke-Glew-Weiss (CGW) model is used to fit the data (black markers) and compared with the results from Deeds (2008) and from (Abraham et al., 2001)-calculated (blue Hexagram, calculated by Revised Method II). The CGW fit in this study agrees to within 2.3 % with two-thirds of the data.

**Deleted:** ure

**Deleted:** S6

**Deleted:** The

**Deleted:** for HFC-23

**Deleted:** by collecting data from

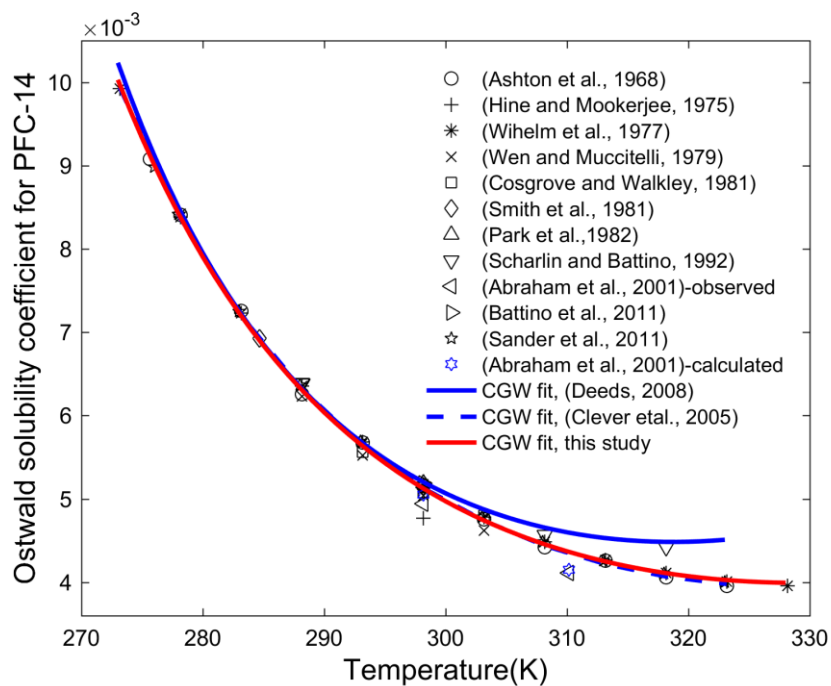


**Fig. S2g.** PFC-14 freshwater solubility (Ostwald solubility coefficients) as a function of temperature based on previous studies (Smith et al., 1981; Park et al., 1982; Scharlin and Battino, 1992; Abraham et al., 2001; Battino et al., 2011; Sander et al., 2011). The Clarke-Glew-Weiss (CGW) model is used to fit the data (black markers) and compared with the results from Deeds (2008), from Clever et al. (2005) and from (Abraham et al., 2001)-calculated (blue Hexagram, calculated by Revised Method II). The CGW fit in this study agrees to within 0.95 % with two-thirds of the data.

Deleted: ure

Deleted: S7

Deleted: The

Deleted: for PFC-14

Deleted: by collecting data from

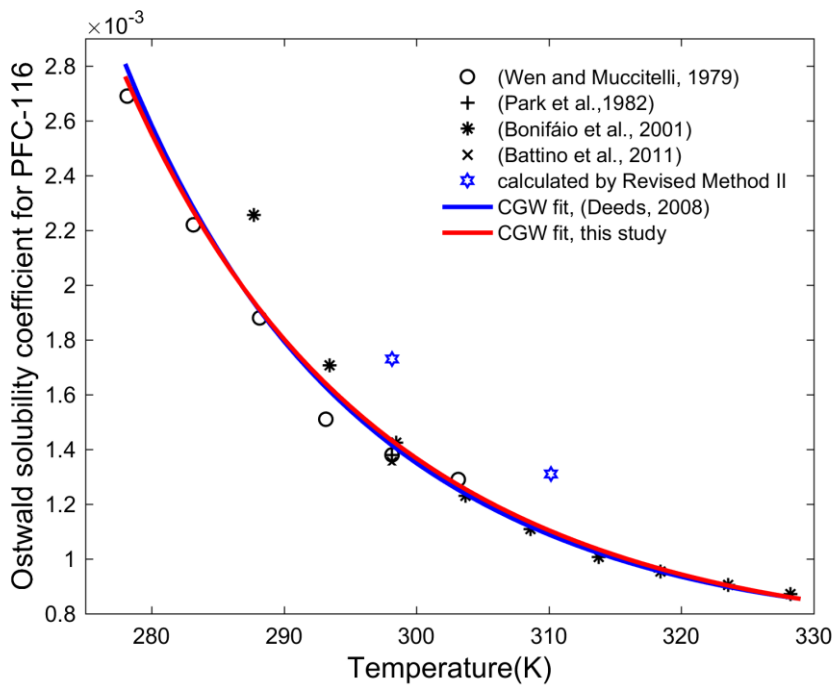


**Fig. S2h.** PFC-116 freshwater solubility (Ostwald solubility coefficients) as a function of temperature based on previous studies (Wen and Muccitelli, 1979; Park et al., 1982; Bonifácio et al., 2001; Battino et al., 2011). The Clarke-Glew-Weiss (CGW) model is used to fit the data (black markers) and compared with the fit results from Deeds (2008) and from the data calculated by Revised Method II (blue Hexagram). The CGW fit in this study agrees to within 3.5 % with two-thirds of the data.

Deleted: ure

Deleted: S8

Deleted: The

Deleted: for PFC-116

Deleted: by collecting data from

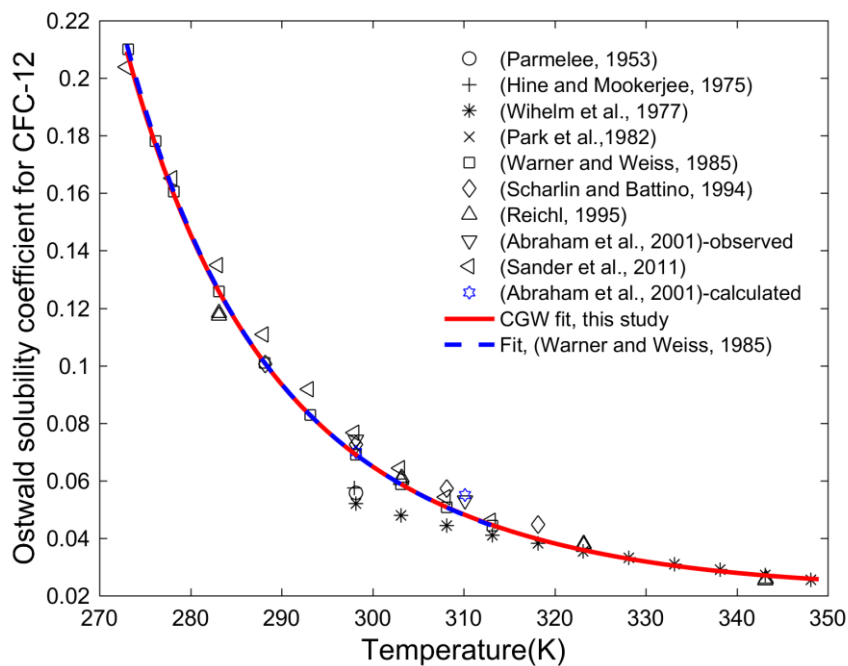


**Fig. S2i.** CFC-12 freshwater solubility (Ostwald solubility coefficients) as a function of temperature based on previous studies (Parmelee, 1953; Hine and Mookerjee, 1975; Wilhelm et al., 1977; Park et al., 1982; Warner and Weiss, 1985; Scharlin and Battino, 1994; Reichl, 1995; Abraham et al., 2001; Sander et al., 2011). The Clarke-Glew-Weiss (CGW) model is used to fit the data (black markers) and compared with the fit results from Warner and Weiss (1985) and the data from (Abraham et al., 2001)-calculated (blue Hexagram, calculated by Revised Method II). The CGW fit in this study agrees to within 6.6 % with two-thirds of the data.

Deleted: ure

Deleted: S9

Deleted: The

Deleted: for CFC-12

Deleted: by collecting data from

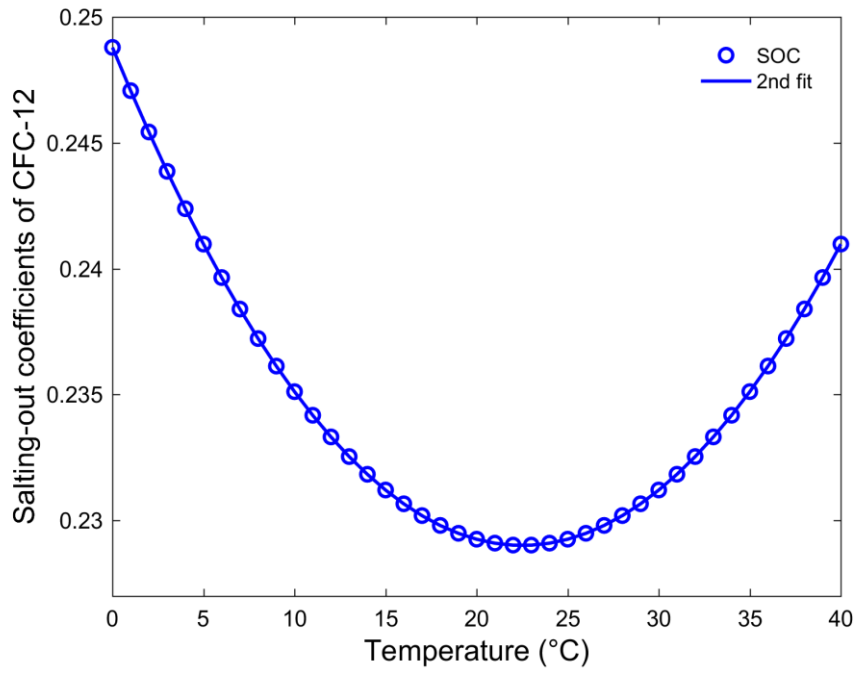


Fig. S3. The relationship between salting-out coefficients (SOC) and temperature for CFC-12 calculated by Eq. (16) based on the data from Warner and Weiss (1985).

Deleted: ure

Deleted: S10

Deleted: the Combined Method

## References

Abraham, M. H., Gola, J. M., Cometto-Muñiz, J. E., and Cain, W. S.: Solvation properties of refrigerants, and the estimation of their water-solvent and gas-solvent partitions, *Fluid Phase Equilib.*, 180, 41-58, doi:10.1016/S0378-3812(00)00511-2, 2001.

Field Code Changed

Formatted: Font: 10 pt, English (U.S.)

Abraham, M. H., Gil-Lostes, J., Corr, S., and Acree, W. E.: Determination of partition coefficients of refrigerants by gas liquid chromatographic headspace analysis, *J. Chromatogr. A*, 1265, 144-148, doi:10.1016/j.chroma.2012.09.085, 2012.

Battino, R., Seybold, P. G., and Campanell, F. C.: Correlations Involving the Solubility of Gases in Water at 298.15 K and 101325 Pa, *Journal of Chemical & Engineering Data*, 56, 727-732, doi:10.1021/je101070h, 2011.

Boggs, J. E., and Buck Jr, A. E.: The solubility of some chloromethanes in water, *J. Phys. Chem.*, 62, 1459-1461, doi:10.1021/j150569a031, 1958.

Bonifácio, R. P., Pádua, A. A. H., and Costa Gomes, M. F.: Perfluoroalkanes in water: Experimental Henry's law coefficients for hexafluoroethane and computer simulations for tetrafluoromethane and hexafluoroethane, *J. Phys. Chem. B*, 105, 8403-8409, doi:10.1021/jp010597k, 2001.

Clever, H. L., Battino, R., Clever, H. L., Jaselskis, B., Clever, H. L., Yampol'skii, Y. P., Jaselskis, B., Scharlin, P., and Young, C. L.: IUPAC-NIST Solubility Data Series. 80. Gaseous Fluorides of Boron, Nitrogen, Sulfur, Carbon, and Silicon and Solid Xenon Fluorides in all Solvents, *J. Phys. Chem. Ref. Data*, 34, 201-438, doi:10.1063/1.1794762, 2005.

Deeds, D. A.: The Natural Geochemistry of Tetrafluoromethane and Sulfur Hexafluoride : Studies of Ancient Mojave Desert Groundwaters, North Pacific Seawaters and the Summit Emissions of Kilauea Volcano, PhD thesis, 2008.

Hine, J., and Mookerjee, P. K.: Structural effects on rates and equilibria. XIX. Intrinsic hydrophilic character of organic compounds. Correlations in terms of structural contributions, *J. Org. Chem.*, 40, 292-298, doi:10.1021/jo00891a006, 1975.

Formatted: Font: 10 pt

HSDB: Hazardous Substances Data Bank, TOXicology data NETwork (TOXNET), National Library of Medicine (US), available at: <http://toxnet.nlm.nih.gov/newtoxnet/hsdb.htm> (last access: 10 April 2015), 2015.

Formatted: Font: 10 pt, English (U.S.)

Hutchinson, M. F., and De Hoog, F.: Smoothing noisy data with spline functions, *Numer. Math.*, 47, 99-106, doi:10.1007/BF01404567, 1985.

Formatted: Font: 10 pt

Formatted: Font: 10 pt, English (U.S.)

Kutsuna, S.: Determination of Rate Constants for Aqueous Reactions of HCFC-123 and HCFC-225ca with OH- Along with Henry's Law Constants of Several HCFCs, *Int. J. Chem. Kinet.*, 45, 440-451, doi:10.1002/kin.20780, 2013.

Formatted: Font: 10 pt

Maaßen, S.: Experimentelle Bestimmung und Korrelierung von Verteilungskoeffizienten in verdünnten Lösungen, Shaker, 1995.

Mclinden, M. O.: Physical properties of alternatives to the fully halogenated chlorofluorocarbons, Scientific assessment of stratospheric ozone, 2, 1990.

Formatted: Font: 10 pt, English (U.S.)

Miguel, A. A. F., Ferreira, A. G. M., and Fonseca, I. M. A.: Solubilities of some new refrigerants in water, *Fluid Phase Equilib.*, 173, 97-107, doi:10.1016/s0378-3812(00)00390-3, 2000.

Miller, B. R., Huang, J., Weiss, R. F., Prinn, R. G., and Fraser, P. J.: Atmospheric trend and lifetime of chlorodifluoromethane (HCFC-22) and the global tropospheric OH concentration, *J. Geophys. Res.*, 103, 13237, doi:10.1029/98jd00771, 1998.

Miller, B. R., Rigby, M., Kuijpers, L. J. M., Krummel, P. B., Steele, L. P., Leist, M., Fraser, P. J., McCulloch, A., Harth, C., Salameh, P., Mühle, J., Weiss, R. F., Prinn, R. G., Wang, R. H. J., O'Doherty, S., Grealley, B. R., and Simmonds, P. G.: HFC-23 (CHF<sub>3</sub>) emission trend response to HCFC-22 (CHClF<sub>2</sub>) production and recent HFC-23 emission abatement measures, *Atmos. Chem. Phys.*, 10, 7875-7890, doi:10.5194/acp-10-7875-2010, 2010.

Montzka, S. A., Butler, J. H., Myers, R. C., Thompson, T. M., Swanson, T. H., Clarke, A. D., Lock, L. T., and Elkins, J. W.: Decline in the tropospheric abundance of halogen from halocarbons: Implications for stratospheric ozone depletion, *Science*, 272, 1318-1322, doi:10.1126/science.272.5266.1318, 1996a.

Montzka, S. A., Myers, R. C., Butler, J. H., Elkins, J. W., Lock, L. T., Clarke, A. D., and Goldstein, A. H.: Observations of HFC-134a in the remote troposphere, *Geophys. Res. Lett.*, 23, 169-172, doi:10.1029/95gl03590, 1996b.

Montzka, S. A., Kuijpers, L., Battle, M. O., Aydin, M., Verhulst, K. R., Saltzman, E. S., and Fahey, D. W.: Recent increases in global HFC-23 emissions, *Geophys. Res. Lett.*, 37, L02808, doi:10.1029/2009gl011195, 2010.

Montzka, S. A., McFarland, M., Andersen, S. O., Miller, B. R., Fahey, D. W., Hall, B. D., Hu, L., Siso, C., and Elkins, J. W.: Recent trends in global emissions of hydrochlorofluorocarbons and hydrofluorocarbons: Reflecting on the 2007 adjustments to the Montreal Protocol, *J. Phys. Chem. A*, 119, 4439-4449, doi:10.1021/jp5097376, 2015.

O'Doherty, S., Cunnold, D. M., Miller, B. R., Mühle, J., McCulloch, A., Simmonds, P. G., Manning, A. J., Reimann, S., Vollmer, M. K., Grealley, B. R., Prinn, R. G., Fraser, P. J., Steele, L. P., Krummel, P. B., Dunse, B. L., Porter, L. W., Lunder, C. R., Schmidbauer, N., Hermansen, O., Salameh, P. K., Harth, C. M., Wang, R. H. J., and Weiss, R. F.: Global and regional emissions of HFC-125 (CHF<sub>2</sub>CF<sub>3</sub>) from in situ and air archive atmospheric observations at AGAGE and SOGE observatories, *J. Geophys. Res.*, 114, doi:10.1029/2009jd012184, 2009.

Oram, D. E., Reeves, C. E., Penkett, S. A., and Fraser, P. J.: Measurements of HCFC-142b and HCFC-141b in the Cape Grim air Archive: 1978–1993, *Geophys. Res. Lett.*, 22, 2741–2744, doi:10.1029/2003JD004277, 1995.

Oram, D. E., Reeves, C. E., Sturges, W. T., Penkett, S. A., Fraser, P. J., and Langenfelds, R. L.: Recent tropospheric growth rate and distribution of HFC-134a (CF<sub>3</sub>CH<sub>2</sub>F), *Geophys. Res. Lett.*, 23, 1949–1952, doi:10.1029/96gl01862, 1996.

Park, T., Rettich, T. R., Battino, R., Peterson, D., and Wilhelm, E.: Solubility of gases in liquids. 14. Bunsen coefficients for several fluorine-containing gases (Freons) dissolved in water at 298.15 K, *J. Chem. Eng. Data*, 27, 324–326, doi:10.1021/je00029a027, 1982.

Parmelee, H. M.: Water solubility of Freon refrigerants, *Refrigerating Engineering*, 61, 1341, 1953.

Prinn, R. G., Weiss, R. F., Arduini, J., Arnold, T., DeWitt, H. L., Fraser, P. J., Ganesan, A. L., Gasore, J., Harth, C. M., and Hermansen, O.: History of chemically and radiatively important atmospheric gases from the Advanced Global Atmospheric Gases Experiment (AGAGE), *Earth System Science Data*, 10, 985, 2018a.

Prinn, R. G., Weiss, R. F., Arduini, J., Arnold, T., Fraser, P. J., Ganesan, A. L., Gasore, J., Harth, C. M., Hermansen, O., Kim, J., Krummel, P. B., Li, S., Loh, Z. M., Lunder, C. R., Maione, M., Manning, A. J., Miller, B. R., Mitrevski, B., Mühle, J., O'Doherty, S., Park, S., Reimann, S., Rigby, M., Salameh, P. K., Schmidt, R., Simmonds, P. G., Steele, L. P., Vollmer, M. K., Wang, R. H., and Young, D.: The ALE/GAGE/AGAGE Network (DB 1001), <http://cdiac.essdive.lbl.gov/ndps/alegagage.html> doi:10.3334/CDIAC/atg.db1001, 2018b.

Reichl, A.: Messung und Korrelierung von Gaslöslichkeiten halogener Kohlenwasserstoffe, *Shaker*, 1995.

Reinsch, C. H.: Smoothing by spline functions, *Numer. Math.*, 10, 177–183, doi:10.1007/BF02162161, 1967.

Sander, S., Abbatt, J., Barker, J., Burkholder, J., Golden, D., Kolb, C., Kurylo, M., Moortgat, G., Wine, P., Huie, R., and Orkin, V.: Chemical Kinetics and Photochemical Data for Use in Atmospheric Studies Evaluation Number 17, Pasadena, CA: Jet Propulsion Laboratory, National Aeronautics and Space Administration, 2011.

Scharlin, P., and Battino, R.: Solubility of CCl<sub>2</sub>F<sub>2</sub>, CClF<sub>3</sub>, CF<sub>4</sub> and c-C<sub>4</sub>F<sub>8</sub> in H<sub>2</sub>O and D<sub>2</sub>O at 288 to 318 K and 101.325 kPa. Thermodynamics of transfer of gases from H<sub>2</sub>O to D<sub>2</sub>O, *Fluid Phase Equilib.*, 95, 137–147, doi:10.1016/0378-3812(94)80066-9, 1994.

Sturrock, G. A., Etheridge, D. M., Trudinger, C. M., Fraser, P. J., and Smith, A. M.: Atmospheric histories of halocarbons from analysis of Antarctic firn air: Major Montreal Protocol species, *J. Geophys. Res.: Atmos.*, 107, doi:10.1029/2002JD002548, 2002.

Thompson, T. M., Butler, J. H., Daube, B. C., Dutton, G. S., Elkins, J. W., Hall, B. D., Hurst, D. F., King, D. B., Kline, E. S., and Laflour, B. G.: Halocarbons and other atmospheric trace species, *Climate Monitoring Diagnostics Laboratory Summary Report*, 27, 115–135, 2004.

Trudinger, C. M., Fraser, P. J., Etheridge, D. M., Sturges, W. T., Vollmer, M. K., Rigby, M., Martinerie, P., Mühle, J., Worton, D. R., and Krummel, P. B.: Atmospheric abundance and global emissions of perfluorocarbons CF<sub>4</sub>, C<sub>2</sub>F<sub>6</sub> and C<sub>3</sub>F<sub>8</sub> since 1800 inferred from ice core, firn, air archive and in situ measurements, *Atmos. Chem. Phys.*, 16, 11733–11754, doi:10.5194/acp-16-11733-2016, 2016.

Wahba, G.: Bayesian "confidence intervals" for the cross-validated smoothing spline, *Journal of the Royal Statistical Society. Series B (Methodological)*, 133–150, 1983.

Warner, M. J., and Weiss, R. F.: Solubilities of chlorofluorocarbons 11 and 12 in water and seawater, *Deep Sea Res. Part A. Oceanogr. Res. Pap.*, 32, 13, doi:10.1016/0198-0149(85)90099-8, 1985.

Wen, W., and Muccitelli, J. A.: Thermodynamics of Some Perfluorocarbon Gases in Water, *J. Solution Chem.*, 8, 22, doi:10.1007/BF00648882, 1979.

Wilhelm, E., Battino, R., and Wilcock, R. J.: Low-Pressure Solubility of Gases in Liquid Water, *Chem. Rev.*, 77, 44, 1977.

Zheng, D., Guo, T., and Knapp, H.: Experimental and modeling studies on the solubility of CO<sub>2</sub>, CHClF<sub>2</sub>, CHF<sub>3</sub>, C<sub>2</sub>H<sub>2</sub>F<sub>4</sub> and C<sub>2</sub>H<sub>4</sub>F<sub>2</sub> in water and aqueous NaCl solutions under low pressures, *Fluid Phase Equilib.*, 129, 197–209, doi:10.1016/S0378-3812(96)03177-9, 1997.

Formatted: Font: 10 pt

Formatted: Font: 10 pt, English (U.S.)

Formatted: Font: 10 pt

Formatted: Font: 10 pt, English (U.S.)